# Quantitative approaches in support of the early development of T-cell redirecting therapies

Dissertation

zur Erlangung des Grades des Doktors der Naturwissenschaften der Naturwissenschaftlich-Technischen Fakultät der Universität des Saarlandes

von

Arthur Van De Vyver

Saarbrücken

2022

# Quantitative approaches in support of the early development of T-cell redirecting therapies

Dissertation

zur Erlangung des Grades des Doktors der Naturwissenschaften der Naturwissenschaftlich-Technischen Fakultät der Universität des Saarlandes

von

Arthur Van De Vyver

Saarbrücken

2022

| | |
|---|---|
| Tag des Kolloquiums: | **12. September 2022** |
| Dekan: | **Prof. Dr. Jörn Eric Walter** |
| Berichterstatter: | **Prof. Dr. Thorsten Lehr**<br>**Prof. Dr. Alexandra K. Kiemer** |
| Vorsitz: | **Prof. Dr. Claus Jacob** |
| Akad. Mitarbeiter: | **Dr. Agnes-Valencia Weiß** |

# Table of Contents

## Publications included in this thesis

I. Predicting Tumor Killing and T-Cell Activation by T-Cell Bispecific Antibodies as a Function of Target Expression: Combining In Vitro Experiments with Systems Modeling

Arthur Van De Vyver, Tina Weinzierl , Miro J Eigenmann, Nicolas Frances, Sylvia Herter, Regula B Buser, Jitka Somandin, Sarah Diggelmann, Florian Limani, Thorsten Lehr, Marina Bacac, Antje-Christine Walz

Mol. Cancer Ther. 2021 Feb;20(2):357-366. doi: 10.1158/1535-7163.MCT-20-0269.

II. A novel approach for quantifying the pharmacological activity of T-cell engagers utilizing in vitro time-course experiments and streamlined data analysis

Arthur Van De Vyver, Miro J Eigenmann, Meric Ovacik, Christian Pöhl, Sylvia Herter, Tina Weinzierl, Tanja Fauti, Christian Klein, Thorsten Lehr, Marina Bacac, Antje-Christine Walz

AAPS J. 2021 Dec 3;24(1):7. doi: 10.1208/s12248-021-00637-2.

III. Cytokine Release Syndrome By T-cell-Redirecting Therapies: Can We Predict and Modulate Patient Risk?

Arthur Van De Vyver, Estelle Marrer-Berger, Ken Wang, Thorsten Lehr, Antje-Christine Walz

Clin Cancer Res. 2021 Nov 15;27(22):6083-6094. doi: 10.1158/1078-0432.CCR-21-0470.

## Contribution report

The author would like to declare his contributions to the publications I, II, and III included in this thesis. The author:

I. Conceptualised project, wrote model code, conducted model fitting and analysis, created graphics, wrote up the manuscript, performed review & editing
II. Wrote model code, conducted model fitting and analysis, performed experiments, created graphics, wrote up the manuscript, performed review & editing
III. Conceptualised project, wrote model code, performed simulations, performed literature search, created graphics, wrote up the manuscript, performed review & editing

## Abbreviations

| Abbreviation | Definition |
|---|---|
| 2D | Two-dimensional |
| 3R | Reduce, Refine, Replace |
| ACT | Adoptive Cell Therapy |
| AIC | Akaike Information Criterion |
| ALL | Acute Lymphoblastic Leukaemia |
| APC | Antigen Presenting Cells |
| AUC | Area Under the Curve |
| AUCE | Area Under the Effect Curve |
| BiTE | Bispecific T-cell Engager |
| CAR | Chimeric Antigen Receptor |
| CBER | Center of Biologics Evaluation Research |
| CD | Cluster of Differentiation |
| CDER | Center of Drug Evaluation Research |
| CDR | Complementarity Determining Region |
| CEA | Carcinoembryonic Antigen |
| CIT | Cancer Immunotherapy |
| Cmax | Maximal Concentration |
| CRS | Cytokine Release Syndrome |
| CV | Coefficient of Variation |
| EC20 | Effective concentration for 20% effect |
| EMA | European Medicines Agency |
| EpCAM | Epithelial Cell Adhesion Molecule |
| Eq. | Equation |
| FACS | Fluorescence-Activated Cell Sorting |
| FDA | Food and Drug Administration |
| FIH | First-in-Human |
| FIM | Fischer Information Matrix |
| FO | First-Order approximation |
| FOCE | First-Order Conditional Estimation |
| GOF | Goodness-of-Fit |
| HED | Human Equivalent Dose |
| ICANS | Immune effector Cell-Associated Neurotoxicity Syndrome |
| ICH | International Conference on Harmonisation of Technical Requirements for Registration of Pharmaceuticals for Human Use |
| IFNγ | Interferon-gamma |

| Abbreviation | Definition |
|---|---|
| IIV | Inter-Individual Variability |
| IL2 | Interleukin-2 |
| IL6 | Interleukin-6 |
| IMP | Investigational Medicinal Product |
| IOV | Inter-Occasion Variability |
| IP | intraperitoneal |
| IV | intravenous |
| Kd | Equilibrium dissociation constant |
| M&S | Modelling and Simulation |
| MABEL | Minimal Anticipated Biological Effect Level |
| MC | Monte Carlo |
| MHC | Major Histocompatibility Complex |
| MIDD | Model-Informed Drug Development |
| N() | Normal Distribution |
| NHL | Non-Hodgkin Lymphoma |
| NHP | Non-Human Primate |
| NLME | Non-Linear Mixed Effects |
| NOAEL | No Observed Adverse Effect Level |
| OFV | Objective Function Value |
| PD | Pharmacodynamics |
| PK | Pharmacokinetics |
| QE | Quasi-Equilibrium |
| QSP | Quantitative Systems Pharmacology |
| r/r | relapsed/refractory |
| RSE% | Relative Standard Error |
| RV | Residual Variability |
| SAEM | Stochastic Approximation Expectation Maximisation |
| SMAC | Supra-Molecular Activation Cluster |
| SS | Steady-State |
| TCB | T-Cell Bispecific antibody |
| TCR | T-Cell Receptor |
| TDCC | T-cell Dependent Cell Cytotoxicity |
| TNFα | Tumour necrosis factor-alpha |
| VPC | Visual Predictive Check |

## Graphical Abstract

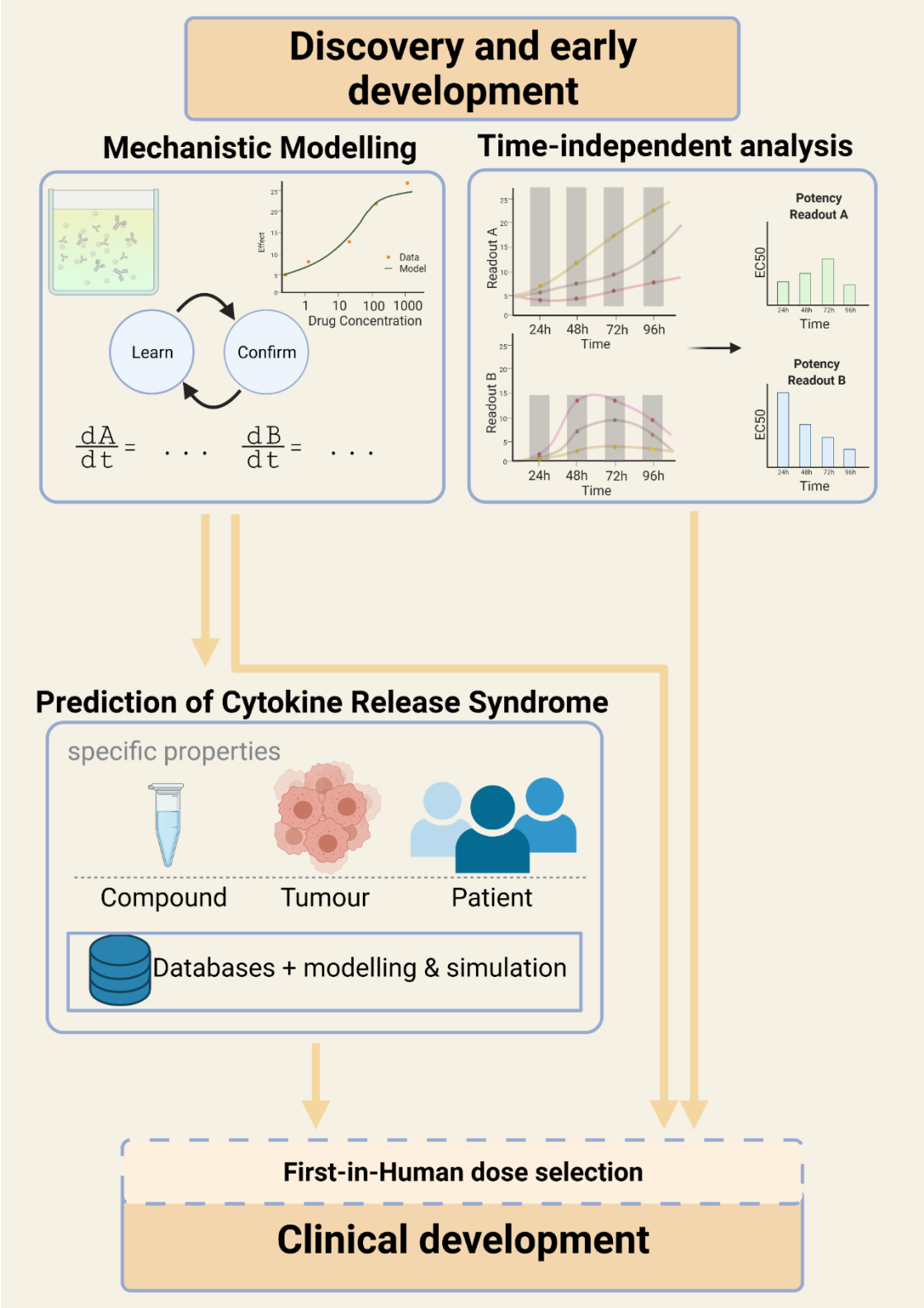

## Summary (EN)

T-cell redirecting therapies such as CD3-bispecific antibodies and CAR-T cells are promising assets in our fight against cancer. By redirecting T-cells towards tumour cells, these therapies induce efficient eradication of tumours. Many questions remain regarding their efficacy and safety in patients. The success of a drug candidate starts with nonclinical investigations before going into patients. This work focused on developing tools to improve the translatability of nonclinical research of T-cell redirecting therapies.

In this work, a mechanistic *in silico* model was developed that integrates an *in vitro* dataset of the pharmacology of cibisatamab, a CD3-bispecific antibody. The model may serve as a tool in early development to explore and quantify the impact of target expression densities on the pharmacology of CD3-bispecifics.

Also, this work proposed the collection of data over multiple time points and designed a new experimental setup and analysis that allows assessing the pharmacology in an unbiased and time-independent manner. As such, the kinetics of experimental readouts can be considered to make informed decisions about the development of the compound and assist in dose selection.

Lastly, the work presents a fresh look on cytokine release syndrome and identifies drug-target disease related factors and individual risk factors as the root cause of CRS. It postulates a combination of mechanistic modelling with real world data to enable individualized risk assessment.

## Summary (DE)

Gerichtete T-Zell-Therapien sind ein vielversprechendes Mittel im Kampf gegen Krebs. Bei dieser Therapie werden T-Zellen auf Tumorzellen gerichtet, was zu einer hocheffizienten Abtötung des Tumors führt. Es bleiben viele Fragen bezüglich ihrer Wirksamkeit und Sicherheit offen. Der Erfolg eines Arzneimittels beginnt mit nichtklinischen Untersuchungen. Diese Dissertation konzentrierte sich auf die Entwicklung Instrumente zur Verbesserung der nichtklinischen Forschung von gerichtete T-Zell-Therapien.

In dieser Dissertation wurde ein mechanistisches In-silico-Modell entwickelt, das einen in-vitro-Datensatz zur Pharmakologie von cibisatamab integriert. Das Modell kann als Werkzeug in der Entwicklung dienen, um die Auswirkungen der Targetdichten auf die Pharmakologie von CD3-bispezifischen Antikörpern zu quantifizieren.

In dieser Dissertation wurde auch ein neuer Versuchsaufbau und Analyse entwickelt, die eine unverzerrte und zeitunabhängige Bewertung der pharmakologischen Aktivität ermöglicht. Auf diese Weise kann die Kinetik der Messwerte berücksichtigt werden. Dies ist von Bedeutung, um fundierte Entscheidungen über die Entwicklung der Wirkstoffe und die Dosisauswahl zu treffen.

Schließlich wirft die Arbeit einen Blick auf das Cytokine Release Syndrome und identifiziert Risikofaktoren als Ursache für CRS und empfiehlt eine Kombination von Modellierung und real-world Daten zur Ermöglichung einer individuellen CRS Risikobewertung bei der Behandlung mit gerichteten T-Zell-Therapien.

# 1. Introduction

## 1.1 Background

Ever since we could recognize tumours as a malignancy, humankind has been looking for ways to combat them. Over the centuries, the use of surgery, herbal tinctures, and even hyperthermia found their way in the fight against cancers [10]. Later on, more medically advanced strategies of radiation and chemotherapy were commonly used, with varying levels of success [11]. Nowadays, media announcements of new and *groundbreaking* immunotherapies - therapies that use the patient's immune system to fight the cancer- are commonplace. The reason for such wide media coverage is undoubtedly due to the promising results that we have so far seen with these kind of therapies [12].

The pretence that the concept of immunotherapy is a child of the 20$^{th}$ and 21$^{st}$ centuries is, however, a false one. A papyrus roll, allegedly written by the Egyptian physician Imhotep, recommends treating tumours by inducing local infections (ca. 2600BC) [13]. The infection would stimulate the immune system that can potentially initiate an attack on the tumour. The first case of *modern* immunotherapy stems from the 1890s, when Dr. William B. Coley injected cancer patients with a concoction of heat-inactivated bacteria (*Streptococcus pyogenes* and *Seratia marcescens*) to induce infection in order to treat malignant sarcomas [14]. He based his hypothesis on frequent literature reports of cancer patients showing spontaneous tumour regression after contracting an infectious disease, and the relatively low prevalence of malignancies in syphilis patients. Because of his radical new idea and its systematic implementation, Coley is now widely seen as the father of immunotherapy.

## 1.2 Rationale for targeted therapies

Non-targeted cytostatics have dominated the oncology scene for a long time [15]. Due to their unspecific mechanism of action, undesired side effects are commonplace during treatment with these early anti-cancer drugs [16]. Alternative therapies, such as kinase inhibitors and monoclonal antibodies, appeared on the scene in the last few decades [17]. These therapies employed a much more targeted approach towards the tumour and showed promising clinical results with reduced propensity for adverse events commonly observed with unspecific treatments [18].

The use of antibodies that bind to a specific tumour antigen and tag them for destruction has proven to be a powerful tool in the physician's repertoire to target tumours. A few notable examples are rituximab (anti-CD20, for the treatment of various B-cell malignancies [19]), trastuzumab (anti-HER2, or the treatment of breast and stomach cancer [20]), and cetuximab (anti-EGFR, for the treatment of colorectal cancers and head-and-neck cancers [21]).

Modern immunotherapy forms a big pillar of targeted therapies. A key player here is the class of checkpoint-inhibitors. These compounds specifically target molecules involved in immune cell activity: immune checkpoints. Well-known examples of immune checkpoints are the PD-1/PD-L1 axis and CTLA4, which will dampen immune responses or induce exhaustion [22]. A variety of monoclonal antibodies has been developed to target these checkpoints, thereby activating immune cells and increasing the chances that tumour cells will be detected, recognized, and destroyed by the patient's own immune system. Additionally, immune-agonistic antibodies that target T-cell co-receptors such as CD28 or 4-1BB can bring T-cells into an elevated state of activity. Stimulating (recombinant) cytokines such as IL2 or IL15 have been used in clinics with varying degrees of success [23, 24] (Figure 1).

However, these targeted therapies did not prove to be the solution for all tumours. A considerable portion of patients are resistant to such treatments; for instance, due to redundant signalling pathways or the presence of tumours that are virtually void of immune cells –an immune desert [25, 26]. Furthermore, removal of the brakes of the immune system can lead to various adverse events, such as disseminated immune activation and tissue damage [22, 27].

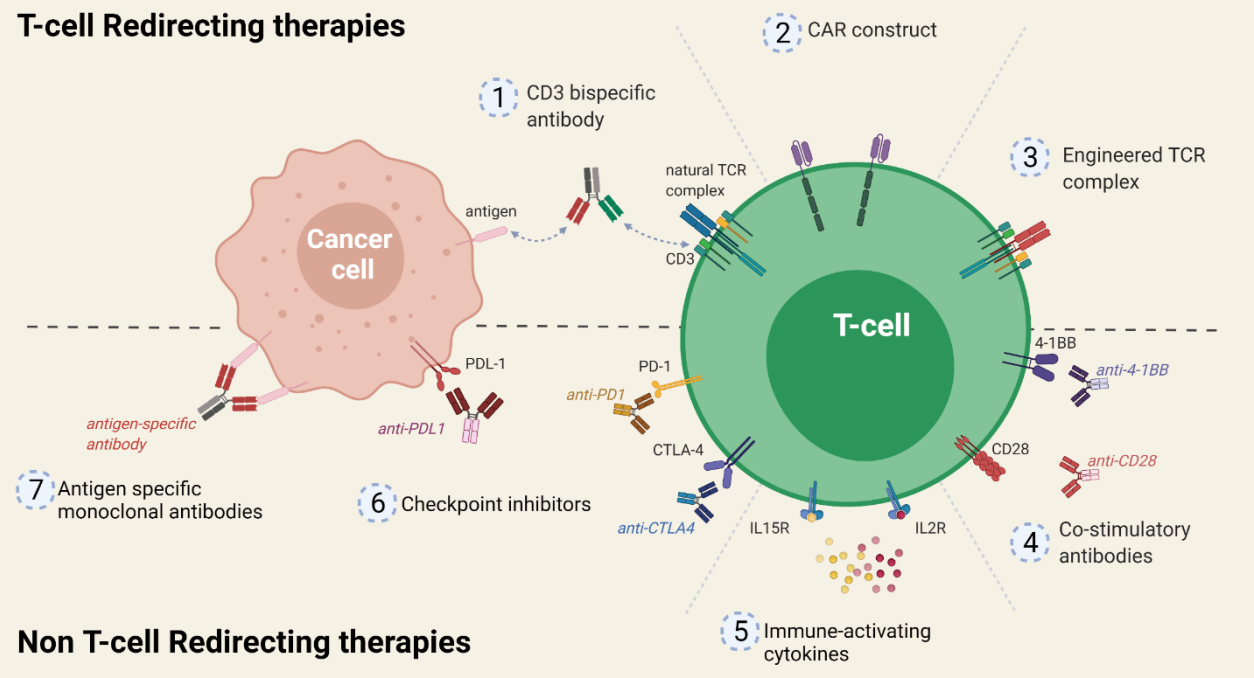


***Figure 1.*** *Overview of the most prominent targeted therapies in oncology. This field contains both T-cell redirecting therapies (top) and Non T-cell redirecting therapies (bottom). ① CD3-bispecifc antibodies cross-link T-cells to tumour cells by binding to CD3 and a tumour antigen; ② CAR constructs are artificially introduced into the T-cell membrane and can recognize a specific tumour antigen, leading to T-cell activation; ③ Engineered TCR complexes have been affinity-matured to bind a specific tumour antigen with much higher affinity; ④ Co-stimulatory antibodies bind stimulatory co-receptors (e.g., CD28, 4-1BB) to trigger T-cell activation; ⑤ Immune-activating cytokines (e.g., IL2, IL15) bind on their respective receptors on T-cells and induce activation and proliferation; ⑥ Checkpoint-inhibitor antibodies block important immune checkpoints that may otherwise dampen immune responses (e.g., CTLA4, PD-1); ⑦ Antigen-specific monoclonal antibodies bind to an antigen that is overexpressed on tumour cells, thereby tagging it for destruction.*

## 1.3 T-cell redirecting therapies

T-cell redirecting therapies are, for industry standards, a relatively novel class of compounds. As a distinct branch of targeted therapies, T-cell redirecting therapies is the umbrella term for various therapeutic modalities that will redirect T-cells towards tumour cells. T-cells are specialised immune cells that make up an important part of the adaptive immune system in humans. They recognize specific foreign antigens and mount an efficient immune response against it. T-cell redirecting therapies take advantage of the highly potent killing mechanisms of activated T-cells to eradicate cancer cells. To achieve this, these therapies rely on the activation of T-cells through recognition of a specific tumour antigen. As such, T-cells are re-targeted *en masse* towards tumour cells that express this specific antigen. Diverse technologies exist to redirect large numbers of T-cells, such as CD3-bispecific antibodies, CAR-T cells, and TCR-T cells (Figure 1). CD3-bispecific antibodies (or antibody fragments) are antibodies that have been engineered to bind to two targets simultaneously. This is in contrast to naturally occurring antibodies or ‘classical’ therapeutic monoclonal

antibodies with two binding arms that both bind the same epitope (figure 2A). The concept of bispecific antibodies has been around for some time and has seen a few therapeutic use cases, for instance in haemophilia (by cross-linking two clotting factors, thereby compensating for the genetic loss of another clotting factor) and in auto-immunity (by sequestering multiple pro-inflammatory cytokines at the same time to prevent excessive inflammation) [28]. CD3-bispecific antibodies are a subclass of bispecific antibodies. They are characterized by their specificity to CD3. CD3 is a subunit of the T-cell receptor (TCR), a complex with which T-cells can recognize antigens and receive activation signals [4]. Besides CD3, these antibodies also have specificity towards a tumour antigen. This means that CD3-bispecific antibodies can bind simultaneously to CD3 on T-cells with one arm and to an antigen on tumour cells with the other arm, thereby cross-linking the two cell types (figure 2B). This crosslinking will mimic a natural immune synapse (see Box A), inducing the T-cells to become active and to eliminate the tumour cell [28]. In a few instances, CD3-bispecific antibodies have shown promising efficacy in patients, with up to 69% objective response rates [29]. Over the years, investigators developed a multitude of construct formats, differing in their molecular weight, valency, and specificity [30].

Chimeric Antigen Receptor (CAR) T-cells are another modality from the class of T-cell redirecting therapies and part of the adoptive cell therapies (ACT). These are highly specialized T-cells that were originally isolated from the patient. These freshly isolated, autologous T-cells are then transfected to express a CAR construct (figure 2D). CARs are large constructs that contain an extracellular domain that recognizes a specific tumour antigen (in the same fashion as a binding arm of an antibody), a transmembrane 'linker', and an intracellular signalling domain. Details on the CAR structure and signalling cascades are reviewed in [31]. Multiple generations of CAR constructs have been developed over the years, each trying to improve upon the previous one by including co-stimulatory domains or other structural changes. After modification, the T-cells will be expanded in great numbers. Afterwards, the patient

Box A | Immunological Synapse

A crucial step in mounting a T-cell immune response is the formation of an immunological synapse between a T-cell and an antigen-presenting cell (APC). APCs are specialised cells that patrol the body and are present in all tissues, on the lookout for foreign antigens. When a foreign antigen is detected, APCs take it up, process it into smaller peptides, and present it to T-cells in secondary lymphoid organs. APCs present these peptides via their Class 2 Major Histocompatibility Complex (MHC-II) to the T-cell Receptor (TCR). In case of intracellular antigens, a similar process takes place except that the main pathway of presentation of the peptides happens via a class 1 MHC, which is found on all nucleated cells in the body [2].

In both cases, the interaction of a peptide-MHC complex and a TCR triggers the build-up of an immunological synapse on the interface between both cells involved. This includes the formation of a Supra-Molecular Activation Cluster (SMAC) that consists of clustered TCRs, adhesion and signalling molecules [4].

The mechanism-of-action of T-cell redirecting therapies relies on mimicking this immunological synapse or on facilitating its formation.

receives an infusion of billions of the re-engineered T-cells to combat their tumour. When a tumour antigen is bound, this will spark a signalling cascade that will lead to activation of the T cell and tumour cell killing. Besides their high efficacy, CAR-T cells are notorious for their high cytokine release potential.

TCR-engineered T cells (TCR-T cells) are another class of ACT. Rather than transducing autologous T cells with a specific construct, the isolated T cells are selected *ex vivo* for specificity towards a specific antigen, followed by affinity-enhancement and expansion [32]. The final product contains billions of T cells trained to target the tumour antigen with much higher affinity than what would be possible to find *in vivo* (figure 2E). Since these T cells still express the canonical, albeit enhanced, TCR on their surface, they target tumour cells in a MHC-restricted manner [33]. This limits its versatility in targeting non-MHC expressed surface antigens that are common targets of CAR-T cells (and many CD3-bispecific antibodies), but opens the door to a whole new repertoire of intracellular antigens expressed on MHC [34]. Multiple clinical trials with TCR-T cells are ongoing [34]. An overview of the different modalities can be found in [34-36].

The first T-cell redirecting therapy to receive market authorization was catumaxomab (Removab®), a CD3-bispecific antibody that binds to EpCAM that is often overexpressed in certain types of cancer. The European Medicines Agency (EMEA) approved catumaxomab in 2009 for the symptomatic treatment of malignant ascites in ovarian carcinoma patients [37]. After intraperitoneal injection, catumaxomab redirects T-cells towards EpCAM-positive cancerous cells floating around in the ascetic fluid. Its mechanism of action allowed the redirection of T-cells towards EpCAM-positive cells and reduced the burden of ascites on patients. Catumaxomab was withdrawn from the market for economic reasons in 2017.

Five years after the first CD3-bispecific antibody was approved, the FDA authorized marketing of the CD19xCD3 bispecific T-cell Engager (BiTE) blinatumomab (Blincyto®) for the treatment of relapsed/refractory Acute Lymphoblastic Leukaemia (ALL) [38]. A few years later, two CAR-T cell therapies that target CD19 achieved approval as well: tisagenlecleucel (Kymriah®) and axicabtagene ciloleucel (Yescarta®) for the treatment of ALL and NHL, respectively [39, 40].

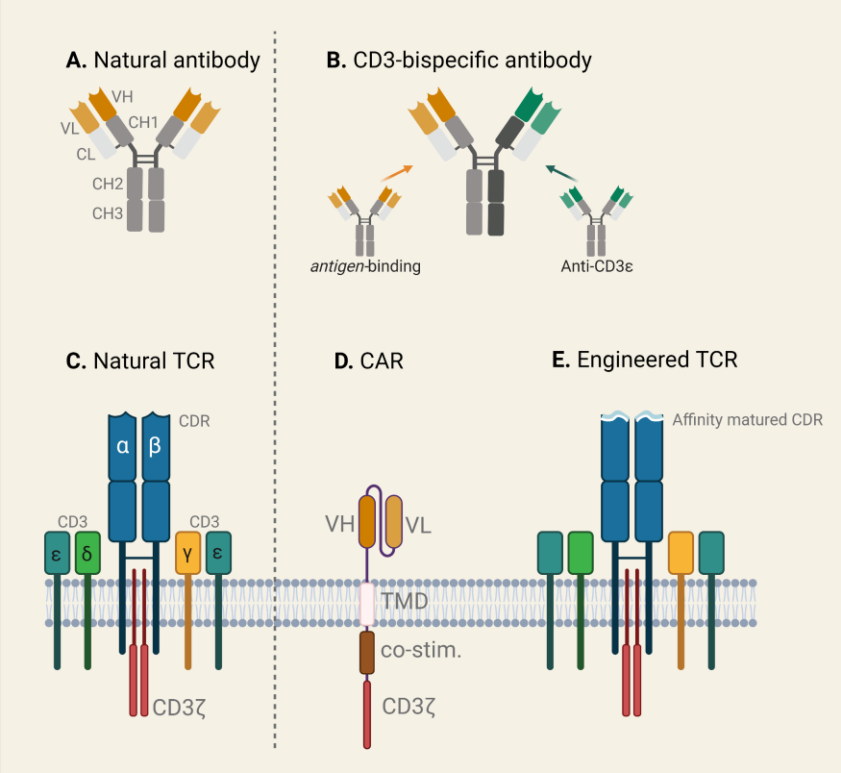


*Figure 2. Structural components of T-cell redirecting therapies and their natural counterparts.* ***A.*** *a natural antibody consists of three main domains: two antigen-binding fragments (Fab) and one 'crystallisable' fragment (Fc). Each domain contains various peptide sequences. The Fc-domain consists of heavy constant chains (CH2 and CH3). Each Fab-domain consists of a constant light (CL) and heavy (CH1) chain, and a variable light (VL) and heavy (VH) domain. The latter two are responsible for antigen binding.* ***B.*** *a CD3-bispecific antibody binds, in contrast to a natural antibody, to two different antigens: a tumour-antigen and the epsilon-chain of CD3. CD3 is a co-stimulatory receptor that is part of the T-cell Receptor Complex (TCR), which is responsible for T-cell activation upon antigen binding. A CD3-bispecific antibody does not need to resemble structurally the Y-shaped natural antibody and exists in many different sizes and formats.* ***C.*** *a simplified depiction of a natural TCR complex, found on T cells. The TCR consists of an α and β subunit anchored into the cell membrane. At the distal end, a Complementarity Determining Region (CDR) is responsible for detecting specific peptides. A crucial part of the TCR signalling machinery is CD3, which consists of various subunits (γ, δ, ε, and ζ).* ***D.*** *a Chimeric Antigen Receptor (CAR) can be considered as a chimera between a TCR and an antibody. The antigen-detecting part consists of the antigen-binding domain of an antibody (VL and VH chains); followed by a transmembrane domain (TMD) that links it to co-stimulatory domains (co-stim., such as CD28 or 4-1BB depending on the generation of the CAR involved). CD3ζ makes up the final part of the construct and is required for signal transduction.* ***E.*** *An engineered TCR looks and functions identical to a natural TCR with the sole difference that the CDR has been artificially affinity-matured in order to exhibit a manifold higher affinity towards the desired antigen.*

## 1.4 Aspects in early drug development.

### 1.4.1 Regulatory Considerations

Before exposing humans to any medicinal product, extensive pharmacological and toxicological profiling is required to ensure patient safety. The primary goal of a First-In-Human (FIH) study is to assess the pharmacology, pharmacokinetics (PK), and safety of an investigational medicinal product (IMP), and to determine a Recommended Phase 2 Dose (RP2D) for further clinical testing [9, 41]. It is crucial to ensure robust translation of nonclinical safety and efficacy data for the selection of a relevant starting dose for the FIH trial. This entails having a good understanding of the nature of the intended target and potential off-

target risks (see section 1.4.2), making informed decisions about the relevance of animal testing (see section 1.4.3), and applying a suitable dose selection strategy (see section 1.4.4). Additionally, it is highly recommended to inform and support dose selection with PK/PD modelling approaches [9]. Phase I studies are carefully designed to maximize safety for the test subjects. Usually –due to rigorous nonclinical testing and good trial planning- Phase I studies go well without noticeable reasons for concern. However, over the last two decades, a few Phase I studies ended with disastrous consequences, indicating that absolute safety cannot be guaranteed [6, 42]. Regulatory agencies have responded in turn with adapted guidelines and requirements in an attempt to prevent such clinical disasters from happening again.

Regulatory agencies and bodies, such as the Food and Drug Administration (FDA), European Medicines Agency (EMEA), and the International Conference on Harmonisation of Technical Requirements for Registration of Pharmaceuticals for Human Use (ICH), have formulated guidelines in support of sponsors and investigators attempting to develop new medicines. For targeted anti-cancer therapies in general, and for T-cell redirecting therapies in particular, the following documents provide guidance in the drug development process from nonclinical testing up to early clinical trials.

*1)* Guideline on strategies to identify and mitigate risks for first-in-human and early clinical trials with investigational medicinal products*. EMA: Committee for Medicinal Products for Human Use (CHMP)* [9]
2) Guidance for Industry: S9 Nonclinical Evaluation for Anticancer Pharmaceuticals. *FDA: Center for Drug Evaluation and Research (CDER) and Center for Biologics Evaluation and Research (CBER)* [43]
3) Guidance for Industry: S6 Addendum to Preclinical Safety Evaluation of Biotechnology-Derived Pharmaceuticals. *FDA: CDER and CBER* [44]
4) Guidance for Industry: Bispecific Antibody Development Programs. *FDA: CDER and CBER* [45]
5) Potency testing of cell-based immunotherapy medicinal products for the treatment of cancer. *EMEA: CHMP* [46]

This is not an exhaustive list by any means, and the regulatory bodies will undoubtedly formulate additional guidelines build on the increasing scientific and translational expertise with such compounds. The Committee for Medicinal Products for Human Use (CHMP) of the EMEA formulated the original guidelines in the aftermath of the TeGenero TGN1412 incident in 2006 [47, 48]. In this controversial incident, various human volunteers received for the first time the novel immune-stimulatory compound TGN1412. They quickly developed severe adverse events. Section 1.4.4 elaborates further on this case and its impact on regulatory guidelines. Briefly, there are multiple –but still debated- potential causes of the unexpected

severe effects observed in humans but all are related to unexpected differences between the tested animal species and humans, and the corresponding lack of translatability [49-51].

The Bial disaster in 2016 prompted the Committee to release an updated version of the original 2007 guidelines [9]. The affected compound in the latter case, BIA-10-2474, is a FAAH enzyme inhibitor developed to increase endocannabinoid levels in plasma to combat neuropathic pain. Similar FAAH inhibitors had proven to be safe in humans and multiple animal species were tested with no observed toxicities except at the highest doses [8]. Yet, after a few uneventful dosing cohorts totalling 84 patients exposed to BIA-10-2474, a healthy volunteer from a multiple ascending dose (MAD) cohort developed clear signs of adverse events after the fifth dose [52]. The volunteer was taken off the trial and was monitored by hospital staff. The next day, the MAD cohort's remaining volunteers proceeded to receive the sixth dose. That day, the affected volunteer's condition deteriorated and the volunteer slipped into a coma, dying a few days later. Four out of five volunteers that received the sixth dose later developed similarly severe symptoms, but survived with long-term sequelae [52]. It is difficult to pinpoint exactly the root cause of this mishap. However, there are two notable aspects highlighted that likely influenced the 2018 revision of the EMEA guidelines. After the trial, an independent research group investigated the MoA of BIA-10-2474 and found that it altered lipid metabolism in a way not seen with similar FAAH inhibitors studied in humans [53]. This suggests that despite being in a class with good tolerability and similar MoA, a compound may still act in an unexpected manner. Additionally, dose selection of BIA-10-2474 relied on the NOAEL approach to ensure human doses remained below those where safety issues in animal species were seen (see section 1.4.4 and Box B). The highest tested dose in humans corresponded to the NOAEL. It was later shown that maximal pharmacological activity in humans is achieved at a dose that is 20-fold lower than the highest tested dose in the trial [8]. These findings reiterate the importance of using human-relevant assays and denounce the reliance on animal findings only. Scientific rationale should be applied when selecting the starting dose and defining the maximal exposure. Having almost doubled in size, the new 2018 guidelines put emphasis on the integration of pharmacokinetic, pharmacodynamic and safety data, the importance of human pharmacology, and conducting dose-exposure-response analysis using PKPD modelling to guide dose selection [54]. As opposed to the first version, the revised version does not consider pharmacology to reflect only nonclinical safety, but now also includes human pharmacology itself [54]. Especially for targeted therapies is human pharmacology important, for exaggerated pharmacology is a dangerous adverse event [55]. This becomes especially a problem at higher doses.

While each document provides specific recommendations, the consensus is the same and the core principle for all is ensuring patient and trial participant safety. Additionally, the guidelines promote the 3R concept

(Reduce, Refine, and Replace animal experimentation) to limit test animal use when alternatives are available.

Phase I trials with anti-cancer therapeutics are usually conducted in cancer patients only instead of healthy volunteers [56]. These patients are often very ill and the administered doses are close to the adverse event levels [43]. Diligent nonclinical testing is vital in order to derive a safe and relevant starting dose to deliver to these patients.

Nonclinical studies prior to phase I are required to demonstrate safety and efficacy. This includes the primary pharmacodynamic properties (e.g., tumour killing, T cell proliferation; markers of desired pharmacological activity) and secondary pharmacodynamic properties (e.g., cytokine release; markers of potential safety concerns), thereby establishing a nonclinical proof of principle [43].

There is an inherent uncertainty involved in early clinical trials concerning the safety and efficacy of an IMP (figure 3). The level of uncertainty is influenced by the amount of knowledge available on and the uniqueness of the mechanism of action, the presence of (safety) biomarkers, the cross-reactivity of the molecule in animal models and the translatability of these animal models, the impact of patient heterogeneity in the clinical trials, the suspicion of pleiotropies or inadequate biological feedback loops, etc. It is important that the potential risks be identified *a priori.* The penultimate goal of nonclinical studies, FIH studies, and early clinical trials is to reduce the amount of uncertainty around an IMP [9]. Generating relevant, high quality nonclinical data is paramount to dissipate some of this uncertainty and to make a more informed decision going forward into the clinical phases. Broader initiatives and joint efforts are helpful in better understanding what causes uncertainty and how to address them. This includes regulatory documents such as the ones reviewed here, cross-sponsor consortia, workshops or whitepapers such as, for instance, a workshop on preclinical and translational safety assessment of CD3 bispecifics [57], or a whitepaper on CRS by Friends of Cancer Research [58]. It requires specific tools capable of integrating these nonclinical findings with clinical or biological knowledge in order to maximise their translational value. The field of modelling and simulation (M&S) provides many such tools suitable to tackle this objective. They can help to describe experimental findings in a quantitative manner [59].

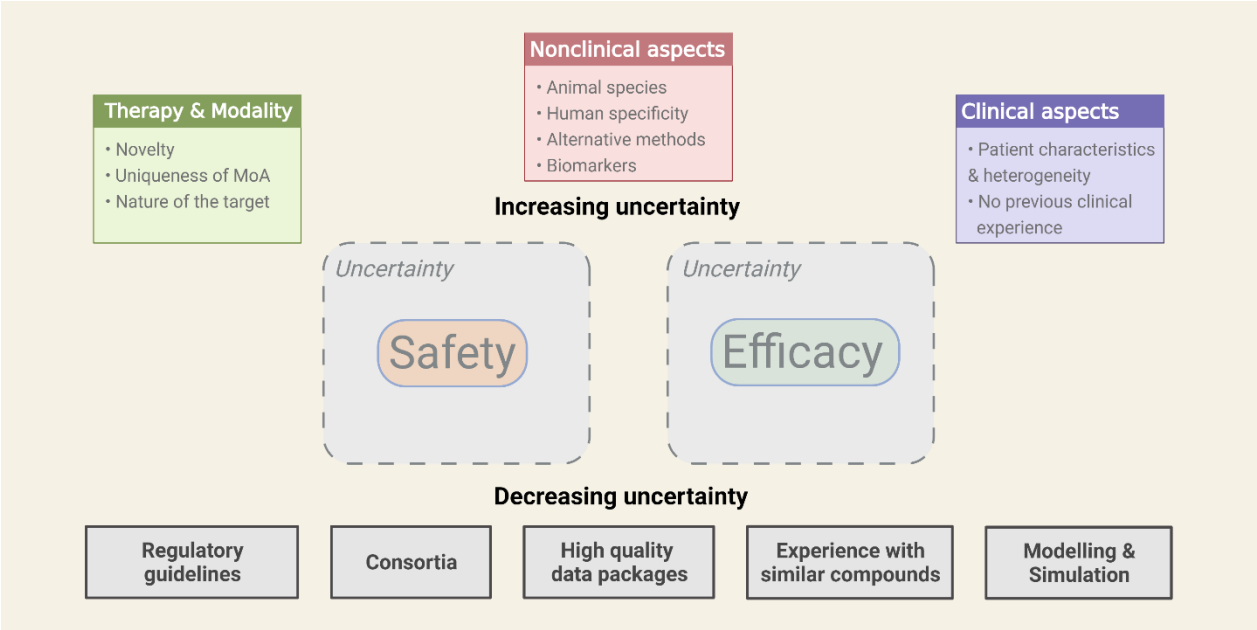


***Figure 3.*** *There is a risk involved with going into human with a new IMP, which investigators cannot readily quantify. The uncertainty that this brings is influenced by various factors such as the novelty of a compound and uniqueness of its mechanism of action. From a nonclinical standpoint, the availability of relevant animal species, alternative methods, or identified biomarkers will influence the inherent level of uncertainty before going into human. In clinics, the heterogeneity of the tested study population may increase uncertainty. On the other hand, clinical experience with similar compounds may decrease uncertainty around the risks involved. Lastly, joint efforts and information sharing including regulatory documents, consortia, and modelling efforts may help dissipate this uncertainty.*

Some tools, such as mechanistic models, also enable the capture of current knowledge about the drug or biological system of interest into a mathematical framework. Such a model is capable of describing the experimental data, but also opens the door to explore alternative experimental scenarios or drug variants by changing the relevant parameters. This can then be supplemented with new experiments whose design was influenced by prior simulations, as a learn-and-confirm cycle. If more is known about a drug and its related pharmacology and biological effects, investigators can make predictions with more confidence, allowing them to explore 'what-if' scenarios and more reliably inform about potential risks.

### 1.4.2 Nature of the target

For new medicinal products, the pharmacological target needs to be studied in detail [9]. The expression pattern and the physiological function of the target of interest may influence the efficacy and safety of the IMP. The occurrence of on- and off-target toxicity may be influenced by the extent of tissue distribution of the compound and the target, which may have implications for dosing selection [60]. Some types of models, such as physiological-based pharmacokinetic (PBPK) models, consider the various tissues in the body and attempt to model the distribution of a drug by means of an elaborate system of equations. PBPK models

integrate *in vitro* knowledge of compound properties or *in vivo* data from animal studies to capture the distribution of the drug [61, 62].

A complex mechanism-of-action is almost inherent to T-cell redirecting therapies. For these modalities, not only the tumour target but also the T-cell activating processes need to be considered. In addition, not only the tumour target but also the T-cell activating machinery at the other end of the therapeutic needs to be well considered. For engineered (CAR- or TCR-) T cells, the tumour target is recognised by a (partly) artificial biological construct that consists of various TCR subunits (e.g., CD3) and co-receptors (e.g., CD28, 4-1BB). CD3-bispecifcs bind simultaneously to the tumour target and to the CD3 subunit. CD3 is part of the T-cell receptor complex and, although it has been well studied, should be considered a high-risk target due to potential pleiotropic effects it may induce and the potential effects on unexpected T-cell activation that this may have [63]. Due to these complexities, developing predictive models for T-cell activity is even more challenging. The immune system relies on various feedback loops and this can be modelled with elaborate mechanistic or systems pharmacology models [64, 65].

For dose selection, PK/PD models allow to relate dose with the drug concentration and its effects. Such models provide a lot of information about the pharmacology of a drug and serve as a good basis for scaling up and predicting the PK/PD in patients. Some of these models have already been developed for various T-cell redirecting therapies [66-68]. For such models to be successful, they should be informed with high quality experimental data.

### 1.4.3 Animal experimentation

Animal testing plays an important role in the preclinical evaluation of anticancer medicinal products and in support of selecting a relevant human dose. Animal models allow investigators to understand the effects of an IMP *in vivo* for the first time. In addition, the selection of dose, schedule or escalation strategy can be facilitated when basic PK analysis is performed in animal species (e.g., half-life, AUC, Cmax) [43]. This information helps to define the range of efficacious concentrations or the concentration for adverse effects.

In order to ensure that findings from animal studies have the potential to be translatable to humans, the relevance of the animal model of choice needs to be demonstrated [9]. Otherwise this may lead to misinterpretation of the results [44]. Relevance of an animal model can be confirmed by assessing the sequence homology of the target, its expression level and distribution pattern, kinetics from ligands and receptors, PK and PD characteristics. Mechanistic models rely on the distinction between drug-specific and system-specific parameters. Drug-specific parameters are inherent to the studied drug and are not expected to change between experiments or individuals, such as the drug's size, stability and affinity. System-related parameters describe the biological system (i.e., an *in vitro* assay, animal species, or patients)

and will vary from one experiment to another, or even between individuals [69]. Experiments should be performed to quantify both the drug- and system-specific parameters. These parameters will, when appropriate scaling is performed to account for species differences in the system-specific parameters, aid in the prediction of drug response in humans.

However, qualitative or quantitative differences in the drug response can occur between animals and humans. This can be due to relative differences in expression level, distribution, affinity values, and truncated downstream events [9, 56]. In addition, similar *in vitro* data is no guarantee for a similar *in vivo* response between animal and human. Due to increased human-specificity of targeted therapies, there is an increase in the uncertainty around patient risk evaluation based on nonclinical studies. The high target-specificity might impair the availability of a relevant animal species as a toxicology model [70]. This warrants a more prudent approach to be taken.

Failing to identify relevant animal species, investigators should refrain from using non-relevant species simply to fulfil regulatory requirements, which often appears to be the case [54]. Instead, the use of transgenic or humanized animals, or the use of surrogate molecules should be considered [44]. Some T-cell redirecting therapies do not cross-react with animal species and must rely on alternative approaches for nonclinical testing (Figure 4) [71, 72].

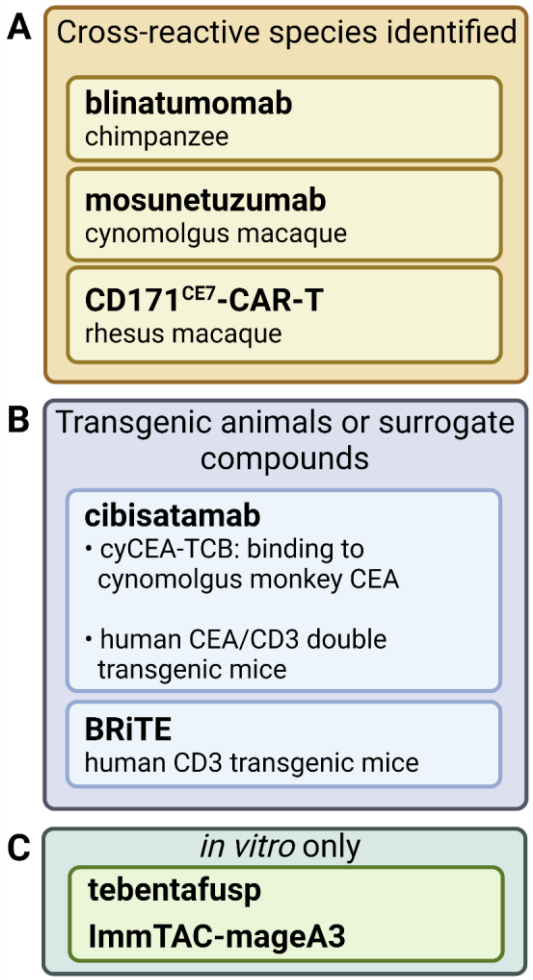


***Figure 4.*** *Examples of T-cell redirecting therapies and the availability of relevant animal species.* ***A.*** *Various non-human primates are relevant test animals as long as there is cross-reactivity with the target.* ***B.*** *In case of cibisatamab, neither approach yielded desirable results* ***C.*** *some compounds target human antigens with such specificity that developing transgenic animals becomes challenging. In these cases, an in vitro-only approach is the only viable option.*

Current experiences with T-cell redirecting therapies show that availability of relevant animal species differs from one compound to the other. For some, relevant animal species exist that cross-react with the binders of the compound (either the tumour target alone or in conjunction with CD3 for CD3-bispecifics). In many cases, these relevant animals are non-human primates (Figure 4A) [38, 73, 74]. When no cross-reactive species are identified, some projects opt for implementing a transgenic animal study (usually with mice) [75] or to deploy a surrogate compound that does bind the animal target (Figure 4B). This does not always yield satisfactory results, as was shown for cibisatamab, a

CD3-bispecific that targets the tumour antigen CEA [76]. In other cases, especially when the compounds exhibits very high human specificity such as TCR-like CD3-bispecifics that target a tumour-specific peptide presented on an MHC-I complex like tebentafusp, an *in vitro*-only approach may be the best choice (Figure 4C) [77]. Irrespective of the availability of relevant animal species, most projects include animal studies with immune-deficient mice that received grafts of human tumour cell lines and injected with human immune cells. This allows the investigator to study the drug effect *in vivo*. However, these xenograft models have limited relevance since they lack for instance a tumour microenvironment and a complete immune system.

### 1.4.4 Dose selection and the need for better strategies

A textbook example that highlights the risk of FIH studies with immune-agonists is the TeGenero TGN1412 tragedy. A phase I study of TGN1412 resulted in life-threatening cytokine release and multi-organ failure in all (n = 6) of the healthy volunteers [6]. TGN1412 is an agonistic anti-CD28 monoclonal antibody that was originally developed for the treatment of B cell chronic lymphocytic leukaemia and rheumatoid arthritis [78]. The starting dose was selected based on the No Observed Adverse Effect Level (NOAEL, see Box B) from a monkey study. Undetected species-differences were at the base of the trial outcome.

Box B **No Observed Adverse Effect Level**

The No Observed Adverse Effect Level, or **NOAEL**, is historically one of the most frequently used strategies to calculate FiH doses [3]. NOAEL refers to the highest tested dose in a relevant animal species that does not elicit a significant increase in observable adverse events as compared to the control group. The NOAEL is converted into a human equivalent dose (HED). A popular method to calculate the HED is via allometric scaling in which scaling of the dose happens in relation to the scaling of a bodily metric (e.g., body weight BW) from animal to human (see inset equation) [5]. There is a whole field of study dedicated to these calculations, which falls beyond the scope of this work.

$$HED = NOAEL * \left(\frac{BW_{animal}}{BW_{human}}\right)^{b}$$

*b* is an allometric exponent used for scaling. After calculation of the HED, usually an additional safety factors is applied to account for any uncertainties.

The use of NOAEL came under scrutiny after the disaster of TeGenero when the HED, even after inclusion of a 160-fold safety factor, elicited severe adverse events in healthy human volunteers. The focus on animal toxicity and lack of pharmacologic context in NOAEL-based dose calculation was criticised [6, 7].

The lethal outcome of the Bial disaster again reinforced the use of alternative methods that focus on human pharmacology instead of on tolerability alone for appropriate dose-exposure-response prediction in order to determine not only the starting dose (MABEL), but also high doses [8, 9].

Due to the learnings from the TeGenero incident, using NOAEL for dose selection for immune-agonists was no longer appropriate. EMEA and FDA released new guidelines, promoting the implementation of an alternative and more holistic dose selection method where all relevant in *vitro* and *in vivo* data needs to be integrated to decide on a safe dose. This method is coined the *Minimally Anticipated Biological Effect Level* (MABEL). The use of MABEL requires a deep understanding of the pharmacology of the target since it can represent any relevant pharmacological marker. Essentially, MABEL is defined, as the exposure required reaching 'minimal' biological effect in a non-clinical study.

The guidelines do not concretely define the term ‘minimal’ nor do they summarise what exactly is considered as ‘biological effect’ [9]. When reviewing the literature, it seems that many investigators to use as MABEL 10-20% of the maximal effect reached for a certain readout in a certain study and, in many cases, the readout of choice is the most sensitive readout, which is the most straightforward to justify [56, 76, 77, 79-81]. The FiH dose is set so that expected human exposure to the drug corresponds to the MABEL. An additional safety factor could be warranted for compounds with a novel or poorly understood mechanism of action or, for instance, when there is uncertainty around the MABEL estimation [9, 56].

A retrospective FDA oncology analysis, reviewing dosing and FiH trial design for 32 antibodies used in immune-oncology, and assessing the utility of animal toxicology studies, has shown that 44% of the FiH doses were at least 2-log units below the dose that could be safely administered to patients [82]. Doses based on animal toxicity were often too high to apply in human.

In another retrospective analysis focusing on CD3-bispecifics, Saber and colleagues concluded that the current MABEL-based methodologies result in doses that are too low to warrant treatment in critically ill patients. Doses calculated from NOAEL and HNSTD in animal studies did retrospectively prove too high in many cases. Dose selection based on 10% or 20% receptor occupancy, as is often the case for immune stimulatory antibodies, proved severely inappropriate for bispecific antibodies. Conversely, doses based on 30% theoretical pharmacological activity seemed to be within safety limits [83].

Since anti-cancer therapies often have a narrow therapeutic index, phase I trials are conducted in cancer patients only [56]. In most of these cases, these patients have exhausted all available treatment options and are turning towards experimental drugs as a last resort. From an ethical point of view, it is unacceptable to treat these patients at doses that are considerably lower than the anticipated pharmacologically active dose [9]. Moreover, starting from a subtherapeutic dose requires many dose-escalation steps to reach clinical efficacy, making the clinical trials more lengthy and costly [84, 85].

Dose-escalation in cancer patients is not limited to the highest dose tested in nonclinical studies and can be continued until dose-limiting toxicities (DLTs) are reached. However, if nonclinical studies showed a steep dose-response curve for a toxicity marker, or failed to identify a toxicity threshold, dose-escalation increments should be reduced. Instead of dose-doublings of half-log increments, fractional increases should be performed [43].

When we consider the current state of knowledge around the class of T-cell redirecting therapies, it becomes apparent that precautions are to be taken when advancing such therapies into clinical trials. The adverse events related to targeted therapeutics are not often caused by off-target toxicities but rather due

to exaggerated pharmacology [55]. The robust integrative analyses applied in FiH dose selection strongly contribute to the relatively safe track record of FIH studies [54].

## 1.5 Nonclinical translatability

Preclinical *in vitro* and *in vivo* assessment is essential to understand better T-cell redirecting therapies, to collect sufficient data to derive a human dose, and to quantify relative patient risks when exposed to the treatments. An important quest is the reliable prediction of cytokine release syndrome in patients. Cytokine release assays are designed to capture the potency and extent of cytokine release induced by a therapy. Despite that these assays are capable of predicting the overall risk in patients, the current pitfall is the lack of absolute translatability, which can be ascribed to the existence of many different assay formats [86] and the considerable donor-to-donor variability [83].

Additionally, animal models that reliably recapitulate CRS are lacking. An FDA oncology analysis reviewed the preclinical and clinical safety profiles of 17 blinded CD3-bispecifics [83]. From those, 10 compounds had cross-reactivity with non-human primates (NHP) for safety assessment. There was however, a discrepancy between the cytokine releases observed in the monkey versus those observed in an *in vitro* assay with NHP or human cells. The authors concluded that animal species overall better tolerated the treatment than patients, and that *in vitro* systems should be considered. This again reinforces the revised EMEA guidelines that emphasize the importance of understanding human pharmacology and the quantification of dose-exposure-response relationships.

The development of physiologically relevant assays is of great importance. The exact developmental landscape of these methods falls beyond the scope of this work, but a relevant part is discussed in [87]. The use of 3-dimensional spheroid cultures opens new doors to studying T-cell-redirecting therapies [88]. These specialized cultures may provide a better understanding of how the immune cells interact with the tumour environment and how tumour accessibility affects the treatment.

It is recommended to make use of a weight-of-evidence approach, integrating *in vitro, ex vivo,* and *in vivo* data as part of the decision-making process. The use of a modelling framework may help to integrate the various sources of data –*in vitro* and *in vivo*- and the current biological knowledge in order to scale it up to, and make predictions about, the human situation. The use of *in vitro* human cell systems or human-derived material could clarify the translation from animal data to human [44]. Moreover, *in vitro* data can be very informative before going into humans. The steepness of the dose-response curves is an example of an interesting metric since risk is a continuous function rather than a discrete (either present or absent) event [48, 56]. This metric can tell us more about the potential dose range and the risks involved by going higher.

Whereas modelling and other quantitative approaches may give guidance to the translational development of a compound, they are ultimately based on prior knowledge and data generated in nonclinical experiments. Any inaccuracies with respect to this information may yield a model that is not predictive. Likewise, if certain variables are ill-defined or yet to be discovered, they cannot be incorporated into a model. To give a related example from the clinical domain, reliable prediction of the extent of cytokine release in patients may not be sufficient to predict the risk for CRS in patients [89, 90]. Other, less overt, variables may not be so easily identified with mechanistic assays such as cytokine release assays or even with animal models. This forms the main topic of one of the projects developed in this work [91].

## 1.6 The role of pharmacometrics in the development of T-cell redirecting therapies

Quantitative approaches have gained a foothold in the drug development space in the last 50 years. Pharmacometrics as a scientific discipline contains many different fields of study that look at drug development in a quantitative fashion with varying degrees of complexity. As was shown in the previous sections, pharmacometrics has the potential to have a huge impact on many parts of the early development process of T-cell redirecting therapies. It can be as simple as establishing a dose-exposure-response relationship for a drug, a linear regression analysis or empirical relationship between variables [92], more elaborate pharmacokinetic/pharmacodynamic models to predict drug exposure and effect in humans, or even full-fledged systems pharmacology models that capture drug-related processes in high detail [62, 67, 93].

Model-informed drug development (MIDD) is becoming more widely accepted by pharmaceutical companies and regulatory bodies. Model-based drug development starts -even before the collection of experimental data- with the design of experiments and the selection of a relevant PK/PD strategy [94]. This is possible thanks to the prospective nature of models and the ability to perform simulations and test hypotheses.

As reviewed by Milton and Horvath, the EMEA guidelines shifted the focus more in favour of risk identification and possible mitigation strategies as opposed to hazard identification, which was the norm before the TeGenero incident [95]. There is a discernible difference between hazard (a qualitative description of the dangers involved with the therapy; e.g., asking “what type of adverse events to we expect?”) and risk (a quantitative measure of the dangers; e.g., asking “what is the likelihood of contracting that adverse event at the anticipated exposure level?”) [47]. A compound with a hazardous profile might have a favourable risk profile as long as systemic exposure is kept low or the compound has a low toxic potential. The complicated and still not fully understood MoA of T-cell redirecting therapies makes them higher risk compounds, even though most hazards may already have been identified. The inclination of risk

to be quantifiable facilitates the use of pharmacometrics approaches. Ideally, pharmacometricians can put a number on the risk an IMP forms to the patient, based on previous experiences and solid understanding of the biology.

In his seminal paper, Sheiner presents the learn-and-confirm paradigm and how it is applied in drug development [96]. Cycles of learning how a drug acts should be followed by cycles of confirming the effective use-case of that drug; first generating a (null) hypothesis followed by an attempt to reject it. He explains that learning cycles are all too often treated as if something needs to be confirmed, and how model-based approaches can help to actually learn from what is known before attempting to confirm anything.

In his paper, Sheiner focuses on the learn-and-confirm cycles encountered in clinical drug development. It can be argued that this paradigm is equally applicable to the nonclinical phase [97, 98]. Nonclinical experiments have the potential to generate a large amount of data that can provide insights into the mechanism-of-action of a drug, implications on the disease, and the best dosing strategies. These insights could be of importance when the drug's clinical viability as a medical product needs to be confirmed, whether it is in an early clinical trial as a proof of concept or in later confirmatory trials [99]. What is needed to propagate these learnings to be of use at later stages is a solid modelling framework.

As outlined in section 1.4.4, investigational medicinal products that seek successful development are required to have all available data integrated in a holistic manner in order to select doses and dosing strategies that are helpful, not detrimental, to the patients. This is especially true for those IMPs that bring along many uncertainties, as is the case for T-cell redirecting therapies. Pharmacometrics and MBDD may be helpful, if not a necessity, to guide these compounds through the drug development process.

The projects outlined in this thesis revolve around the use of pharmacometrics in the early drug development of T-cell redirecting therapies. The first project attempted to describe the pharmacology of a CD3-bispecific antibody in a quantitative manner in order to understand better the influence of drug- and cell-related parameters on its activity. A mechanistic model was developed that displays the use-case of a learn-and-confirm cycle with *in vitro* data. The model succeeded in predicting an experimental outcome based on the target expression level of tumour cells that were targeted with a CD3-bispecific antibody. Moreover, the project exposes and discusses the relationship between T-cell activation and immune synapse formation in a way that has not been presented before. The second project identifies and tackles a recurrent problem with compounds exerting a complex mechanism of action, such as T-cell redirecting therapies. The pharmacology of these drugs triggers many processes that take place on different timescales. This makes it challenging to compare potencies between readouts. This project focused on the development of a novel method of analysing experimental data by integration over time. The generation of time-

independent insights in the pharmacology of these drugs may help to more confidently rank compounds and select safe starting doses in an unbiased manner. The third project reviews factors that may contribute to the development of cytokine release syndrome in cancer patients treated with T-cell redirecting therapies and distinguishes between drug-target-related factors and individual patient risk factors. The root causes of CRS formation in some patients are still enigmatic, but understanding them is very important to ensure patient safety and successful clinical development of the compounds. As an outlook, it is proposed to conduct an exhaustive analysis based on real-world data combined with mechanistic modelling in order to predict individual patient risks and pave the way for precision dosing. These projects have the common goal of providing robust tools and insights that are of use to the model-based drug development of T-cell redirecting therapies.

# 2. Aims of thesis

The objective of this work was to contribute to active areas of pharmacometrics and early drug development of T-cell redirecting therapies, and to identify and address gaps in our knowledge about their pharmacology and safety considerations. Each project looked from a different angle at the development of T-cell redirecting therapies, with a central focus on quantitative approaches. Each project has been published in a peer-reviewed scientific journal.

## 2.1 Project I

It is a widely accepted assumption that the pharmacology of CD3-bispecifics requires the formation of trimeric complexes (the so-called immune synapses) to trigger a response. The formation of these trimeric complexes depends on many different variables, such as binding affinity and antigen expression levels, from which the exact relationships have not been fully elucidated yet. The aim of this project was to better characterize the influence of target expression on the pharmacology of cibisatamab, a CD3-bispecifc antibody that targets carcinoembryonic antigen (CEA). To this end, the project combined an extensive *in vitro* study with a tailored systems pharmacology model in order to capture the *in vitro* pharmacology of cibisatamab on different tumour cell lines in a quantitative manner. The model was to be used to investigate the predictive potential of target expression levels on the pharmacology of CD3-bispecifcs and to establish a better understanding of the link between immune synapse formation, T-cell activation, and tumour cell killing.

## 2.2 Project II

*In vitro* experiments play an important role in the early development of CD3-bispecific antibodies. Due to the involvement of the immune system, the mechanism-of-action of CD3-bispecifics is complex and involves many different processes that occur on different timescales (e.g., target engagement, cytokine release, T-cell activation and proliferation, and tumour cell killing). Despite this complexity, *in vitro* investigations of novel CD3-bispecific antibodies usually limit the recording of data to a single or -at most- two time points. This risks that important insights into the mechanism-of-action are missed and that comparisons between readouts or compounds become irrelevant or biased. The deliverable of this project is to develop tailored and less labour intensive *in vitro* experiments with more frequent time recording and develop a methodology to assess the data in a time-independent manner.

## 2.3 Project III

The promising therapeutic potential of T-cell redirecting therapies comes with a caveat: the risk for severe adverse events. One of the most prominent adverse events exhibited in this class of therapies is cytokine release syndrome (CRS). CRS is a life-threatening adverse event and originates from an uncontrolled release of cytokines by the immune system and the inability of the human body to respond in kind. The objective of this project was to review thoroughly the factors triggering CRS formation. The novelty of this project is to look at both nonclinical and clinical evidence simultaneously, and to consider the role that M&S and mechanistic models may play in the prediction of cytokine release. Briefly, the project attempts to answer the question why some patients develop CRS whereas others do not and why mechanistic models fed with our current biological knowledge may be insufficient to predict CRS risk in each patient. The project emphasizes that there is a distinction between cytokine release and CRS and that it is important to understand why some patients respond differently to cytokine release. In the end, the projected goal is to formulate a solution to the prediction problem through a stratagem of combining mechanistic modelling with a risk-scoring algorithm and to provide insights that are useful to nonclinical investigators and clinicians alike.

# 3. Methods

This section summarises the methodologies that were central to the presented work. The experimental framework used throughout the assays and the theoretical background and rationale of the pharmacometrics approaches are presented here. The peer-reviewed articles for each project within this work summarise the materials and methods in detail and are found in Section 4.

## 3.1 In vitro experimentation

### 3.1.1 Assay set-up

Two-dimensional *in vitro* co-cultures are common practice in nonclinical testing of candidate compounds against cancer [100]. In these assays, various cell types of interest are cultured together in small-volume wells (e.g., 96-well plates with a well volume of 250µL) and incubated with the test agent. For T-cell redirecting therapies, both tumour cells and T cells need to react with each other and are thus co-cultured (Figure 5) [101]. The most important measurements from there T-cell dependent cellular cytotoxicity (TDCC) assays are tumour cell killing, T-cell activation, and cytokine release.

In practice, the start time of an assay corresponds to the time point at which the candidate compound (test agent) is added to the co-culture. Recording of this time is important in order to ensure reliable stopping times when measurements are made. The assay should be repeated at various drug concentrations (including a control group) that span the anticipated sigmoidal dose-response curve (see section 1.4.4). The same setup can be repeated under various experimental conditions (e.g., target expression differences, different drug candidates and affinity variants, etc.).

Recording data at multiple time points enables capturing of the time course of various readouts (see section 2.2). It is advisable to duplicate the number of assay plates depending on the number of time points that need to be measured. Like this, each time a 'fresh' well will be probed. This will prevent any experimental artefacts due to dilution or condensation of the well contents due to previous measurements.

### 3.1.2 Cytometry: FACS versus incuCyte

Measuring tumour cell viability is key to assessing an anti-cancer drug's cytotoxic potential and is a core metric in the large majority of *in vitro* pharmacology studies of these pharmaceuticals. Various methods exist, either a biochemical assay (measuring a soluble marker of tumour cell viability, or killing, such as lactate dehydrogenase (LDH) [102] or Chromium-51 [103] release assays) or a cytometric assay (directly measuring or counting the tumour cells). Biochemical assays are easier to perform. The drawback of these assays is that they provide an indirect measurement; i.e., the number of dead or alive tumour cells needs to be calculated form the biochemical readout.

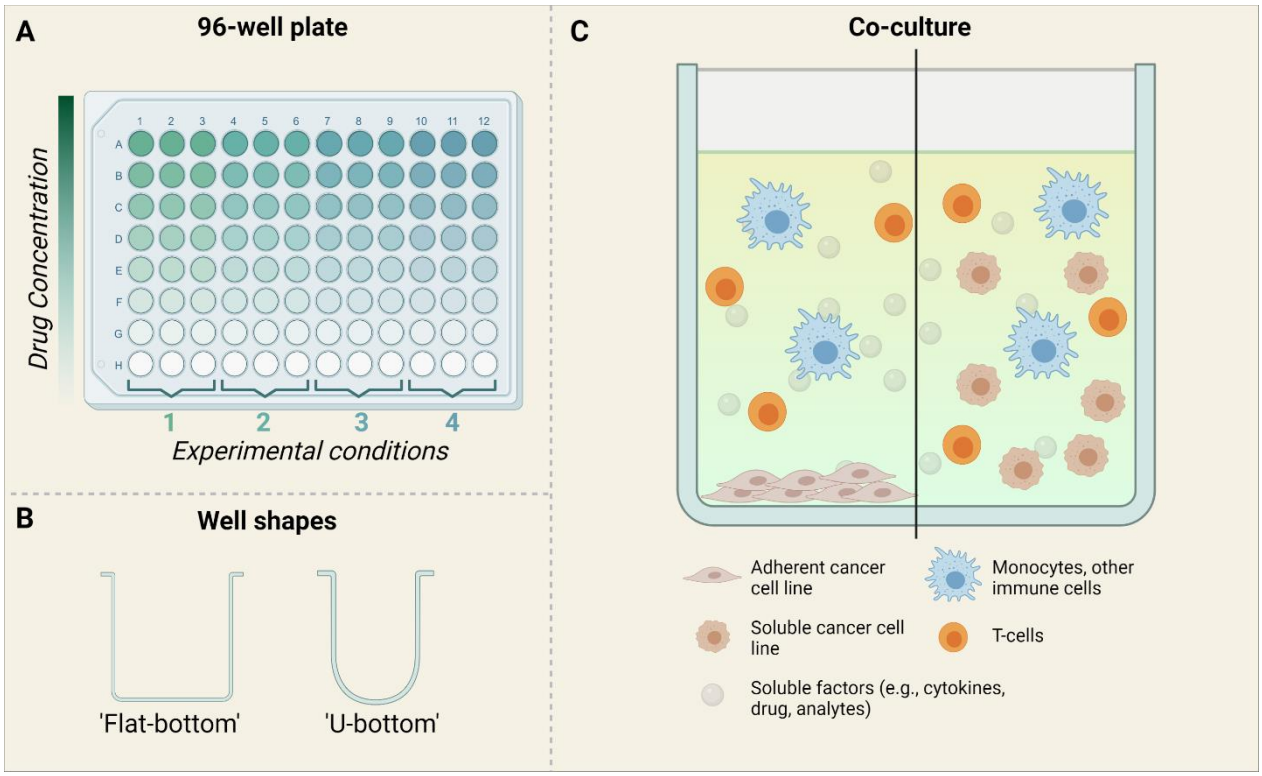


**Figure 5.** The set-up of 2D co-culture experiments is often performed in 96-well plates, which allow for relatively high throughput. **A.** A 96-well plate consists of 8 rows and 12 columns. The exact setup will depend on the specific project requirements. In this work, drug concentrations were titrated from row A (highest concentration) down to row H (control group). Each experimental condition was replicated three times (e.g., columns A-C). This allows four experimental conditions to be tested on a single plate. **B.** The bottom of an individual well can either be flat or round (U-shaped). The choice of well shape depends on the specific experiment. **C.** Contents of a single well under co-culture conditions for testing of T-cell redirecting therapies. The cancer cell line of choice can either be adherent to the well surface (left hand side) or soluble in the medium (right hand side). The cancer cells are co-cultured with human immune cells, which at a minimum contain T-cells and are often including myeloid cells such as monocytes, neutrophils, etc.

Cytometric approaches rely on (semi)direct measurements of the tumour cells, hence providing a more interpretable number of killed tumour cells. The staple of these approaches is Fluorescence-Activated Cell Sorting (FACS) cytometry. FACS allows the multi-parametric analysis of multiple cell types simultaneously and proved to be an indispensable tool in many scientific disciplines, including cancer and immunological research [104]. The principles and methodologies are discussed in [105]. In the case of TDCC assays, at the predetermined time points (see section 3.1.1 above), the wells will be prepared and its cell contents measured with the FACS cytometer. Investigators will often look at the presence of T-cells (CD3 marker), markers of T-cell activation (e.g., CD69, CD25), T-cell exhaustion (e.g., PD-1, TIM-3), intracellular cytokines

(e.g., stores of IL6), and number of viable tumour cells (e.g., through counting the number of cells with the corresponding morphology, or using a live-dead dye) [106].

While FACS technology improved over the years since its inception, more recently researchers have developed alternative approaches. An approach that is gaining widespread adoption is real-time cell monitoring. Various technologies exist, such as impedance-based [107] or image-based [108] real-time cell monitoring. Throughout this work, the image-based technology incuCyte was used and will be discussed further.

An image-based tool such as incuCyte consists of a cell incubator with an integrated fluorescence microscope. This technology has a few prerequisites about the TDCC assay preparation. In order for the microscope to pick up fluorescence, the cells or cell markers need to be fluorescent. This is achieved through cells that have been stably transfected (e.g., nuclear labelling), transiently transfected (dye taken up by cell, but will dissipate over time) or with fluorescent antibodies binding specific cell markers [109, 110].

The proposition of real-time monitoring is not entirely correct since the microscope takes images at a certain time interval (e.g., every two or three hours). Nevertheless, incuCyte takes measurements with a temporal resolution that is manifold higher than those found in classical FACS protocols are. Moreover, since measurements happen automatically, incuCyte-based approaches are less work-intensive since no separate time points need to be sampled and measured by the investigator.

### 3.1.3 Cytokine release assays

Cytokine release forms an integral part of the nonclinical study package of many T-cell redirecting therapies. There are various methods to measure and quantify the concentration of released cytokines within an assay.

The method used throughout this work is the Cytometric Bead Array (CBA) and is based on the FACS principle (see section 3.1.2 above). The basic principles of the CBA are discussed in [111]. Briefly, at the predetermined time point, the assay plate is centrifuged and a small volume of the supernatant is aspirated. This aspirate contains the soluble contents of the assay, including released cytokines. Small microbeads are added to the aspirate. These microbeads are covered in antibodies that are specific for a cytokine (e.g., IL6). The CBA technology allows multiplexing, meaning that multiple cytokines can be detected within a single run simply by adding the corresponding microbeads to the aspirate. After a period of equilibration, fluorophore-labelled antibodies are added that are specific to the cytokines of interest.

A flow cytometer can measure and quantify the signal emitted by the fluorophores that are indirectly bound to the cytokines. Since every cytokine is bound to another kind of fluorophore that is distinct from the others

in their excitation and emission spectra, the cytometer can measure them simultaneously [112]. By the use of a standard curve with cytokines of known concentration, the CBA assay enables the calculation of exact concentrations through interpolation. This is extremely helpful for interpretation of the results, comparison across assays, and for use in modelling efforts.

## 3.2 Mechanism-based model development

The following section highlights the key components of the mechanistic model developed in Project 1 [113]. The model structure, equations and assumptions are presented here. These model components originate from seminal papers that were unrelated to the modelling of the pharmacology of CD3-bispecifics, but they have proven to be of great use in other models, including a few on CD3-bispecifics [68, 79, 114, 115]. The model consists of three main components of which the first one is the formation of trimeric complexes between the drug, CD3 and the tumour antigen [116]. This is modelled assuming independent interactions between these factors and based on their initial concentrations. Next, trimeric complex formation is assumed to trigger the activation of cytotoxic T-cells, the kinetics of which were experimentally determined and modelled using a transit compartment model. Lastly, activated T-cells induce lysis of the tumour cells. The growth and T-cell mediated killing of tumour cells was captured experimentally and modelled using a logistic growth term and a sigmoidal kill term. Each model component is described in detail below.

### 3.2.1 Trimeric complex formation

The formation of trimeric complexes relies on the binding between CD3, tumour antigen, and the CD3-bispecific antibody. These binding events can be modelled in a sequential manner with a system of ordinary differential equations (ODEs), see Equations 1-4. Binding events between multiple binding partners have been modelled before, for instance to model the interaction between GTP-binding proteins [117]. A system of four coupled ODEs is the most commonly used method to model trimeric complex formation [66, 68, 74, 114, 115, 118]. The model assumes independent binding events between the different binding partners. This signifies that the CD3-bispecific can either bind CD3 or tumour antigen first, without interference of the other binding partner. The dimer that follows from this interaction is then capable of binding the remaining binding partner. There is no direct interaction between CD3 and the tumour antigen.

As a generic example, the sequential binding between three entities can be considered with the following state variables: A, B, and C are respectively the drug of interest, free antigen B, and free antigen C. AB and AC are the dimers between drug A and antigen B or C, respectively. ABC is the trimeric complex (Figure 6).

$$\frac{dA}{dt} = -kon_B * B * A - kon_C * C * A + koff_B * AB + koff_C * AC \quad \text{(Eq. 1)}$$

$$\frac{dAB}{dt} = kon_B * B * A - koff_B * AB + koff_C * ABC - kon_C * C * AB \quad \text{(Eq. 2)}$$

$$\frac{dAC}{dt} = kon_C * C * A - koff_C * AC + koff_B * ABC - kon_B * B * AC \quad \text{(Eq. 3)}$$

$$\frac{dABC}{dt} = kon_B * AC * B + kon_C * AB * C - (koff_B + koff_C) * ABC \quad \text{(Eq. 4)}$$

With the following initial conditions.

$$A_{(t=0)} = Drug\ Concentration\ \left[\frac{nanomole}{liter}\right]$$

$$B_{(t=0)}\ \&\ C_{(t=0)} = \frac{target\ density * cell\ concentration}{10^{-9} * N_a}\ \left[\frac{nanomole}{liter}\right]$$

$$\mathrm{AB}_{(t=0)} = \mathrm{AC}_{(t=0)} = \mathrm{ABC}_{(t=0)} = 0\ \left[\frac{nanomole}{liter}\right]$$

$N_a$ is the Avogadro constant. The concentration of free antigen is captured in the following arithmetic function:

$$B = B_{(t=0)} - AB - ABC \quad \text{(Eq. 5)}$$

$$C = C_{(t=0)} - AC - ABC \quad \text{(Eq. 6)}$$

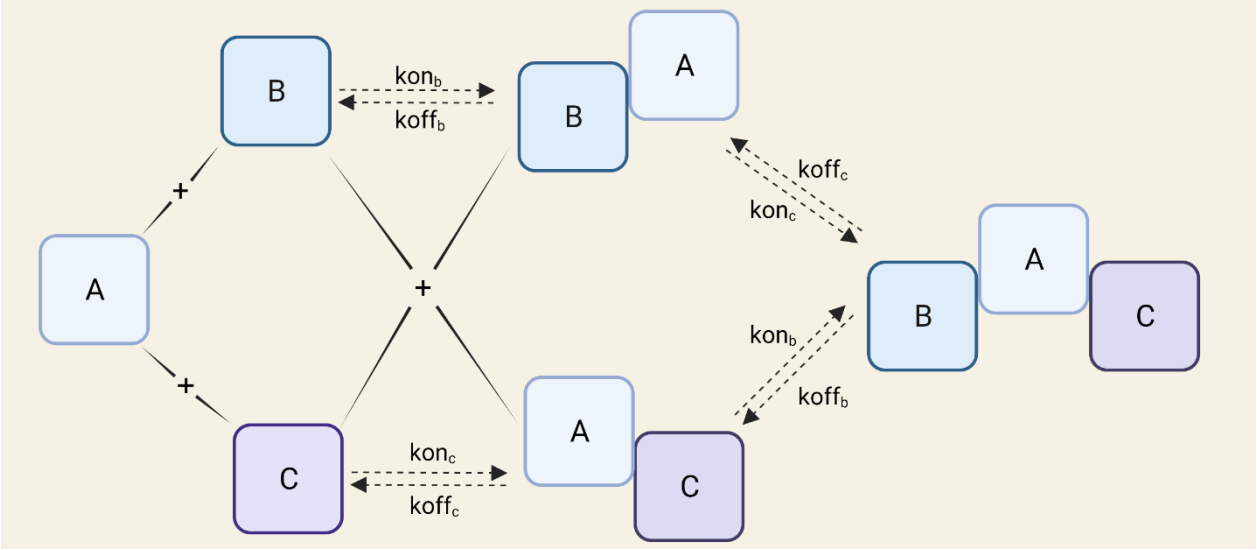


*Figure 6. Schematic representation of the immune synapse model as described in equations 1-4. Trimeric complexes are formed between three separate entities (A, B, C) of which A is considered the CD3-bispecific antibody, and B and C are the tumour and CD3 antigens. Sequential binding events will lead to the formation of dimers between A and either B (AB) or C (AC). The dimers can bind with the remaining antigen through the free binding arm on A. The reactions are governed by second-order association rates and first-order dissociation rates.*

### 3.2.2 Signal transduction

The formation of trimeric complexes will trigger the activation of T-cells, but T-cell activation only occurs at later time points. In order to capture the delay between trimeric complex formation and T-cell activation, a signal transduction model was implemented [119].

Lobo and Balthasar presented the original signal transduction model to capture the delayed pharmacodynamic effect of a chemotherapeutic agent on a culture of tumour cells [119]. Existing cell phase-specific and nonspecific models could not capture this delay. Whereas its original use was to capture delayed cytotoxic effects, the model is also suitable to describe delayed T-cell activation (Figure 7).

The signal transduction is triggered by a stimulation cue (Equation 7), which will depend on a certain biological function. In the case of Project 1, this biological function is a sigmoidal model in function of the number of trimeric complexes per cell [113]. The Potency term defines the number of trimeric complexes per cell that induces half-maximal T-cell activation. $E_{max}$ is the maximal extent of T-cell activation. Delta ($\delta$) is a new term introduced in Project 1 that accounts for differences in target expression density between the cell line that is being tested and the reference cell line, which was used to estimate the model parameters. This parameter was included under the assumption that the potency of the drug does not change between cell systems, but the extent of T-cell activation can change under the influence of varying target expression densities. There are three transit compartments ($delay_1$, $delay_2$, $delay_3$) through which the signal needs to be transduced before it can exert an effect on T-cell activation (Equations 8-10). The transit rate is governed by $3/\tau$ with $\tau$ (tau) the transit time. In the original paper from Lobo and Balthasar, the transit rate was taken as $1/\tau$, whereas Project 1 resorted to the use of $3/\tau$ as was done previously [114, 120-122]. However, this choice was arbitrary and this does not change the model structure nor performance.

$$Stimulation = \frac{E_{max} * \delta * Trimeric\ Complex_{per\ cell}}{Potency + Trimeric\ Complex_{per\ cell}} \quad \text{(Eq. 7)}$$

$$\frac{ddelay1}{dt} = \frac{3}{\tau}(Stimulation - delay1) \quad \text{(Eq. 8)}$$

$$\frac{ddelay2}{dt} = \frac{3}{\tau}(delay1 - delay2) \quad \text{(Eq. 9)}$$

$$\frac{ddelay3}{dt} = \frac{3}{\tau}(delay2 - delay3) \quad \text{(Eq. 10)}$$

$$\text{delay1}_{(t=0)} = \text{delay2}_{(t=0)} = \text{delay3}_{(t=0)} = 0$$

$delay_3$ triggers the activation of T-cells by increasing in input rate (Equation 11). For maintaining mass-balance, there is an outflow of activated T-cells, governed by the rate $k_{out}$

$$\frac{dTcell_{activated}}{dt} = k_{in} * (1 + delay3) * F_b - k_{out} * Tcell_{activated} \quad \text{(Eq. 11)}$$

$$Tcell_{activated_{(t=0)}} = baseline$$

The baseline concentration of activated T-cells under steady-state conditions adheres to the following relationship:

$$Baseline = \frac{kin}{kout} \quad \text{(Eq. 12)}$$

The net inflow of activated T-cells is not assumed to continue indefinitely and, over time, activated T-cells may lose their activation markers, get exhausted or die off. The exact mechanism for this purpose is of low importance, but it is crucial to include a model component that captures this type of behaviour

Friberg and colleagues developed a model on myelosuppression after chemotherapy, which involves a similar delayed signal transduction as the one presented by Lobo and Balthasar. In their model, chemotherapeutic regimens will affect the proliferation of certain sensitive subsets of hematopoietic cells [123]. This will then propagate through multiple maturation steps before its impact can be seen in the pool of circulating (mature) blood cells. In addition, this model includes a novel feedback loop that ensures homeostasis in the pool of hematopoietic cells and circulating blood cells (Equations 13-17).

This feedback loop was included in Project 1 (term $F_b$ in equation 11) to capture the reduced rate of T-cell activation when the pool of activated T-cells is already large. $F_b$ is the ratio of baseline activated T-cells over activated T-cells that went through the transduction process. The transit compartments are now called $k_1$, $k_2$, and $k_3$ to make the distinction from equations 8-10.

$$\frac{dk1}{dt} = k_{out} * (Tcell_{activated} - Baseline) - k_{out} * k1 \quad \text{(Eq. 13)}$$

$$\frac{dk2}{dt} = k_{out} * k1 - k_{out} * k2 \quad \text{(Eq. 14)}$$

$$\frac{dk3}{dt} = k_{out} * k2 - k_{out} * k3 \quad \text{(Eq. 15)}$$

$$k1_{(t=0)} = k2_{(t=0)} = k3_{(t=0)} = 0$$

$$\frac{dFeedback}{dt} = k_{out} * k3 - k_{out} * (Feedback - Baseline) \quad \text{(Eq. 16)}$$

$$Feedback_{(t=0)} = Baseline$$

$$F_b = \frac{Baseline}{Feedback} \quad \text{(Eq. 17)}$$

### 3.2.3 Tumour cell kinetics

Tumour cells are an active entity and will expand over time and various tumour growth models exist to capture their behaviour (Figure 8). The growth rate of a specific population of tumour cells can be estimated based on their growth curves. Under physiological conditions, tumour cells cannot grow indefinitely; their growth is restrained due to a lack of space and a limited supply of resources, as is the case for *in vitro* cell culture assays. At higher tumour cell concentrations, the rate of growth will reduce and the growth curve will flatten out at the maximal concentration of tumour cells that the system can support (also called the carrying capacity). Therefore, it was chosen to use a logistic growth model with $k_g$ the exponential growth rate and K the carrying capacity (Equation 18, first term).

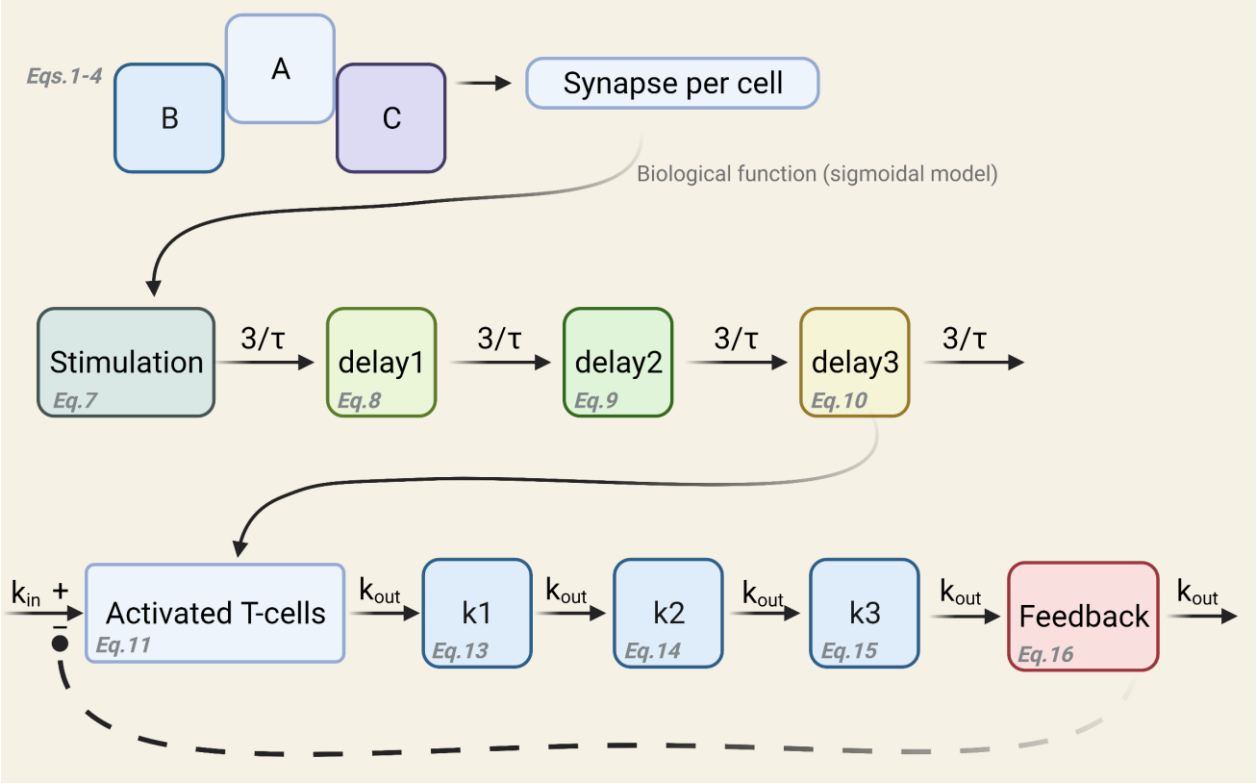


***Figure 7.*** *Schematic representation of the mechanisms involved in T-cell activation as described in equations 5-13. The formation of trimeric complexes (Eqs.1-4) leads to a specific number of immune synapses per tumour cell, which will govern T-cell activation through a signal transduction cascade (Eqs.7-10). The signal transduction leads to a slower build-up of T-cell activation by providing a delayed boost in the inflow of activated T-cells (Eq.11). Accumulation of activated T-cells will dampen over time the activation of other T-cells. This dampening over time is captured with another signal transduction cascade with feedback loop (Eqs.13-17).*

$$\frac{dTumour}{dt} = growth_{rate} * Tumour\left(1 - \frac{Tumour}{carryingCapacity}\right) - Tumour * \text{kill}_{rate} \quad \text{(Eq. 18)}$$

$$Tumor_{(t=0)} = initial\ concentration\ of\ tumour\ cells$$

Upon treatment, the concentration of tumour cells will go down due to specific killing of the tumour cells. The simplest way to capture this is with a first-order kill rate. The killing will thus depend on the kill rate and the remaining concentration of tumour cells (Equation 18, last term).

In Project 1, the tumour kill rate is a function of the amount of activated cytotoxic T-cells and follows a sigmoidal relationship (Equation 19). Since there is an assumed baseline activity of T-cells, tumour killing is only elicited (i.e., $\text{kill}_{rate}$ > 0) when the concentration of activated T-cells exceeds baseline levels. Furthermore, the steepness of the kill curve is under the influence of a hill-factor (h).

$$kill_{rate} = \frac{Max\_kill_{rate} * (Tcell_{activated} - baseline)^h}{Potency^h + (Tcell_{activated} - baseline)^h} \quad \text{(Eq. 19)}$$

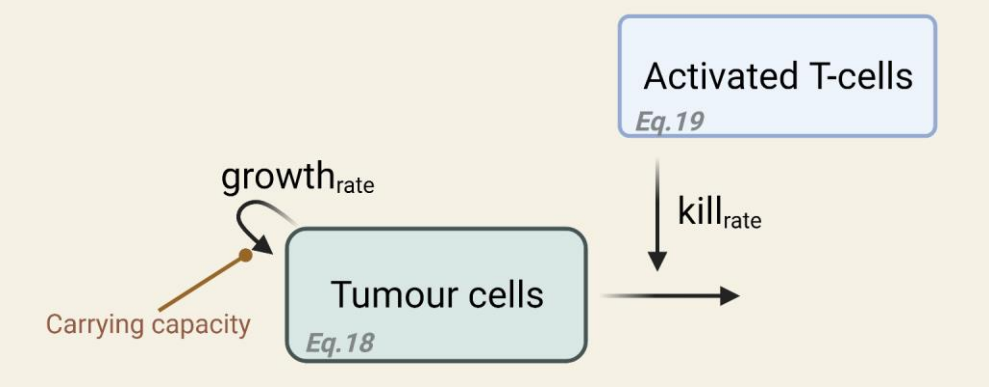


***Figure 8.*** *Schematic representation of tumour growth kinetics and the effect of T-cell activation on specific tumour cell killing, as described in equations 18-19. Tumour cells grow with a specific growth rate until a maximal density that supports cell sustenance, the carrying capacity. Considerable killing of tumour cells is achieved through large numbers of activated T-cells. The killing kinetics follow a sigmoidal function (Eq.19).*

### 3.2.4 Modelling strategy

The structural model was developed using a Non-Linear Mixed Effects (NLME) approach in order to capture both structural parameter estimates and variability between experiments. NLME modelling is an advanced type of population modelling and was described by Sheiner in the 1970s [124, 125]. NMLE models are mainly employed to capture inter-individual (i.e., between-subject) variability in clinical trials as is extremely useful to quantify sources of variability. NLME models are equally useful in cases of nonclinical experimental data, where variability between assays and replicates can be quantified.

NLME models break down into two main components: fixed and random effects. This lends NLME its name of being a model of mixed effects. The fixed effects describe the parameters that describe the whole study

population: the population parameters (designated THETA, θ). THETA describes the typical parameter value in the population and is related to the structural model. It is more than likely that the fixed effects alone cannot well describe the data from each individual since each individual will be different to some extent. Modellers will try to explain this variability between individuals through covariates such as body weight or age in patients, or cell culture conditions in *in vitro* systems. However, even after accounting for covariate effects, it is still probable that there is variability that remains unexplained and cannot be captured with the fixed effects model. Even though it remains unexplained, the NMLE method allows to quantify this variability through random effects [124]. Random effects are parameters related to the statistical model and represent the distribution of all individual parameters.

NLME models follow the principle of nested hierarchy in the random effects. This means that there are multiple sources of random (i.e., unexplained) variability that can be identified. At a minimum, the random variability consists of inter-individual variability (IIV) and residual variability (RV) [124]. Another frequently used random effect is inter-occasion variability (IOV) that deals with variability within an individual that was studied at separate occasions [126]. IOV played no part in this work and will not be considered further.

IIV quantifies the extent to which the individual parameters differ from the population parameters and is referred to as ETA (η). ETA is in many cases assumed to follow a normal distribution centred on zero with standard deviation OMEGA (ω) (Equation 20). OMEGA is therefore useful to summarise the IIV for a parameter.

$$\eta_i \sim N(0, \omega^2) \qquad \text{(Eq. 20)}$$

With i standing for the i-th individual in the population. Individuals each have their own specific value of ETA for a model parameter, with each ETA sampled from the same distribution.

The actual individual parameter value can be described in terms of the population parameter THETA and the individual ETA. The most common method to describe the individual parameter in these terms is with an exponential distribution (Equation 21). Since many PK/PD parameters are right-skewed, they are log-normally distributed. When log-transforming the parameters, the IIV becomes additive to the population parameters (Equation 22), i.e., there is a constant variance around the log-transformed population parameter.

$$\theta_i = \theta_{pop} * e^{\eta_i} \qquad \text{(Eq. 21)}$$

$$\ln(\theta_i) = \ln(\theta_{pop}) + \eta_i \qquad \text{(Eq. 22)}$$

With $\theta_i$ the individual parameter and $\theta_{pop}$ the population parameter.

Similar to IIV models, the structure of RV models can take different shapes and the modeller needs to choose the error model that best describes the noise around the data (such as additive, proportional, or exponential error models).

The purpose of fitting a model to a set of data is to find model parameter values that best describe the data. That is, we want to maximize the likelihood of finding back our data given the model parameters (Equation 23).

$$\arg\max(L(y|\theta)) \qquad \text{(Eq. 23)}$$

The maximum likelihood estimation (MLE) will determine the vector of parameters θ so that the likelihood of the observed data becomes maximal, i.e., its derivative becomes zero (Equation 24).

$$L'(y|\theta) = \frac{d\,L(y|\theta)}{d\theta} = 0 \qquad \text{(Eq. 24)}$$

It is unlikely that an analytical solution to the MLE problem is available for nonlinear systems such as NLME. The solution will need to be approximated numerically. In case of NMLE models, the MLE needs to consider both fixed (θ) and random (η, ε) effects.

The obtained likelihood feeds into an equation to calculate an objective function value (OFV), which is used to assess model performance. The OFV is often taken as minus two times the logarithm of the likelihood (-2*LogL) [127]. When the likelihood increases, the OFV decreases. The key drawback of the classical OFV method in model comparison is the difficulty handling complex models with many parameters. Increasingly complex models may fit the data better, but potentially at the cost of less generalizability. Alternative OFV have been developed to deal with increasing model complexity, such as the Akaike Information Criterion (AIC), which has been used in this work [128] (Equation 25).

$$AIC = -2 * Log(Likelihood) + 2 * n_{parameters} \qquad \text{(Eq. 25)}$$

A penalty factor is added to the objective function so that highly parametrized models do not necessarily improve the OFV. A model structure that reduces the AIC with more than 2 points is considered superior to the previous model structure [127]. It is however important to realise that such objective functions serve as a tool in model assessment and that decision making should not be based solely on their value [128].

### 3.2.5 Monte Carlo simulations

The Monte Carlo (MC) simulation is a mathematical method to capture variability or uncertainty in simulations. The method relies on random sampling from a probability distribution and is of great use in many engineering disciplines and other branches that rely on uncertainty in data. By leveraging from a probability distribution, the Monte Carlo method can provide a degree of randomness to an otherwise deterministic simulation. This is important to capture potential scenarios that deviate from the 'expected' outcome, especially when going to the extremes.

In context on NLME models, the results will consist of fixed (i.e., deterministic) and random effects. As described in section 3.2.4, the estimated population parameters ($\theta_i$) capture the whole population whereas the random effects ($\eta_i$; as implied by the name) provide sufficient randomness around the population parameter in order to capture the unexplained variability exerted by the study population. The random sampling from the probability distribution of the random effects ($\eta \sim N(0, \omega^2)$) can serve as a basis to run an MC simulation and capture the level of uncertainty we expect to see in a simulation.

To achieve this, the MC method samples the random effect from the i-th population parameter ($\theta_i$), $\eta_{i,j}$, from its normal distribution with mean zero and standard deviation ω.

$$\eta_{i,s} = N(0, \omega^2) \qquad s \in [1, T] \qquad \text{(Eq. 26)}$$

$$\theta_{i,s} = \theta_i * \exp(\eta_{i,j}) \qquad \text{(Eq. 27)}$$

With T being the total number samples taken by the MC method. After sampling the random effects (Equation 26) and calculating the individual parameters (Equation 27), the MC method simulates the model with a total of T sets of individual parameters.

These simulations can be visualized and provide an idea about the uncertainty of the parameters. Overlaying a dataset with the model prediction and the 5$^{th}$ and 95$^{th}$ percentiles of the MC simulation can serve as a good basis for model validation.

## 3.3 Time-independent analysis

### 3.3.1 NCA: AUCE calculation

As implied by its name, the area-under-the-curve (AUC) is the calculated surface area underneath the curve of interest. Non-compartmental analysis (NCA) often relies on AUC as a powerful descriptor of the pharmacokinetics of a drug [129].

In addition, AUC does have a place in pharmacodynamics to capture important properties of a drug. For instance, investigators used AUC values to compare various antimalarial drugs and to determine which drug achieved the best protection against anaemic events in infected children [130]. The AUCs of pharmacodynamic –effect– curves (also called AUCEs) allow the interpretation of a readout without the need to consider any time-dependencies.

Calculation of the AUC(E) requires integration of the curve of interest over time (Equation 28). The trapezoidal rule is a numerical integration method that provides a good approximation of this integral and is usually applied in PK/PD analyses (Equation 29) [131].

$$AUC = \int_{t_{first}}^{t_{last}} f(x)dx \qquad \text{(Eq. 28)}$$

$$AUC = \sum_{t_i}^{N} \frac{f(t_{i-1})+f(t_i)}{2} * (t_i - t_{i-1}) \qquad \text{(Eq. 29)}$$

Equation 29 describes the linear trapezoidal rule. Others such as the logarithmic trapezoidal rule exist and are of importance in non-compartmental analyses [131]. These fall outside the scope of this work.

### 3.3.2 Estimation of time-independent potency

Calculation of AUCE values provides a single value for each tested drug concentration. This is a time-independent metric of drug effect at a specific drug concentration. In order to generate meaningful AUCE values, sufficient time points should be captured in the experiments. At least three time points are required to perform an adequate assessment of the time course of a drug.

Investigators can use AUCE values in identical fashion as dose-response data generated from single-time point analyses. This means that pharmacodynamic models such as a sigmoidal relationship can be fit to dose-AUCE curves (Equation 30).

$$AUCE = AUCE_0 + \frac{E_{max} * Drug}{EC_{50} + Drug} \qquad \text{(Eq. 30)}$$

With $AUCE_0$ the AUCE at baseline, $E_{max}$ the maximal effect, *Drug* the drug concentration, and $EC_{50}$ the drug concentration at which half-maximal effect is achieved. The drug's potency, $EC_{50}$, is now a time-independent metric.

### 3.3.3 Threshold concentrations

Not every biological process or dose-response relationship follows a sigmoidal model. This deviation may have a biological origin (e.g., zero-order reactions, bell-shaped dose-response curves). More probable, however, is a suboptimal experimental design that fails to capture the full range of dose responses from no

effect up to maximal effect. In such instances, it may be challenging to fit a model from the sigmoid class of functions to the data and, in turn, reliably estimate drug potencies.

For example, if the dose-range does not capture the maximal drug effect ($E_{max}$), both $E_{max}$ and $EC_{50}$ may become unidentifiable. In these cases, alternative models such as a threshold model may provide metrics that summarize pharmacological activity. A threshold model enables the estimation of the threshold drug concentration that triggers the initiation of pharmacological activity [132]. This can be a surrogate metric when no sigmoidal relationship can be determined. Equation 31 is fit to the AUCE data in order to estimate the threshold concentration.

$$AUCE = AUCE_0 + S * (Drug - Drug_{threshold}) * P^+ \quad \text{(Eq. 31)}$$

Where $Drug_{threshold}$ is the threshold drug concentration to elicit a pharmacological effect, S is the slope of increasing pharmacological activity with increasing drug concentrations over the threshold concentration, and $P^+$ is a derived variable. A derived variable will change value based on certain conditions from within the equation:

$$\begin{cases} P^+ = 0 \; if \; Drug < Drug_{threshold} \\ P^+ = 1 \; if \; Drug \geq Drug_{threshold} \end{cases}$$

This is important to prevent a negative pharmacological effect when the drug concentration is still inferior to the threshold concentration.

# 4. Results

## 4.1 Project I: Predicting tumour killing and T-cell activation by T-Cell Bispecific antibodies as a function of target expression: combining in vitro experiments with systems modelling.

Van De Vyver AJ, Weinzierl T, Eigenmann MJ, Frances N, Herter S, Buser RB, et al. Predicting tumor killing and T-cell activation by T-Cell Bispecific antibodies as a function of target expression: combining in vitro experiments with systems modeling. Molecular Cancer Therapeutics. 2020:molcanther.0269.2020. doi: 10.1158/1535-7163.MCT-20-0269.

## 4.2 Project II: A novel approach for quantifying the pharmacological activity of T-cell engagers utilizing in vitro time-course experiments and streamlined data analysis

Van De Vyver A, Eigenmann M, Ovacik M, Pohl C, Herter S, Weinzierl T, et al. A Novel Approach for Quantifying the Pharmacological Activity of T-Cell Engagers Utilizing In Vitro Time Course Experiments and Streamlined Data Analysis. The AAPS journal. 2021;24(1):7. doi: 10.1208/s12248-021-00637-2.

## 4.3 Project III: Cytokine release syndrome by T-cell-redirecting therapies: can we predict and modulate patient risk?

Van De Vyver AJ, Marrer-Berger E, Wang K, Lehr T, Walz A-C. Cytokine release syndrome by T-cell-redirecting therapies: can we predict and modulate patient risk? Clinical Cancer Research. 2021:clincanres.0470.2021. doi: 10.1158/1078-0432.ccr-21-0470.

# 5. Discussion

Drug development is a long and complicated process with an overall low probability of success. In a Nature editorial from 2011, the editors reviewed attrition rates of up to 95% of the anti-cancer drugs in preclinical development [133]. They pointed out that suboptimal preclinical strategies are an important contributor to this attrition at later stages of drug development. Since then, the situation has improved and the pharmaceutical industry may have averted a ‘productivity crisis’ [134]. Nevertheless, challenges remain, with strict regulatory requirements, complex mechanisms of action, concerns about nonclinical translatability, and fragile patient populations. For a nascent class of treatments such as T-cell redirecting therapies, a well thought-out development strategy and the leveraging of state-of-the-art methodologies are therefore all the more important.

One aspect that underwent big changes down the line is the role of modelling and simulation in drug development. Back in 2004, the FDA proposed the use of Model-Based Drug Development in order to improve pharmaceutical productivity [135]. In recent times, modelling and simulation plays a critical role in the development of some drugs, either to design or even replace a clinical trial, or to improve their

probability of success [136]. The next few paragraphs will summarise the background and key results from each project, and paint a wider picture of their applicability.

Developing a model that can serve as an exploratory tool in the early development of CD3-bispecific antibodies formed the rationale for the first project in this work. The link between target expression, target binding, immune synapse formation, and effect on tumour killing was not well understood. An extensive *in vitro* data set combined with a tailored mechanistic model allowed us to capture the pharmacological activity of cibisatamab. Moreover, the model was predictive for another experiment with a tumour cell line that exhibited a much lower target expression level, showing that cibisatamab only induced minimal cell killing of cells with low target levels. The model was also predictive for an unrelated experiment that tested cibisatamab against more than 100 different cell lines with varying target expression levels. The data showed that cibisatamab triggers tumour cell killing when the tumour cells express more than 10'000 target molecules on their cell surface. The model correctly predicted this expression threshold. The development of this model followed the learn-and-confirm paradigm. The learning phase comprised the fitting of the model, its performance was then assessed with the prediction in another cell line (confirming). These findings were then used to further optimise the model (learning) until a final model was obtained. This model was then used for the prediction of pharmacology in a large and unrelated dataset (confirming), leading to satisfactory results.

An important attribute of models is the possibility to simulate. Through simulations, one can visualise alternative scenarios or test hypotheses. The mechanistic model presented in project 1 breaks down in three main components: synapse formation, T-cell activation, and tumour cell killing. The inclusion of activated T-cells (i.e., $CD8^{+}CD25^{+}$ T-cells) as a mechanistic component backed-up by data and linked to tumour cell killing was a novelty presented in this model.

For other purposes, we can zoom in on individual model parts to understand better their behaviour. As shown in the peer-reviewed article (see section 4.1), the model predicts a bell-shaped relationship when plotting synapse number in function of drug concentration. This prediction is not backed-up by data, since methods to visualise and quantify synapse formation are still lacking (although this may change in the future [137, 138], and a non-CD3 bispecific construct did exhibit bell-shaped binding behaviour [139]). The assumption of the bell-shaped relationship is based on stoichiometric considerations of a binding event between three entities (i.e., between the bispecific antibody, tumour target, and CD3) and is currently the most widely applied assumption in modelling efforts around CD3-bispecifics [66, 68, 79, 114, 140]. Zooming in on the next step in the model, plotting T-cell activation in function of the number of synapses per cell shows a peculiar characteristic of the model. Namely, two distinct processes drive T-cell activation. Firstly,

T-cell activation follows a sigmoidal relationship in function of immune synapses formed per tumour cell. Secondly, the target expression density on tumour cells governs the amplitude of T-cell activation. To achieve this, the model included an adaptive 'fudge factor' in the sigmoidal model. If the cell line of interest expresses higher levels of target than the cell line on which the model was built, then there would a larger than proportional increase in T-cell activation. Alternatively, a cell line with a lower expression level would invoke a less than proportional increase in amplitude of T-cell activation. This fudge factor is not found in similar models from literature and was a novelty introduced in this model.

What is interesting to this, however, is that this behaviour can be visualised by plotting T-cell activation in function of synapse formation. Simulations from different cell lines would not overlap and the data would agree with the simulations. The last step of this exercise is plotting tumour killing in function of T-cell activation, which shows that the model perfectly captures the relationship between activated T-cells and tumour cell killing. This three-pronged approach, although it does not add any new data to what was shown before during model prediction, nevertheless manages to put the insights behind the mechanism-of-action and the model assumptions into a new light.

In order to translate this model to the human situation, it should be integrated with a PK model to predict the local drug concentration at the site of action. Moreover, the local tumour and T-cell concentrations are important input parameters. As this model has been developed on *in vitro* data of a single CD3-bispecific antibody, cibisatamab, the first step would be to apply this model to other compounds and investigate its performance. In any case, the model considers the most important parts of CD3-bispecific pharmacology and forms a good basis for further model development and model translation. In its current form, the model is perfectly suited to explore the impact on pharmacology by different expression levels and binding affinities.

Modelling and simulation is playing an increasingly important role in nonclinical research and it forms an important tool for assay design, compound selection, and simply for exploratory analysis. Where robust preclinical research really begins, however, is with the collection of qualitative and meaningful data. Two-dimensional *in vitro* assays are –besides animal testing- probably the most used experimental set-up in preclinical drug research. Back in 1906, Ross G. Harrison published the first experiment with a cell culture when he studied nerve growth in the field of neuro-embryology [141]. The cell culture assays used today benefit from a century's worth of experience and technological advancements. It would be rather unfair to make any technical comparisons between the cell culture experiments performed in this work and those from Harrison. However, it is worthwhile to draw some parallels on how the measurements are being made. In Harrison's experiment, he performed serial sampling and documented the daily growth of some nerve

and brain structures for multiple days. Additionally, he documented the almost real-time lengthening of a nerve fibre over a period of 25 to 50 minutes. It is clear that, although Harrison did not plan to perform any sort of modelling on the data (the first PubMed entry on modelling and simulation was published in 1959 [142]), he captured time course data in detail. Nowadays, cell culture assays are a cornerstone of the preclinical research in immune-oncology and are key to gain information about cytotoxicity, T-cell behaviour, and cytokine release. What is usually the case, however, is that these assays are read out at one or perhaps two time points (e.g., 24h, 48h) and this data is then propagated in the rest of the preclinical development of that drug. It seems like current investigators generate data with less temporal resolution from cell culture assays than Harrison did with an embryo in a plate in the early 1900s.

Why this matters is the following. Immuno-oncology drugs –and thus T-cell redirecting therapies- function with a complex mechanism-of-action that involves many biological actors, including various T-cell subsets, tumour cells, multiple families of cytokines, etc. Many of those function on different timescales. For instance, the release of Interleukin-2 (IL2) usually occurs early on in the assay. IL2 binds to CD25 (an IL2-receptor) on T-cells, is taken up by the T-cell, induces T-cell activation, and prompts an increase in the expression of additional CD25 [65]. Due to this cycle, IL2 levels may peak early on whereas CD25 expression is induced at a later time point.

When a single measurement is taken from an *in vitro* assay, this is effectively a 'snapshot' of the biology of the system and the pharmacology of the drug. To continue the narrative of the IL2-CD25 cycle, depending of the time point of choice, the data will either show a high level of IL2 in the assay (in case of an early time point) or a high number of CD25-positive T-cells (in case of a later time point) but not both.

Besides differences in amplitude, the potency of the drug on a certain readout may also shift from one time point to the other as was shown in the peer-reviewed article (see section 4.2). This may have considerable implications on the future development of that drug and even on its probability of success. The derived drug potencies are used for ranking candidate compounds or for calculation of a FiH dose. Considering that the apparent potency of a drug can change if a snapshot analysis is done, time point selection may have a direct impact on the dose administered to patients (see section 1.4.4 for more information about dose selection strategies).

The new approach developed in Project 2 proposes the collection of data at multiple time points for each readout, hence providing a clearer image about the kinetics of the biological processes. To facilitate comparison of potencies and remove the bias when it comes to selecting a time point, project 2 proposes the use of a time-independent analysis. This is achieved through integration of the dose-response curves

over time, thereby generating an AUCE value for each tested drug concentration. These AUCE values are used in the same manner as actual dose-response data to calculate the potency: a time-independent potency.

This time-independent potency, which has not been subjected to any time point selection bias, combined with knowledge on the readout's amplitude changes over time, may provide a good basis for MABEL dose selection. Moreover, there is an increased appeal to use the most relevant rather than the most sensitive assay to calculate the MABEL dose [143]. The time-independent analysis may be an excellent tool to derive the most relevant MABEL since it takes into account kinetic differences over time for each readout in both their potency and amplitude. This richness of information may enable investigators to make informed decisions on the relevance of certain readouts and influence dose selection. In the peer-reviewed manuscript, a retrospective calculation of the MABEL dose based on a time-independent assay for cibisatamab resulted in a higher dose than the original. Rather than focusing on the most sensitive assay (tumour cell killing), the approach took interleukin-6 (IL6) release (an important safety marker) as the most relevant readout. By integrating knowledge on efficacy (tumour killing potency) and the upper-limit of safety (based on amplitude and potency of IL6 release), an informed decision on a relevant dose could be made.

Having a closer look at the guidelines for Nonclinical Evaluation for Anticancer Pharmaceuticals, it appears warranted to modify existing nonclinical protocols to less standard procedures in order to study novel properties in the class of pharmaceuticals [43]. The time-independent analysis of nonclinical data proposed in this work is indeed a diversion from classical testing, but may be warranted and justified given the complex and pleiotropic mechanism-of-action of T-cell redirecting therapies.

Even though clinical trials to study T-cell redirecting therapies have proven to be generally safe, still too many patients succumb to the consequences of cytokine release syndrome, an adverse event linked to these therapies. For instance, during the clinical development of blinatumomab, 3.5% of the patients spread over six clinical trials (phase I up to phase III) perished due to treatment related adverse events, including CRS [80]. The root causes of severe CRS remain unknown and it is still unclear why some patients are unsusceptible to it while others experience severe outcomes.

The rationale behind the undertaking of Project 3 was to shed a new light on the biological factors influencing CRS formation. Project 3 breaks down cytokine release syndrome into two distinct parts: (1) cytokine release on the biological level and (2) its manifestation into a clinical symptom. By making this distinction, Project 3 and the accompanied peer-reviewed article (see section 4.3) shed a new light on CRS formation and propose a possible solution to the lack of predictive potential of mechanistic models.

The release of certain cytokines (such as IL6, TNFα, IFNγ) is influenced by the so-called drug-target-disease related factors. These factors -on the most basic level- will affect the amount of target engagement that takes place between the tumour cell and the T-cells. The larger the extent of target engagement, the higher the pharmacological activity, including the release of cytokines. Project 3 identified the dose, target abundancy, target accessibility in the human body, binding affinity, the involved types of T-cells, and the amount of T-cells present as the main factors contributing to the extent of cytokine release. Prior knowledge about these factors may help to anticipate the ranges of cytokine release in patients. What is more difficult to anticipate is how individual patients will react to the cytokine excursion upon treatment with a T-cell redirecting therapy. Some patients will experience not as much as a strong fever, whereas others may suffer from high-grade CRS even with only low plasma concentrations of the cytokines [89, 90]. This disparity between cytokine release and clinical symptoms of CRS makes it difficult to predict in individual patients. Putting a number on the anticipated cytokine levels in plasma is of limited use when these levels cannot be translated into an individual risk. Information on individual patient risk factors and the effect on CRS formation by T-cell redirecting therapies is still lacking.

The analysis performed in Project 3 concluded that *in silico* methods might play an important role in deciphering the exact link between T-cell redirecting therapies and CRS formation in patients. Mechanistic models exist that can capture various drug-target-disease related factors to predict the extent of cytokine release [67, 115]. Some models are equally capable of assessing various dosing regimens or even the dampening impact of mitigation strategies, such as step-up dosing for CD3-bispecific antibodies [121, 122]. These models are however insufficient to predict individual patient risk. Clinical experience shows that individual patients react differently to cytokine release and that no two patients are alike [89, 90]. Mechanistic models on cytokine release are thus unable to predict the CRS severity in different patients. Developing a modelling framework that considers both cytokine release and CRS severity in patients requires extensive analysis of real-world data from electronic health records and patient databases that record patient characteristics such as comorbidities, the received treatment, and the clinical outcomes. The combination of mechanistic modelling with insights gained from real-world data may be an important step in the direction of individualised patient safety for T-cell redirecting therapies.

As proposed by van Iersel on structured risk assessment for First-in-Human studies, the risk in a patient is proportional to the vulnerability of that patient and animal species to the IMP, the exposure to the IMP and how it is related to toxicity, and the toxicity findings from nonclinical studies [1]. The risk is also inversely proportional to the risk mitigation that is in place. For drugs aimed at treating critically ill patients, such as

T-cell-redirecting therapies, it can be argued that not only risk, but also rather the risk-benefit for the patient is the most important consideration.

If we draw the line from the equation presented by van Iersel and the findings from Project 3, we can assign the different pillars that are involved in the prediction and modulation of cytokine release syndrome to the different factors involved in the equation (figure 9). As such, patient-related risk factors may represent subject vulnerability, drug-target-disease related factors may dictate the extent of exposure to toxicity, and nonclinical findings shed a light on the potential toxicity to be expected during treatment.

Unfortunately, the risk to which patients are exposed in FiH trials cannot readily be quantified nor does previous experience with similar compounds provide a reliable prediction of potential risk [1]. Nevertheless, each piece of information may help to create a picture of the risk and it is therefore essential that extensive and robust nonclinical testing is performed prior to entry-into-human studies and that experience from similar compounds is recorded and considered.

Figure 9 illustrates the multifactorial nature of patient risk such as CRS and the importance of integrative analyses. Knowledge on both drug-target-disease related factors, predicting their impact on cytokine release with mechanistic models, and leveraging real-world data to gain insights in individual patient risk factors are all part of the equation.

Lastly, note that risk covers only one part of the equation. As presented in section 1.4 and figure 3, uncertainty around the risk also commands attention. Both the aspects '*What we know*' and '*What we know that we do not know*' should be considered when informed decisions about the IMP are ought to be made.

This risk and its uncertainty, and how both can be reduced, play a central role in the early drug development process. It is recommended to make use of a weight-of-evidence approach, integrating *in vitro, ex vivo,* and *in vivo* data, and *in* silico insights as part of the decision-making process.

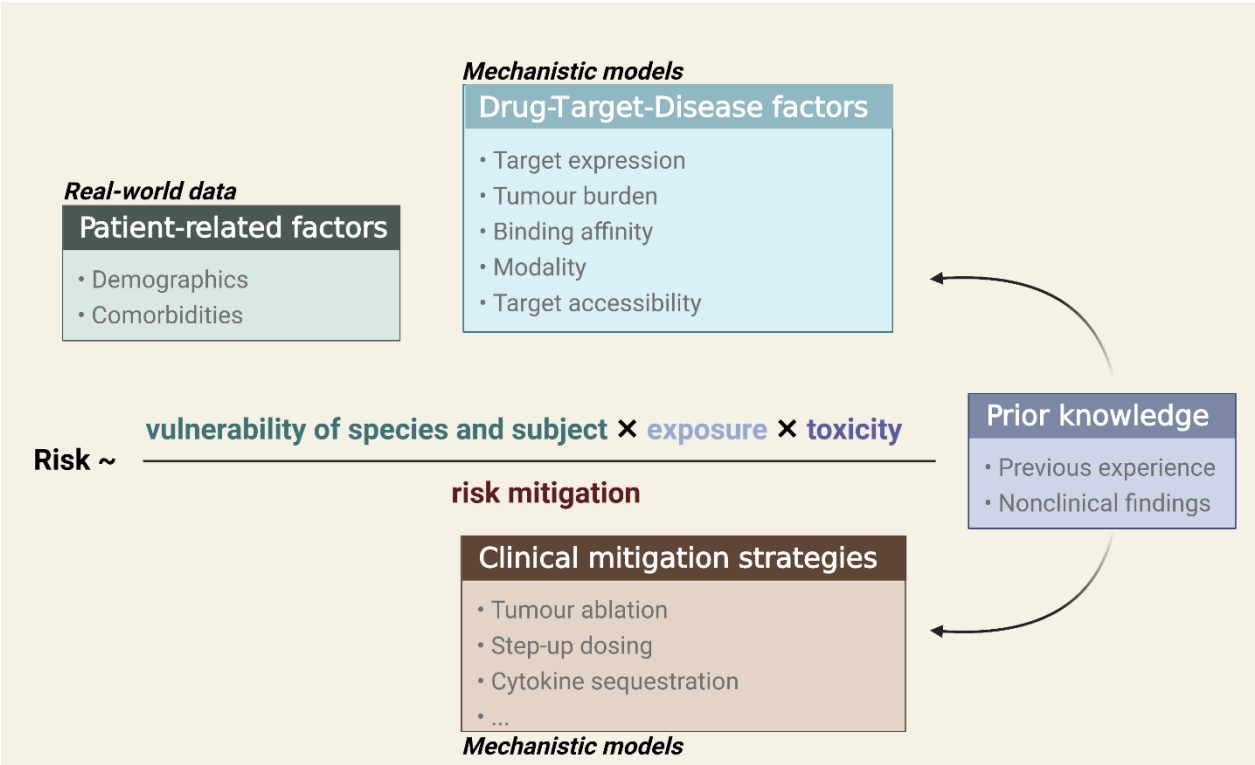


*Figure 9. The risk for a patient in a FiH trial is proportional to the vulnerability of the patient, the exposure to toxicity, the expected toxicity profile and the inverse of the implemented mitigation strategies, according to the equation from van Iersel and colleagues [1]. The boxes represent the findings from Project 3 and how these are related to the equation of risk. The bold/italic text represents the in silico methods suited to support the prediction of risk from each box. Both real-world data and mechanistic modelling means will be required in order to make predictions on individual patient risk. Information from prior studies or nonclinical findings can help in better understanding the other pillars of risk.*

## 6. Outlook & Limitations

Thanks to detailed guidelines, rigorous science, and increasing expertise, early clinical studies are generally safe despite their high-risk setting and complicated preparation. However, it is clear that there are many knowledge gaps that need to be filled by the regulators, sponsors, and investigators. Increasingly complex and multimodal therapies only add up to the challenge of going through a safe –and successful- early drug development process.

Each project presented in this thesis aimed to provide support to the early drug development process of T-cell redirecting therapies. Project 1 focused on the development of mechanistic *in silico* models to better characterize the *in vitro* pharmacology of CD3-bispecifics and to serve as a predictive tool when designing new experiments. Project 2 is the culmination of a time-independent experimental set-up and complementary analysis that provides a holistic understanding of the pharmacology and that may fit

perfectly in the regulator-issued integrative analyses for FiH studies. Finally, Project 3 sheds a light on the factors that influence the risk for developing CRS after treatment with T-cell redirecting therapies, a health hazard that not only lurks in FiH trials but also forms a serious issue at later stages of the drug development process.

The primary focus of this work was to provide guidance and insights to a few aspects of the nonclinical and translational development of T-cell redirecting therapies. It achieved its original objectives by delivering tools and ideas that can be applied throughout the drug development process. The outcomes from these projects should not be considered as endpoints but rather as steps in the right direction. Some current limitations identified in the projects –and potential future steps to overcome them- are summarised hereunder.

The drug-response model from Project 1 leaves room to become more mechanistic. The relationship between synapse formation and T-cell activation tells us that additional mechanisms are involved and that the empirical fudge factor (i.e., the $\delta$-term in equation 5, section 3.2.2) on target expression density is required to reliably capture this behaviour. However, the fudge factor on its own does not provide a satisfactory mechanistic explanation for this behaviour and more research is warranted to elucidate this. In addition, the impact of varying binding affinities has not been explored in detail. Referring to basic T-cell biology, it is well possible that changes in binding reaction kinetics elicit bigger changes than what would be expected based on the anticipated change in trimeric complex formation [144]. More complicated model components, such as those based on the principles of kinetic proofreading [145], would therefore be required. In its current form, the model was validated with data from cibisatamab, but was not expanded to other CD3-bispecifics. Similar data packages should be generated with other compounds and the model performance should be assessed. In addition, the model focuses on T-cell activation and tumour cell killing as biological endpoints. However, as was widely discussed throughout this work, cytokine release is an important part of the pharmacology of CD3-bispecifics and is currently lacking in the model. Inclusion of mechanisms of cytokine release would benefit the translational relevance of the model.

Project 2 presents a new methodology to assess the pharmacology of T-cell redirecting therapies in a holistic manner. Since this methodology relies on an *ad hoc* analysis of generated data, it cannot be used, unlike computational models, to explore 'what-if' scenarios or make predictions of future experiments. Its strength lies in enabling unbiased analysis of pharmacology data in a time-independent manner.

Project 3 in itself discussed an important limitation of mechanistic models; models unable to predict the risk for CRS in individual patients. The project presents a potentially powerful solution through a

combination of mechanistic modelling -to predict cytokine release and to identify the optimal dosing regimen tailored to the drug of interest- and a statistical model to predict individual risk. To be successful, such a framework entails the development of mechanistically sound models and the collection of real-world data on CRS and patient characteristics. Such a framework can be further developed and applied in early drug development (e.g., for compound ranking) or in clinical practice as a clinical decision tool for precision dosing.

It bears mentioning that this work did not touch upon some aspects that have equally important implications for the future of T-cell redirecting therapies. Both immunogenicity and neurotoxicity come to mind. We speak of immunogenicity when the body mounts an immune response against the administered drug. This is a common problem in case of biologics such as antibodies since these drugs are big enough to be easily recognised by the immune system as a foreign object. When a drug is subjected to an immunogenic response, this may have severe consequences for the PK/PD profile of that drug, potentially rendering it ineffective. Many research efforts, including modelling, go into deciphering the exact mechanisms behind immunogenicity and in finding out how to prevent/combat them. Neurotoxicity forms, together with CRS, the primary toxicity risk by T-cell redirecting therapies. Its pathophysiology (and its potential link with cytokine release) are not well understood. Neurotoxicity –also known in this context as immune effector cell-associated neurotoxicity syndrome (ICANS) - is a severe side effect that may have a lethal outcome. It is therefore crucial that its mechanisms are studied.

The situation in which T-cell redirecting therapies reside is a tricky one. Their novelty, their high-risk character, and our previous experiences dictate us to play on safe and treat patients with low doses when first going into clinics. We are aware that these first low doses are unlikely to provide any clinical benefit to the receiving patients; patients that are severely ill and enrolled in these clinical trials with the hope on a miracle cure. Less conservative approaches on the other hand may result in doses that are unsafe for an already fragile patient population. It becomes an ethical dilemma, as much as it is a scientific one. The only way out of this stalemate is with robust science. If there is one take-away message from this work, let it be that the field of drug development is vast with many different scientific disciplines that each benefit from collaboration and integration, and that a holistic and strategic understanding of the available resources is crucial for success. This means the integration of non-clinical, clinical, real world, and literature data wherever it makes sense scientifically. As shown as case examples in this work and encouraged by health authorities with the MIDD initiative, it may not surprise that pharmacometrics as a discipline stands a good chance on being this integrator.

## 7. Acknowledgements

First and foremost, I want to thank Antje Walz for her tireless guidance and kindness throughout the last four and a half years that I spent at Roche. My thesis would never have achieved this level of quality if it were not for you. Your critical thinking, scientific curiosity, holistic understanding of drug development, and –most importantly- your willingness to share all this experience with me have shaped me into an actual scientist and I will be forever grateful for that. I look forward to continue collaborating and to solve interesting scientific questions together!

I also want to thank Miro Eigenmann, especially for his friendship and for essentially being a mentor to me when I first started as a master student and later as a PhD student. Always happy to share your insights, you taught me a lot over the past years and I have very much enjoyed working together with you.

A very big thank you to all colleagues at Roche for creating such a welcoming and inspiring atmosphere. In particular, I want to thank Nicolas Frances for always having his door open when I had a modelling question or problem. I want to thank Estelle Marrer-Berger for her contagious enthusiasm and her willingness to share her boundless knowledge with me. Likewise, I want to thank Ken Wang for her wisdom and support in the different projects. I am also grateful to Simone Lang, Melanie Knobloch, and Simon Keiser in Schlieren for having my back during experiments. Many thanks to Marina Bacac and Tina Weinzierl for mentoring me in Schlieren. Also a sincere thank you to Thierry Lavé, Sherri Dudal, Niels Janssen, and Benjamin Ribba for taking me under their wings and help me navigate my way through Roche.

I want to thank Prof. Thorsten Lehr for agreeing on being my academic supervisor and allowing me to pick his brain and benefit from his experience when working on the projects that make up this thesis. I also want to thank Prof. Alexandra Kiemer for kindly agreeing on being my scientific supervisor and for reviewing the thesis.

The PharMetrX program has played an important role in my training as a scientist and I would like to thank Prof. Charlotte Kloft and Prof. Wilhelm Huisinga for this opportunity to benefit from their expert guidance. Many kudos to Cornelia Böhnstedt for the flawless coordination. Likewise, I want to thank all PharMetrX students for the great dynamics during the courses, get-togethers, and conferences. A special thank you to Lukas Kovar for the interesting discussions we had during and after the courses, while enjoying a Berliner Kindl.

I want to thank my mom, Martine, and my dad, Patrick, for their unconditional love and support throughout my entire life and making me the person who I am today. You both are my source of inspiration and motivation. Also a thank you to my (not so) little brothers Jérôme and Henri. It is always a nice homecoming when the two of you are around.

I want to thank my love Kelly for her care and support, and her never-ending curiosity in my research. By asking critical questions, you managed to influence a critical aspect in one of the projects, which aided in its further development. I love you and I love discussing science with you.

Furthermore, I want to thank my best friends Sven, Jerome, Gilles, Diederik, and Bavo for always having my back and for the countless great times that we had – and still will have- together.

This list is of course by no means exhaustive and there are many more people to thank for their kind words, support, and curiosity.

The Figures and graphical abstract presented as part of this dissertation have been created with Biorender.com

## 8. References

1. van Iersel, M.T., H.E. Greenberg, and M.L. Westrick, *Structured Risk Assessment for First-in-Human Studies.* Therapeutic Innovation & Regulatory Science, 2017. **51**(3): p. 288-297.
2. Abbas, A., A. Lichtman, and S. Pillai, *Major Histocompatibility Complex Molecules and Presentation to T Lymphocytes*, in *Cellular and Molecular Immunology*, Elsevier, Editor. 2012, Elsevier Saunders: Philadelphia, PA. p. 109-136.
3. Suh, H.Y., et al., *Determination of the starting dose in the first-in-human clinical trials with monoclonal antibodies: a systematic review of papers published between 1990 and 2013.* Drug design, development and therapy, 2016. **10**: p. 4005-4016.
4. Smith-Garvin, J.E., G.A. Koretzky, and M.S. Jordan, *T Cell Activation.* Annual Review of Immunology, 2009. **27**(1): p. 591-619.
5. Banavar, J.R., et al., *A general basis for quarter-power scaling in animals.* Proceedings of the National Academy of Sciences of the United States of America, 2010. **107**(36): p. 15816-15820.
6. Attarwala, H., *TGN1412: From Discovery to Disaster.* Journal of Young Pharmacists, 2010. **2**(3): p. 332-336.
7. Horvath, C.J. and M.N. Milton, *The TeGenero Incident and the Duff Report Conclusions: A Series of Unfortunate Events or an Avoidable Event?* Toxicologic Pathology, 2009. **37**(3): p. 372-383.
8. Kaur, R., P. Sidhu, and S. Singh, *What failed BIA 10–2474 Phase I clinical trial? Global speculations and recommendations for future Phase I trials.* Journal of Pharmacology & Pharmacotherapeutics, 2016. **7**(3): p. 120-126.
9. European Medicines Agency, *Guideline on strategies to identify and mitigate risks for first-in-human and early clinical trials with investigational medicinal products*

*(EMEA/CHMP/SWP/28367/07 Rev. 1)*, Committee for Medicinal Products for Human Use (CHMP), Editor. 2017, EMEA: London, United Kingdom. p. 1-22.
10. Kucerova, P. and M. Cervinkova, *Spontaneous regression of tumour and the role of microbial infection--possibilities for cancer treatment.* Anti-cancer drugs, 2016. **27**(4): p. 269-277.
11. Christakis, P., *The birth of chemotherapy at Yale. Bicentennial lecture series: Surgery Grand Round.* The Yale journal of biology and medicine, 2011. **84**(2): p. 169-172.
12. Kruger, S., et al., *Advances in cancer immunotherapy 2019 – latest trends.* Journal of Experimental & Clinical Cancer Research, 2019. **38**(1): p. 268.
13. Jessy, T., *Immunity over inability: The spontaneous regression of cancer.* Journal of natural science, biology, and medicine, 2011. **2**(1): p. 43-49.
14. McCarthy, E.F., *The toxins of William B. Coley and the treatment of bone and soft-tissue sarcomas.* The Iowa orthopaedic journal, 2006. **26**: p. 154-158.
15. Kummar, S., et al., *Drug development in oncology: classical cytotoxics and molecularly targeted agents.* Br J Clin Pharmacol, 2006. **62**(1): p. 15-26.
16. Palumbo, M.O., et al., *Systemic cancer therapy: achievements and challenges that lie ahead.* Front Pharmacol, 2013. **4**: p. 57.
17. De Angelis, C., *Side effects related to systemic cancer treatment: are we changing the Promethean experience with molecularly targeted therapies?* Current oncology (Toronto, Ont.), 2008. **15**(4): p. 198-199.
18. Adams, V.R., *Adverse Events Associated with Chemotherapy for Common Cancers.* Pharmacotherapy: The Journal of Human Pharmacology and Drug Therapy, 2000. **20**(7P2): p. 96S-103S.
19. Pierpont, T.M., C.B. Limper, and K.L. Richards, *Past, Present, and Future of Rituximab-The World's First Oncology Monoclonal Antibody Therapy.* Front Oncol, 2018. **8**: p. 163.
20. Boekhout, A.H., J.H. Beijnen, and J.H.M. Schellens, *Trastuzumab.* The oncologist, 2011. **16**(6): p. 800-810.
21. Vincenzi, B., et al., *Cetuximab: from bench to bedside.* Curr Cancer Drug Targets, 2010. **10**(1): p. 80-95.
22. Azoury, S.C., D.M. Straughan, and V. Shukla, *Immune Checkpoint Inhibitors for Cancer Therapy: Clinical Efficacy and Safety.* Curr Cancer Drug Targets, 2015. **15**(6): p. 452-62.
23. Conlon, K.C., et al., *Redistribution, hyperproliferation, activation of natural killer cells and CD8 T cells, and cytokine production during first-in-human clinical trial of recombinant human interleukin-15 in patients with cancer.* J Clin Oncol, 2015. **33**(1): p. 74-82.
24. Soiffer, R.J., et al., *Expansion and manipulation of natural killer cells in patients with metastatic cancer by low-dose continuous infusion and intermittent bolus administration of interleukin 2.* Clin Cancer Res, 1996. **2**(3): p. 493-9.
25. Beatty, G.L. and W.L. Gladney, *Immune Escape Mechanisms as a Guide for Cancer Immunotherapy.* Clinical Cancer Research, 2015. **21**(4): p. 687-692.
26. Liu, D., R.W. Jenkins, and R.J. Sullivan, *Mechanisms of Resistance to Immune Checkpoint Blockade.* American journal of clinical dermatology, 2019. **20**(1): p. 41-54.
27. Martins, F., et al., *Adverse effects of immune-checkpoint inhibitors: epidemiology, management and surveillance.* Nature Reviews Clinical Oncology, 2019. **16**(9): p. 563-580.
28. Sedykh, S.E., et al., *Bispecific antibodies: design, therapy, perspectives.* Drug Design, Development and Therapy, 2018. **12**: p. 195-208.
29. Coyle, L., et al., *Open-Label, phase 2 study of blinatumomab as second salvage therapy in adults with relapsed/refractory aggressive B-cell non-Hodgkin lymphoma.* Leukemia & Lymphoma, 2020: p. 1-10.
30. Spiess, C., Q. Zhai, and P.J. Carter, *Alternative molecular formats and therapeutic applications for bispecific antibodies.* Molecular Immunology, 2015. **67**(2, Part A): p. 95-106.

31. Lindner, S.E., et al., *Chimeric antigen receptor signaling: Functional consequences and design implications.* Science Advances, 2020. **6**(21): p. eaaz3223.
32. Rath, J.A. and C. Arber, *Engineering Strategies to Enhance TCR-Based Adoptive T Cell Therapy.* Cells, 2020. **9**(6): p. 1485.
33. Li, D., et al., *Genetically engineered T cells for cancer immunotherapy.* Signal Transduction and Targeted Therapy, 2019. **4**(1): p. 35.
34. Zhao, L. and Y.J. Cao, *Engineered T Cell Therapy for Cancer in the Clinic.* Frontiers in Immunology, 2019. **10**(2250).
35. Ma, S., et al., *Current Progress in CAR-T Cell Therapy for Solid Tumors.* International journal of biological sciences, 2019. **15**(12): p. 2548-2560.
36. Suurs, F.V., et al., *A review of bispecific antibodies and antibody constructs in oncology and clinical challenges.* Pharmacology & Therapeutics, 2019. **201**: p. 103-119.
37. Fan, G., et al., *Bispecific antibodies and their applications.* Journal of hematology & oncology, 2015. **8**: p. 130-130.
38. Przepiorka, D., et al., *FDA Approval: Blinatumomab.* Clin Cancer Res, 2015. **21**(18): p. 4035-9.
39. FDA NEWS RELEASE. *FDA approves CAR-T cell therapy to treat adults with certain types of large B-cell lymphoma*. [Online Press Release] 03/21/2018 [cited 2021 July 19th]; Available from: https://www.fda.gov/news-events/press-announcements/fda-approves-car-t-cell-therapy-treat-adults-certain-types-large-b-cell-lymphoma.
40. FDA NEWS RELEASE. *FDA approval brings first gene therapy to the United States*. [Online Press Release] 03/26/2018 [cited 2021 July 19th]; Available from: https://www.fda.gov/news-events/press-announcements/fda-approval-brings-first-gene-therapy-united-states.
41. Hazim, A., et al., *Relationship Between Response and Dose in Published, Contemporary Phase I Oncology Trials.* J Natl Compr Canc Netw, 2020. **18**(4): p. 428-433.
42. Nolop, K., *Bial trial disaster.* British Journal of Clinical Pharmacology, 2016. **82**(2): p. 561-561.
43. FDA Center for Drug Evaluation and Research and Center for Biologics Evaluation and Research, *Guidance for Industry: S9 Nonclinical Evaluation for Anticancer Pharmaceuticals*. 2010, FDA Maryland. p. 0-12.
44. FDA Center for Drug Evaluation and Research and Center for Biologics Evaluation and Research, *Guidance for Industry: S6 Addendum to Preclinical Safety Evaluation of Biotechnology-Derived Pharmaceuticals*. 2012, FDA Maryland. p. 0-16.
45. FDA Center for Drug Evaluation and Research and Center for Biologics Evaluation and Research, *Guidance for Industry: Bispecific Antibody Development Programs*. 2021, FDA Maryland. p. 10.
46. European Medicines Agency, *Potency testing of cell-based immunotherapy medicinal products for the treatment of cancer* Committee for Medicinal Products for Human Use (CHMP), Editor. 2016, EMEA: London, United Kingdom. p. 1-8.
47. Milton, M.N. and C.J. Horvath, *The EMEA Guideline on First-in-Human Clinical Trials and Its Impact on Pharmaceutical Development.* Toxicologic Pathology, 2009. **37**(3): p. 363-371.
48. European Medicines Agency, *Guideline on strategies to identify and mitigate risks for first-in-human and early clinical trials with investigational medicinal products (EMEA/CHMP/SWP/28367/07 Rev. 1)*, Committee for Medicinal Products for Human Use (CHMP), Editor. 2007, EMEA: London, United Kingdom. p. 1-12.
49. Nguyen, D.H., et al., *Loss of Siglec expression on T lymphocytes during human evolution.* Proceedings of the National Academy of Sciences, 2006. **103**(20): p. 7765.
50. Hansel, T.T., et al., *The safety and side effects of monoclonal antibodies.* Nature Reviews Drug Discovery, 2010. **9**(4): p. 325-338.
51. Eastwood, D., et al., *Monoclonal antibody TGN1412 trial failure explained by species differences in CD28 expression on CD4+ effector memory T-cells.* British journal of pharmacology, 2010. **161**(3): p. 512-526.

52. Funck-Brentano, C. and J. Ménard, *The BIAL/Biotrial case of death of a human volunteer in the first-in-human study of BIA 10-2474: Are we missing the fundamentals?* Presse Med, 2016. **45**(9): p. 719-22.
53. van Esbroeck, A.C.M., et al., *Activity-based protein profiling reveals off-target proteins of the FAAH inhibitor BIA 10-2474.* Science, 2017. **356**(6342): p. 1084.
54. van Gerven, J. and M. Bonelli, *Commentary on the EMA Guideline on strategies to identify and mitigate risks for first-in-human and early clinical trials with investigational medicinal products.* Br J Clin Pharmacol, 2018. **84**(7): p. 1401-1409.
55. Brennan, F.R., et al., *Safety and immunotoxicity assessment of immunomodulatory monoclonal antibodies.* mAbs, 2010. **2**(3): p. 233-255.
56. Muller, P.Y., et al., *The minimum anticipated biological effect level (MABEL) for selection of first human dose in clinical trials with monoclonal antibodies.* Curr Opin Biotechnol, 2009. **20**(6): p. 722-9.
57. Kamperschroer, C., et al., *Summary of a workshop on preclinical and translational safety assessment of CD3 bispecifics.* Journal of Immunotoxicology, 2020. **17**(1): p. 67-85.
58. Friends of Cancer Research, *Harmonizing the Definition and Reporting of Cytokine Release Syndrome (CRS) in Immuno-Oncology Clinical Trials [White paper]*. 2021, Friends of Cancer Research: Washington, D.C.
59. Viceconti, M., et al., *In silico trials: Verification, validation and uncertainty quantification of predictive models used in the regulatory evaluation of biomedical products.* Methods, 2021. **185**: p. 120-127.
60. Leedale, J., et al., *A Combined In Vitro/In Silico Approach to Identifying Off-Target Receptor Toxicity.* iScience, 2018. **4**: p. 84-96.
61. Jones, H.M., et al., *Application of PBPK modelling in drug discovery and development at Pfizer.* Xenobiotica, 2012. **42**(1): p. 94-106.
62. Eigenmann, M.J., et al., *Interstitial IgG antibody pharmacokinetics assessed by combined in vivo- and physiologically-based pharmacokinetic modelling approaches.* The Journal of Physiology, 2017. **595**(24): p. 7311-7330.
63. Guy, C.S., et al., *Distinct TCR signaling pathways drive proliferation and cytokine production in T cells.* Nature immunology, 2013. **14**(3): p. 262-270.
64. Hart, Y., et al., *Design principles of cell circuits with paradoxical components.* Proceedings of the National Academy of Sciences, 2012. **109**(21): p. 8346.
65. Hart, Y., et al., *Paradoxical signaling by a secreted molecule leads to homeostasis of cell levels.* Cell, 2014. **158**(5): p. 1022-1032.
66. Betts, A., et al., *A Translational Quantitative Systems Pharmacology Model for CD3 Bispecific Molecules: Application to Quantify T Cell-Mediated Tumor Cell Killing by P-Cadherin LP DART((R)).* Aaps j, 2019. **21**(4): p. 66.
67. Singh, A.P., et al., *Development of a quantitative relationship between CAR-affinity, antigen abundance, tumor cell depletion and CAR-T cell expansion using a multiscale systems PK-PD model.* mAbs, 2020. **12**(1): p. 1688616-1688616.
68. Campagne, O., et al., *Integrated Pharmacokinetic/Pharmacodynamic Model of a Bispecific CD3xCD123 DART Molecule in Nonhuman Primates: Evaluation of Activity and Impact of Immunogenicity.* Clin Cancer Res, 2018. **24**(11): p. 2631-2641.
69. Danhof, M., et al., *Mechanism-based pharmacokinetic-pharmacodynamic (PK-PD) modeling in translational drug research.* Trends in Pharmacological Sciences, 2008. **29**(4): p. 186-191.
70. Lynch, C.M., B.W. Hart, and I.S. Grewal, *Practical considerations for nonclinical safety evaluation of therapeutic monoclonal antibodies.* MAbs, 2009. **1**(1): p. 2-11.
71. Van Norman, G.A., *Limitations of Animal Studies for Predicting Toxicity in Clinical Trials: Is it Time to Rethink Our Current Approach?* JACC: Basic to Translational Science, 2019. **4**(7): p. 845-854.

72. Van Norman, G.A., *Limitations of Animal Studies for Predicting Toxicity in Clinical Trials: Part 2: Potential Alternatives to the Use of Animals in Preclinical Trials.* JACC. Basic to translational science, 2020. **5**(4): p. 387-397.
73. Künkele, A., et al., *Preclinical Assessment of CD171-Directed CAR T-cell Adoptive Therapy for Childhood Neuroblastoma: CE7 Epitope Target Safety and Product Manufacturing Feasibility.* Clinical Cancer Research, 2017. **23**(2): p. 466.
74. Ferl, G.Z., et al., *A Preclinical Population Pharmacokinetic Model for Anti-CD20/CD3 T-Cell-Dependent Bispecific Antibodies.* Clinical and Translational Science, 2018. **11**(3): p. 296-304.
75. Gedeon, P.C., et al., *A Rationally Designed Fully Human EGFRvIII:CD3-Targeted Bispecific Antibody Redirects Human T Cells to Treat Patient-derived Intracerebral Malignant Glioma.* Clinical Cancer Research, 2018. **24**(15): p. 3611.
76. Dudal, S., et al., *Application of a MABEL Approach for a T-Cell-Bispecific Monoclonal Antibody: CEA TCB.* J Immunother, 2016. **39**(7): p. 279-89.
77. Harper, J., et al., *An approved in vitro approach to preclinical safety and efficacy evaluation of engineered T cell receptor anti-CD3 bispecific (ImmTAC) molecules.* PLOS ONE, 2018. **13**(10): p. e0205491.
78. Fain, J. and S.C. Gad, *TGN1412*, in *Encyclopedia of Toxicology (Third Edition)*, P. Wexler, Editor. 2014, Academic Press: Oxford. p. 521-522.
79. Chen, X., et al., *Mechanistic Projection of First-in-Human Dose for Bispecific Immunomodulatory P-Cadherin LP-DART: An Integrated PK/PD Modeling Approach.* Clin Pharmacol Ther, 2016. **100**(3): p. 232-41.
80. Schaller, T.H., et al., *First in human dose calculation of a single-chain bispecific antibody targeting glioma using the MABEL approach.* J Immunother Cancer, 2020. **8**(1).
81. Ryan C. Patricia, et al. *In Vitro MABEL Approach for Nonclinical Safety Assessment of MEDI-565 (MT111)* in *ALTEX Proceedings, World Conference 8*. 2011. Montreal: Springer Spektrum.
82. Saber, H., et al., *An FDA oncology analysis of immune activating products and first-in-human dose selection.* Regulatory Toxicology and Pharmacology, 2016. **81**: p. 448-456.
83. Saber, H., et al., *An FDA oncology analysis of CD3 bispecific constructs and first-in-human dose selection.* Regul Toxicol Pharmacol, 2017. **90**: p. 144-152.
84. Kola, I. and J. Landis, *Can the pharmaceutical industry reduce attrition rates?* Nature Reviews Drug Discovery, 2004. **3**(8): p. 711-716.
85. Schuhmacher, A., O. Gassmann, and M. Hinder, *Changing R&D models in research-based pharmaceutical companies.* Journal of translational medicine, 2016. **14**(1): p. 105-105.
86. Grimaldi, C., et al., *Cytokine release: A workshop proceedings on the state-of-the-science, current challenges and future directions.* Cytokine, 2016. **85**: p. 101-108.
87. Zanoni, M., et al., *3D tumor spheroid models for in vitro therapeutic screening: a systematic approach to enhance the biological relevance of data obtained.* Scientific Reports, 2016. **6**: p. 19103.
88. Chang, C.-H., et al., *Combination Therapy with Bispecific Antibodies and PD-1 Blockade Enhances the Antitumor Potency of T Cells.* Cancer Research, 2017. **77**(19): p. 5384-5394.
89. Del Valle, D.M., et al., *An inflammatory cytokine signature predicts COVID-19 severity and survival.* Nature Medicine, 2020. **26**(10): p. 1636-1643.
90. Teachey, D.T., et al., *Identification of Predictive Biomarkers for Cytokine Release Syndrome after Chimeric Antigen Receptor T-cell Therapy for Acute Lymphoblastic Leukemia.* Cancer Discovery, 2016. **6**(6): p. 664-679.
91. Van De Vyver, A.J., et al., *Cytokine release syndrome by T-cell-redirecting therapies: can we predict and modulate patient risk?* Clinical Cancer Research, 2021: p. clincanres.0470.2021.

92. Sato, J., et al., *Correlation and linear regression between blood pressure decreases after a test dose injection of propofol and that following anaesthesia induction.* Anaesth Intensive Care, 2003. **31**(5): p. 523-8.
93. Trivedi, A., R.E. Lee, and B. Meibohm, *Applications of pharmacometrics in the clinical development and pharmacotherapy of anti-infectives.* Expert review of clinical pharmacology, 2013. **6**(2): p. 159-170.
94. Lalonde, R.L., et al., *Model-based Drug Development.* Clinical Pharmacology & Therapeutics, 2007. **82**(1): p. 21-32.
95. European Medicines Agency, *ICH guideline Q9 on quality risk management (EMA/CHMP/ICH/24235/2006)*, Committee for Human Medicinal Products, Editor. 2006, EMEA. p. 1-20.
96. Sheiner, L.B., *Learning versus confirming in clinical drug development.* Clin Pharmacol Ther, 1997. **61**(3): p. 275-91.
97. Danhof, M., et al., *The future of drug development: the paradigm shift towards systems therapeutics.* Drug Discovery Today, 2018. **23**(12): p. 1990-1995.
98. Kimmelman, J., J.S. Mogil, and U. Dirnagl, *Distinguishing between exploratory and confirmatory preclinical research will improve translation.* PLoS biology, 2014. **12**(5): p. e1001863-e1001863.
99. Steinmetz, K.L. and E.G. Spack, *The basics of preclinical drug development for neurodegenerative disease indications.* BMC neurology, 2009. **9 Suppl 1**(Suppl 1): p. S2-S2.
100. Jensen, C. and Y. Teng, *Is It Time to Start Transitioning From 2D to 3D Cell Culture?* Frontiers in Molecular Biosciences, 2020. **7**(33).
101. Olivo Pimentel, V., et al., *A novel co-culture assay to assess anti-tumor CD8+ T cell cytotoxicity via luminescence and multicolor flow cytometry.* Journal of Immunological Methods, 2020. **487**: p. 112899.
102. Kaja, S., et al., *Quantification of Lactate Dehydrogenase for Cell Viability Testing Using Cell Lines and Primary Cultured Astrocytes.* Curr Protoc Toxicol, 2017. **72**: p. 2.26.1-2.26.10.
103. Baumgaertner, P., et al., *Chromium-51 (51Cr) Release Assay to Assess Human T Cells for Functional Avidity and Tumor Cell Recognition.* Bio-protocol, 2016. **6**(16): p. e1906.
104. McKinnon, K.M., *Flow Cytometry: An Overview.* Curr Protoc Immunol, 2018. **120**: p. 5.1.1-5.1.11.
105. Cossarizza, A., et al., *Guidelines for the use of flow cytometry and cell sorting in immunological studies (second edition).* Eur J Immunol, 2019. **49**(10): p. 1457-1973.
106. Mousset, C.M., et al., *Comprehensive Phenotyping of T Cells Using Flow Cytometry.* Cytometry Part A, 2019. **95**(6): p. 647-654.
107. Kiesgen, S., et al., *Comparative analysis of assays to measure CAR T-cell-mediated cytotoxicity.* Nature Protocols, 2021. **16**(3): p. 1331-1342.
108. Huang, G.L., et al., *A multivariate, quantitative assay that disentangles key kinetic parameters of primary human T cell function in vitro.* PLOS ONE, 2020. **15**(11): p. e0241421.
109. Lovell, G.F., et al., *Use of fluorescent Fab/Ab complexes and IncuCyte live-cell analysis to dynamically track cell surface markers and cell populations in mixed cultures.* The Journal of Immunology, 2018. **200**(1 Supplement): p. 46.11.
110. Essen Bioscience. *Incucyte® Nuclight Reagents*. [Product information] [cited 2021 August 9th]; Available from: https://www.essenbioscience.com/en/communications/incucyte-nuclight-reagents/.
111. Morgan, E., et al., *Cytometric bead array: a multiplexed assay platform with applications in various areas of biology.* Clinical Immunology, 2004. **110**(3): p. 252-266.
112. BD Biosciences. *BD Cytometric Bead Array: Multiplexed Bead-Based Immunoassays*. 2009 [cited 2021 August 9th]; Available from: https://www.bd.com/resource.aspx?IDX=17701.

113. Van De Vyver, A.J., et al., *Predicting tumor killing and T-cell activation by T-Cell Bispecific antibodies as a function of target expression: combining in vitro experiments with systems modeling.* Molecular Cancer Therapeutics, 2020: p. molcanther.0269.2020.
114. Jiang, X., et al., *Development of a Target cell-Biologics-Effector cell (TBE) complex-based cell killing model to characterize target cell depletion by T cell redirecting bispecific agents.* MAbs, 2018. **10**(6): p. 876-889.
115. Hosseini, I., et al., *Mitigating the risk of cytokine release syndrome in a Phase I trial of CD20/CD3 bispecific antibody mosunetuzumab in NHL: impact of translational system modeling.* npj Systems Biology and Applications, 2020. **6**(1): p. 28.
116. Van De Vyver, A.J., et al., *PAGE 28 (2019) Abstr 9077 [www.page-meeting.org/?abstract=9077]: in vitro PK/PD modeling of immunological synapse-based tumor cell killing and immune activation to predict in vitro efficacy of T-Cell Bispecifics.*, in *PAGE*. 2019: Stockholm, Sweden.
117. Cardelli, L., et al., *A process model of Rho GTP-binding proteins.* Theoretical Computer Science, 2009. **410**(33): p. 3166-3185.
118. Chen, W., et al., *One size does not fit all: navigating the multi-dimensional space to optimize T-cell engaging protein therapeutics.* mAbs, 2021. **13**(1): p. 1871171.
119. Lobo, E.D. and J.P. Balthasar, *Pharmacodynamic modeling of chemotherapeutic effects: application of a transit compartment model to characterize methotrexate effects in vitro.* AAPS pharmSci, 2002. **4**(4): p. E42-E42.
120. Krzyzanski, W., *Interpretation of transit compartments pharmacodynamic models as lifespan based indirect response models.* J Pharmacokinet Pharmacodyn, 2011. **38**(2): p. 179-204.
121. Jiang, X., et al., *Development of a minimal physiologically-based pharmacokinetic/pharmacodynamic model to characterize target cell depletion and cytokine release for T cell-redirecting bispecific agents in humans.* European Journal of Pharmaceutical Sciences, 2020. **146**: p. 105260.
122. Chen, X., et al., *A Modeling Framework to Characterize Cytokine Release upon T-Cell-Engaging Bispecific Antibody Treatment: Methodology and Opportunities.* Clin Transl Sci, 2019. **12**(6): p. 600-608.
123. Friberg, L.E., et al., *Model of chemotherapy-induced myelosuppression with parameter consistency across drugs.* J Clin Oncol, 2002. **20**(24): p. 4713-21.
124. Mould, D.R. and R.N. Upton, *Basic concepts in population modeling, simulation, and model-based drug development.* CPT: pharmacometrics & systems pharmacology, 2012. **1**(9): p. e6-e6.
125. Sheiner, L.B., B. Rosenberg, and K.L. Melmon, *Modelling of individual pharmacokinetics for computer-aided drug dosage.* Comput Biomed Res, 1972. **5**(5): p. 411-59.
126. Abrantes, J.A., et al., *Handling interoccasion variability in model-based dose individualization using therapeutic drug monitoring data.* British journal of clinical pharmacology, 2019. **85**(6): p. 1326-1336.
127. Mould, D.R. and R.N. Upton, *Basic concepts in population modeling, simulation, and model-based drug development-part 2: introduction to pharmacokinetic modeling methods.* CPT: pharmacometrics & systems pharmacology, 2013. **2**(4): p. e38-e38.
128. Dziak, J.J., et al., *Sensitivity and specificity of information criteria.* Briefings in bioinformatics, 2020. **21**(2): p. 553-565.
129. Gabrielsson, J. and D. Weiner, *Non-compartmental analysis.* Methods Mol Biol, 2012. **929**: p. 377-89.
130. Sowunmi, A., et al., *Use of area under the curve to evaluate the effects of antimalarial drugs on malaria-associated anemia after treatment.* Am J Ther, 2011. **18**(3): p. 190-7.
131. Purves, R.D., *Optimum numerical integration methods for estimation of area-under-the-curve (AUC) and area-under-the-moment-curve (AUMC).* J Pharmacokinet Biopharm, 1992. **20**(3): p. 211-26.

132. Lutz, W.K. and R.W. Lutz, *Statistical model to estimate a threshold dose and its confidence limits for the analysis of sublinear dose-response relationships, exemplified for mutagenicity data.* Mutat Res, 2009. **678**(2): p. 118-22.
133. Hutchinson, L. and R. Kirk, *High drug attrition rates—where are we going wrong?* Nature Reviews Clinical Oncology, 2011. **8**(4): p. 189-190.
134. Pammolli, F., et al., *The endless frontier? The recent increase of R&D productivity in pharmaceuticals.* Journal of translational medicine, 2020. **18**(1): p. 162-162.
135. Kim, T.H., S. Shin, and B.S. Shin, *Model-based drug development: application of modeling and simulation in drug development.* Journal of Pharmaceutical Investigation, 2018. **48**(4): p. 431-441.
136. Lim, H.-S., *Evolving role of modeling and simulation in drug development.* Translational and clinical pharmacology, 2019. **27**(1): p. 19-23.
137. Stamova, S., et al., *Generation of single-chain bispecific green fluorescent protein fusion antibodies for imaging of antibody-induced T cell synapses.* Anal Biochem, 2012. **423**(2): p. 261-8.
138. Kamakura, D., et al., *Mechanism of action of a T cell-dependent bispecific antibody as a breakthrough immunotherapy against refractory colorectal cancer with an oncogenic mutation.* Cancer Immunology, Immunotherapy, 2021. **70**(1): p. 177-188.
139. Dustin, M.L., et al., *Quantification and modeling of tripartite CD2-, CD58FC chimera (alefacept)-, and CD16-mediated cell adhesion.* J Biol Chem, 2007. **282**(48): p. 34748-57.
140. Schropp, J., et al., *Target-Mediated Drug Disposition Model for Bispecific Antibodies: Properties, Approximation, and Optimal Dosing Strategy.* CPT: Pharmacometrics & Systems Pharmacology, 2019. **8**(3): p. 177-187.
141. Harrison, R.G., *Observations on the living developing nerve fiber.* Proceedings of the Society for Experimental Biology and Medicine, 1906. **4**(1): p. 140 - 143.
142. Harmon, L.D., *Artificial Neuron.* Science, 1959. **129**(3354): p. 962-3.
143. Leach, M.W., et al., *Strategies and Recommendations for Using a Data-Driven and Risk-Based Approach in the Selection of First-in-Human Starting Dose: An International Consortium for Innovation and Quality in Pharmaceutical Development (IQ) Assessment.* Clinical Pharmacology & Therapeutics, 2021. **109**(6): p. 1395-1416.
144. McKeithan, T.W., *Kinetic proofreading in T-cell receptor signal transduction.* Proceedings of the National Academy of Sciences, 1995. **92**(11): p. 5042.
145. Lever, M., et al., *Phenotypic models of T cell activation.* Nat Rev Immunol, 2014. **14**(9): p. 619-29.

## 9. Attached manuscripts

***Manuscript 1***

## *Predicting tumour killing and T-cell activation by T-Cell Bispecific antibodies as a function of target expression: combining in vitro experiments with systems modelling.*

*Arthur Van De Vyver, Tina Weinzierl, Miro Eigenmann, Nicolas Frances, Sylvia Herter, Regular B. Busser, Jitka Somandin, Sarah Diggelmann, Florian Limani, Thorsten Lehr, Marina Bacac, Antje-Christine Walz*

Journal: AACR Molecular Cancer Therapeutics

Publishing date: December 9th 2020

DOI: 10.1158/1535-7163.MCT-20-0269

URL: https://mct.aacrjournals.org/content/20/2/357.long

# Predicting Tumor Killing and T-Cell Activation by T-Cell Bispecific Antibodies as a Function of Target Expression: Combining *In Vitro* Experiments with Systems Modeling

Arthur J. Van De Vyver[1,2], Tina Weinzierl[3], Miro J. Eigenmann[1], Nicolas Frances[1], Sylvia Herter[3], Regula B. Buser[4], Jitka Somandin[3], Sarah Diggelmann[3], Florian Limani[3], Thorsten Lehr[2], Marina Bacac[3], and Antje-Christine Walz[1]

## ABSTRACT

Targeted T-cell redirection is a promising field in cancer immunotherapy. T-cell bispecific antibodies (TCB) are novel antibody constructs capable of binding simultaneously to T cells and tumor cells, allowing cross-linking and the formation of immunologic synapses. This in turn results in T-cell activation, expansion, and tumor killing. TCB activity depends on system-related properties such as tumor target antigen expression as well as antibody properties such as binding affinities to target and T cells. Here, we developed a systems model integrating *in vitro* data to elucidate further the mechanism of action and to quantify the cytotoxic effects as the relationship between targeted antigen expression and corresponding TCB activity. In the proposed model, we capture relevant processes, linking immune synapse formation to T-cell activation, expansion, and tumor killing for TCBs *in vitro* to differentiate the effect between tumor cells expressing high or low levels of the tumor antigen. We used cibisatamab, a TCB binding to carcinoembryonic antigen (CEA), to target different tumor cell lines with high and low CEA expression *in vitro*. We developed a model to capture and predict our observations, as a learn-and-confirm cycle. Although full tumor killing and substantial T-cell activation was observed in high expressing tumor cells, the model correctly predicted partial tumor killing and minimal T-cell activation in low expressing tumor cells when exposed to cibisatamab. Furthermore, the model successfully predicted cytotoxicity across a wide range of tumor cell lines, spanning from very low to high CEA expression.

## Introduction

T-cell bispecific antibodies and antibody fragments are promising modalities in the field of cancer immunotherapy (1). They bind simultaneously to CD3 on T cells and a specific antigen on tumor cells. This will result in crosslinking of T cells and tumor cells, causing the formation of immune synapses that will promote activation of T cells and granzyme-induced apoptosis of tumor cells (2–4). TCBs can redirect non-naive T cells irrespective of their specificity, thereby inducing a polyclonal T-cell response (5).

Cibisatamab is a novel TCB construct that targets a membrane-proximal epitope of human carcinoembryonic antigen (CEA) and CD3 epsilon-chain. Further compound characteristics are summarized in the Supplementary Section S1.1.

CEA is a surface antigen that is mainly found on the apical side of columnar cells in the colon, where it is expressed at low densities (6). CEA is often overexpressed in gastrointestinal tumors, where also its expression is no longer polarized to the apical side. Due to being largely tumor specific, CEA is an attractive target for targeted therapies against gastrointestinal tract neoplasms (7).

For such bispecific molecules, drug effect requires formation of ternary complexes between tumor and T cells, leading to activation of T cells. These ternary complexes result in the formation of immunologic synapses that mimic naturally formed synapses between antigen-specific T cells and tumor cells. This implies that the effects of TCBs are complex and multifactorial, and cannot be directly related to the concentration of the compound. Mathematical models have been proposed to understand the complex relationship between target expression, target affinity, T-cell infiltration, activation, proliferation, and drug effects (8–10). Such models are helpful in exploring the potential impact of altering experimental conditions and predicting the outcome of untested scenarios, thus assisting in the design of new experiments and informing on desired compound properties.

Campagne and colleagues proposed a model to capture the exposure–response relationship for TCBs in cynomolgus monkeys with respect to T-cell trafficking, T-cell–mediated tumor lysis, and the formation of antidrug antibodies (8). Jiang and colleagues developed a mechanistic model, based on *in vitro* data sets, assuming that immune synapse formation is driving the drug effect and linked this to drug and system-specific parameters across different compounds and cell lines (9). The model predicted cytotoxicity at single time points and showed the impact on cell killing by both system and compound related properties, such as E:T ratios and binding affinities. Betts and colleagues employed a translational model during nonclinical development of LP-DART, a proprietary-format TCB targeting P-Cadherin, to support clinical dosing regimen projection. They linked the synapse-based model to *in vivo* pharmacokinetics (PK) to

[1]Roche Pharma Research and Early Development, Pharmaceutical Sciences, Roche Innovation Center, Basel, Switzerland. [2]Saarland University, Department of Clinical Pharmacy, Saarbrücken, Germany. [3]Roche Pharma Research and Early Development, Cancer Immunotherapy Department 2, Roche Innovation Center, Zürich, Switzerland. [4]Roche Pharma Research and Early Development, Large Molecule Research, Roche Innovation Center, Zürich, Switzerland.

**Note:** Supplementary data for this article are available at Molecular Cancer Therapeutics Online (http://mct.aacrjournals.org/).

**Corresponding Author:** Arthur J. Van De Vyver, F. Hoffmann-La Roche, Grenzacherstrasse 124, Basel 4070, Switzerland. Phone: 41-7871-58333; E-mail: arthur.van_de_vyver@roche.com

Mol Cancer Ther 2021;20:357–66

**doi:** 10.1158/1535-7163.MCT-20-0269

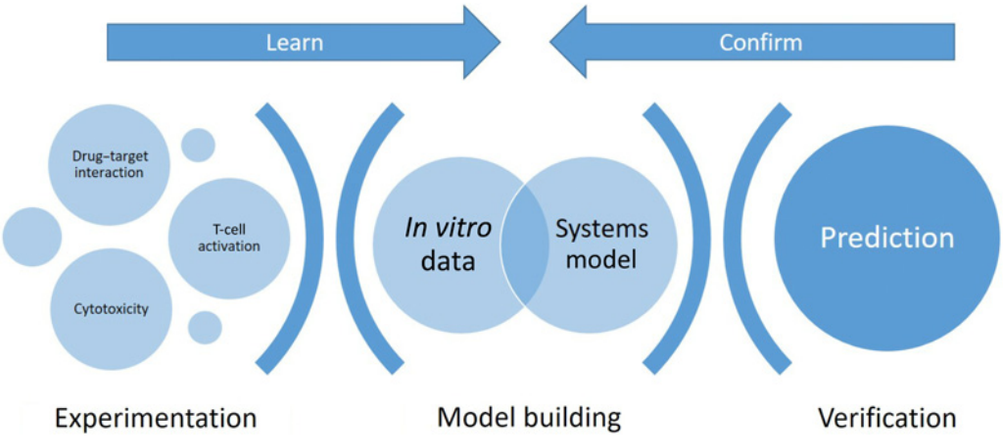


**Figure 1.**
Learn-and-Confirm paradigm: the generation of tailored *in vitro* data to build and inform a systems-type model. The predictive performance of the model can be tested with another dataset, which can help refine the model further.

characterize TCB plasma concentrations and *in* vivo efficacy in xenograft mice (10). This mechanistic model was also used to project the *in vitro* minimally anticipated biological effect level (MABEL) from LP-DART to *in vivo* as an alternative to determine the first-in-human dose (11).

Here, we propose a modeling framework that predicts drug-induced T-cell activation and tumor cell killing in relation to drug concentration, target expression, and target antigen affinity. Therefore, we conducted tailored *in vitro* experiments and generated a longitudinal *in vitro* dataset to inform the model. We developed our model in conjunction with a learn-and-confirm paradigm, using tailored experimental data from a low and high expression cell line (**Fig. 1**). We built the model with the data of the high target expressing cell line and tested the predictive power of the model with the dataset of the low expression tumor cell line. Using that approach, we show that the model can predict *in vitro* cytotoxicity induced by cibisatamab, based on the surface expression density of CEA. The application of such a learn-and-confirm methodology entails the generation of an informative *in vitro* dataset over several time points that spans multiple tested concentrations. In summary, the proposed model is a tool complementary to experimentation. It allows the investigator to test hypotheses, to explore conditions that go beyond the performed experiments, and to probe the understanding behind the mechanism of action.

## Materials and Methods

### *In vitro* experiments

MKN45 (high CEA expressing tumor, CEA density range 230,000–690,000/cell) and CX1 (low CEA expressing tumor, CEA density range 2,000–11,000/cell) were used as target cell lines. To determine tumor cell lysis and T-cell activation, tumor cells were stained with 1.75 μmol/L eFluor670 (#65-0840-85; ebioscience) and PBMCs were isolated from fresh human blood with Histopaque-1077 density gradient method (#10771, Sigma Aldrich) and stained with 0.2 μmol/L CFSE (#21888, Sigma Aldrich). A total of 30,000 target cells (MKN45 or CX1) were seeded in flat-bottom 96-well plates and co-cultured with 300,000 PBMCs per well to attain an E:T of 10:1 (assay medium RPMI1640 + 2% FCS + 1% GlutaMax). Cibisatamab dilutions were added to reach the required total TCB concentrations (6, 32, 160, 800, 4,000, 20,000, and 100,000 pmol/L). For the negative control, 50 μL of assay medium was added. All assays were performed in triplicate. The co-cultures were incubated for 24, 48, 72, 96, and 168 hours at 37°C in a humidified incubator. At the indicated time points, supernatants were collected and FACS analysis was performed to quantify cell killing, T-cell activation, and cytokine release (Supplementary Section S1).

### Model development

A set of ordinary differential equations (ODE) was developed to describe the formation of immune synapses by cibisatamab, triggering activated T cells ($CD25^+$), and T-cell–mediated tumor cell killing. **Figure 2** represents the schematic of the model. All parameters and their description are listed in Supplementary Table S1.

### Target engagement and immune synapse formation

Immune synapse formation was modeled in a well-stirred setting assuming sequential and independent binding processes between the molar free fractions of cibisatamab (*TCB*), CEA antigen (*CEA*), and CD3e (*CD3*), which implies that binding to the first target does not affect the binding affinity to the second target. For simplicity reasons, we assume that cibisatamab has only one binding arm for CEA. When *TCB* binds to *CEA* or *CD3*, dimers between *TCB* and *CEA* (*CEAdim*) or *TCB* and *CD3* (*CD3dim*) are formed, respectively. *CEAdim* and *CD3dim* can subsequently bind *CD3* and *CEA*, respectively, to form a ternary complex (*Synapse*) between the three entities (**Fig. 2A**). *Synapse* formation is described by Eqs. A to D. It should be noted that cibisatamab binding to soluble CEA that was shed from tumor cells is negligible and was not accounted for in the model (3).

$$\frac{dTCB}{dt} = -kon_R * CEA * TCB - kon_{CD3} * CD3 * TCB + koff_R * CEA_{dim} + koff_{CD3} * CD3_{dim} \quad \text{(A)}$$

$$TCB(0) = \text{Drug concentration } [\text{nmol/L}]$$

$$\frac{dCEA_{dim}}{dt} = kon_R * CEA * TCB - koff_R * CEA_{dim} + koff_{CD3} * Synapse - kon_{CD3} * CD3 * CEA_{dim} \quad \text{(B)}$$

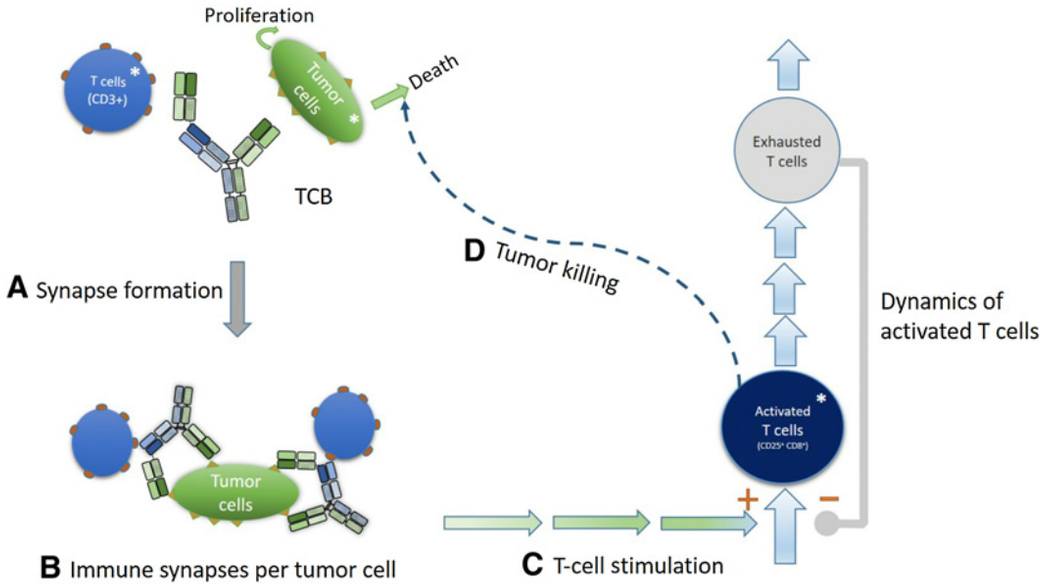


**Figure 2.**

Systems pharmacology model of TCBs redirecting and activating T cells to kill antigen-specific tumor cells. In the model, a TCB will bind sequentially to its targets (CD3 on T cells and a specific antigen on tumor cells) to form ternary complexes, also called immunologic synapses (**A**). This will result in a certain amount of synapses formed on the surface of each tumor cell (**B**). The average synapse density per cell induces an activation of cytotoxic T cells, indicated by CD25 positivity (**C**). Activated T cells directly induce the killing of tumor cells (**D**). Within the dynamics of T-cell activation, stimulation is counter balanced by a negative feedback (gray arrow with rounded head). *, Components on which observations were made. A more detailed structural model schematic found in Supplementary Material.

$$\frac{dCD3_{dim}}{dt} = kon_{CD3} * CD3 * TCB - koff_{CD3} * CD3_{dim} + koff_R * Synapse - kon_R * CEA * CD3_{dim} \quad (C)$$

$$\frac{dSynapse}{dt} = kon_R * CD3_{dim} * CEA + kon_{CD3} * CEA_{dim} * CD3 - (koff_R + koff_{CD3}) * Synapse \quad (D)$$

$$CEA_{dim}(0) = CD3_{dim}(0) = Synapse(0) = 0\ [\text{nmol/L}]$$

Total concentrations of CEA and CD3e are derived from the respective cell concentrations (Eq. E). Antigen expression per cell is assumed to remain constant. Surface expression of CD3 was fixed at 50,000/cell (internal data). The rates *kon* and *koff* are the respective association and dissociation constants between cibisatamab and CEA ($kon_R$ and $koff_R$) or CD3e ($kon_{CD3}$ and $koff_{CD3}$). Only the KD for binding to CD3 and the FRET $IC_{50}$ for binding to CEA were known. Therefore, both *koff* values were taken as 3.6 $h^{-1}$ and both *kon* values were derived as *kon* = *koff*/(*KD or* $IC_{50}$).

$$\text{Antigen}_{\text{total}} = 10^9 \times \frac{\text{Cell concentration} \times \text{Antigen density}}{N_a}\ [\text{nmol/L}] \quad (E)$$

## CD25 induction and T-cell activation

It is assumed that the density of immune synapses per cell is one of the drivers behind T-cell activation (**Fig. 2B**), and that activated T cells express CD25 on their surface which we monitored in the *in vitro* experiments. Bimolecular complexes between cibisatamab and CEA ($CEA_{dim}$) or CD3e ($CD3_{dim}$) are inactive. The molar concentration of immune synapses is converted into a density of an absolute number of immune synapses/cell and averaged by the total number of tumor cells per microliter (Eq. F). The number of synapses/cell will elicit a delayed stimulation on $CD8^+$ T cells, which was monitored by CD25 expression (Eqs. G–L).

$$Synapse_{cell} = \frac{Synapse * N_A * 10^{-6}}{Tumor\ cells * 10^9}\left[Cell^{-1}\right] \quad (F)$$

$$STIM = \frac{\delta * Emax * Synapse_{cell}}{Complex50 + Synapse_{cell}} \quad (G)$$

$$\delta = \frac{CEA_{expression}}{CEA_{expression}^{reference}} \quad (H)$$

$$k_{tr} = \frac{3}{\tau}\left[h^{-1}\right]$$

$$\frac{ddelay1}{dt} = k_{tr}(STIM - delay1) \quad (I)$$

$$\frac{ddelay2}{dt} = k_{tr}(delay1 - delay2) \quad (J)$$

$$\frac{ddelay3}{dt} = k_{tr}(delay2 - delay3) \quad (K)$$

$$\text{delay1}(0) = \text{delay2}(0) = \text{delay3}(0) = 0$$

The stimulatory drug effect on T cells (*STIM*) is dependent on the number of immune synapses per cell ($Synapse_{cell}$) and the relative tumor target expression, captured by a scaling factor $\delta$, accounting for differences in CEA expression between the experimental data and a reference system (Eq. H). For the presented case, the reference system is MKN45. This stimulation of T cells is delayed relative to the

formation of the synapses and is described by a sigmoidal function where $E_{max}$ represents maximal stimulation by immune synapses, multiplied with the relative target expression. The number of immune synapses per tumor cell required to reach half-maximal killing is given by Complex50. The transit compartments $delay_1$, $delay_2$, and $delay_3$ dampen the stimulatory effect of STIM on CD25 induction on $CD8^+$ cells (Eqs. I–K). $K_{tr}$ is the transit rate from one compartment to the other and equals 3/tau.

$$\frac{dCD25}{dt} = k_{in}{}^{*}\,(1 + delay3)^{*}\,\frac{Reg0}{Reg} - k_{reg}{}^{*}\,CD25 \qquad \text{(L)}$$

$$\mathrm{CD25}(0) = CD25_{baseline}[\mathrm{cells}/\mu\mathrm{L}]$$

$$CD25_{baseline} = \frac{k_{in}}{k_{out}}\left[\frac{\mathrm{cells}}{\mu\mathrm{L}}\right] \qquad \text{(M)}$$

$$\frac{dTransit1}{dt} = k_{reg}{}^{*}\,(CD25 - CD25_{baseline}) - k_{reg}{}^{*}\,Transit1 \qquad \text{(N)}$$

$$\frac{dTransit2}{dt} = k_{reg}{}^{*}\,Transit1 - k_{reg}{}^{*}\,Transit2 \qquad \text{(O)}$$

$$\frac{dTransit3}{dt} = k_{reg}{}^{*}\,Transit2 - k_{reg}{}^{*}\,Transit3 \qquad \text{(P)}$$

$$Transit1(0) = Transit2(0) = \mathrm{Transit3}(0) = 0\left[\tfrac{\mathrm{cells}}{\mu\mathrm{L}}\right]$$

$$\frac{dReg}{dt} = k_{reg}{}^{*}\,Transit3 - k_{reg}{}^{*}\,(Reg - Reg0) \qquad \text{(Q)}$$

$$\mathrm{Reg}(0) = \mathrm{Reg0}\left[\tfrac{\mathrm{cells}}{\mu\mathrm{L}}\right]$$

The gradual increase in $CD25^+CD8^+$ T cells is captured with a delay compartment linked to a signal transduction cascade with a feedback loop and captures the transient T-cell activation (**Fig. 2C**). The synthesis rate of $CD25^+$ T cells is given by *kin*, and *kreg* is the rate of CD25 turnover (Eq. L). Depending on the amount of $Synapse_{cell}$ formed, $delay_3$ will add up to *kin*. The output rate of CD25-positivity is given by $k_{reg}$ and can be calculated assuming a steady state (Eq. M). A negative feedback loop is described with three transit compartments ($Transit_1$, $Transit_2$, $Transit_3$). The transit compartments will flow into the *Reg* compartment, which has an inhibitory effect on *kin* (Eqs. N–Q) and is depicted by the light-grey rounded arrow at the far right of **Fig. 2** (12).

### Tumor cell killing by activated T cells

A control group without cibisatamab treatment was used to study unperturbed tumor growth for both CX1 and MKN45. The control group was used to derive the tumor-related parameters growth rate ($k_g$) and carrying capacity (*K*), which are specific for each cell line. Unperturbed growth is described by a logistic function with parameters for tumor growth rate ($k_g$) and maximal tumor capacity (*K*). From the tumor growth rate, the tumor doubling time ($t_d$) can be derived (Eq. R)

$$t_d = \frac{\ln 2}{k_g} \qquad \text{(R)}$$

The killing of tumor cells is driven by the increase in $CD25^+CD8^+$ T-cell concentration over baseline and is described by a sigmoidal function (Eq. S, **Fig. 2D**). The $CD25^+CD8^+$ T cells are baseline corrected to eliminate cytotoxic activity in the control group. The maximal rate of tumor killing is proportional to the tumor growth rate. Parameter kappa ($\kappa$) is the proportionality constant between tumor growth rate and maximal killing.

$$\frac{dTumor}{dt} = k_g{}^{*}\,Tumor\left(1 - \frac{Tumor}{K}\right) - Tumor{*}\frac{kg^{*}\,\kappa^{*}\,(CD25 - CD25_{baseline})^{h}}{CD25_{50}{}^{h} + (CD25 - CD25_{baseline})^{h}} \qquad \text{(S)}$$

$$Tumor(0) = iniTumor\left[\frac{cells}{\mu L}\right]$$

All model parameters and their description are listed in Supplementary Table S1.

### Model verification

To verify the robustness of the model, the estimated parameter values obtained during model building with MKN45 (*kin, tau, Emax, Complex50,* $CD25_{baseline}$, $CD25_{50}$, *h,* $\kappa$) were used as an input to predict the outcome of the assays on CX1 (low CEA-expressing). Cell line specific parameters ($k_g$, *K*, CEA-expression level) were changed accordingly (**Table 1**). Cell line-specific parameters were either measured or estimated from the untreated sample. Predictions of tumor cell and T-cell profiles were overlaid with observed data.

As an external validation, the model was used to simulate an unrelated dataset presented by Bacac and colleagues (3), where they show cytotoxicity in function of CEA expression levels. Tumor cytotoxicity at 48 hours after incubation with 20 nmol/L cibisatamab was simulated across a 7-log CEA-density range. Cytotoxicity was calculated as (1 − Treatment/Control) × 100%. Simulations were overlaid and compared with published data (3). A Monte Carlo simulation of 250 iterations was run to capture the random effects estimated by the model. Random effects for $k_g$ and *K* were fixed at 0.3 to account for greater variability between cell lines.

### Parameter estimation

Model parameter estimation was performed with nonlinear mixed-effects modeling in Monolix (version 2018R2; Lixoft). Monolix employs the stochastic-approximation expectation maximization (SAEM) algorithm. Model verification and simulations were performed in Berkeley-Madonna (version 8.3.18; University of California, Berkeley). Diagnostic plots comparing observed versus predicted values and visual predictive checks assessing goodness-of-fit were used to check model performance. The precision of the estimations

**Table 1.** Cell line–specific parameters.

| Parameter | MKN45 (model building) | CX1 (model verification) | Origin |
|---|---|---|---|
| CEA surface expression ($cell^{-1}$) | 230,000 | 11,000 | Measured |
| Growth rate ($hour^{-1}$) | 0.058 | 0.114 | Estimated |
| Carrying capacity (cells) | 326 | 278 | Estimated |
| Initial tumor concentration (cells/μL) | 5.8 | 1.04 | Estimated |

Cell line–specific parameters were changed for model verification purposes. These were either measured experimentally or estimated from the respective control samples.

and the identifiability of the parameters were assessed by means of diagnostic criteria such as the relative standard error (RSE) and parameter shrinkage.

### Cell line characterization

MKN45 (AAC 409) and CX1 (AAC 129) were obtained from DSMZ. Authentication of MKN45 was performed by Microsynth AG in 2018 to confirm identity. No authentication was performed on CX1. No mycoplasma testing was performed prior to the study. Both cell lines' CEA expression levels were determined with QIFIKIT (Agilent Dako), as described elsewhere (3). Cell lines have been in culture for 1 to 4 months at the start of the experiments.

## Results

### Prediction of T-cell activation and tumor cell killing with a mechanistic systems model

In high expression tumor cell line MKN45 (230,000 CEA/cell), we modeled the time course of T-cell activation captured by the number of $CD25^+CD8^+$ T cells (**Fig. 3A**) and of tumor cells (**Fig. 3B**) in the presence and absence of cibisatamab. Overlay of model prediction (solid line) with observed data (triplicate means, symbols) are shown. Individual triplicate observations are shown in Supplementary Fig. S2.

With regards to T-cell activation, we observed a dose-dependent increase in $CD25^+CD8^+$ T cells (**Fig. 3A**, symbols) with maximal levels of activated T cells of 164 cells/μL observed in high dose groups (4,000—100,000 pmol/L). In the control group, number of activated T cells was low (∼3 cells/μL) and only slight changes were observed throughout the observation period. T-cell activation reached maximal levels after approximately 4 days, followed by a decrease in CD25 expression observed at 7 days. We observed gradual and dose-dependent increases in immune checkpoints TIM-3 and PD-1 (Supplementary Fig. S3). The decline in activated T cells at later time points may be explained by these inhibitory mechanisms. Activated T cells remain considerably elevated compared with baseline after 1 week incubation.

Tumor cell growth was monitored over time in the presence and absence of cibisatamab (**Fig. 3B**) in MKN45. In the control group, tumor cell growth was characterized with exponential growth phase during the first 3 days reaching a plateau at 168 hours. From the control group, the estimated tumor growth rate was 0.058 $hour^{-1}$ (RSE 6.48%) resulting a doubling time of 12 hours (**Fig. 3B**) and the estimated carrying capacity was 326 cells/μL (RSE 9%; **Table 1**). In the presence of cibisatamab, we observed a dose-dependent decrease of tumor cell growth. Almost complete tumor growth reduction occurred at high cibisatamab concentrations (4,000–100,000 pmol/L). In addition to the dose-dependent effects on activated T cells and tumor growth inhibition, we observed a dose-dependent effect on cytokine release (Supplementary Fig. S3). In this study, we observed an early IL2 release that triggers T-cell activation and CD25 induction.

In summary, the model well captured the time course of T-cell activation (**Fig. 3A**, solid lines) and tumor cell growth (**Fig. 3B**, solid lines) in control and treated group across a broad dose range of cibisatamab. The model parameters were estimated with good precision, with the highest RSE below 45% (Supplementary Table S2). The diagnostic plots showed overall good model performance (Supplementary Figs. S4 and S5). At lower TCB concentrations, some observations fall outside the 90% prediction intervals in Supplementary Fig. S4A. It should be noted that this misspecification is only observed for very low T-cell numbers (∼3–18 cells/μL). At these levels, the accuracy of the assay may not be sufficient to reliably measure the exact T-cell numbers.

### Prediction of T-cell activation and cytotoxicity in a low expressing tumor cell line

For model verification, we tested whether the model could predict the activity of cibisatamab acting on a tumor cell line (CX1) with much lower surface expression of CEA (11,000/cell) based on the model built on the high expression cell line MKN45 (230,000/cell). Therefore, we simulated the expected time course of $CD25^+CD8^+$ T cells (**Fig. 4A**, solid line) and tumor cells (**Fig. 4B**, solid line) and overlaid it with the observed data (**Fig. 4A** and **B**, symbols, triplicate means). For the simulations, we used the estimated parameters we obtained from fitting the model to the dataset with MKN45 and replaced only cell line-specific parameters by accounting for the differences between the cell lines. These were target expression and the tumor growth parameters which was estimated from the control group (**Table 1**). For CX1, the estimated tumor growth rate was 0.114 $hour^{-1}$ (RSE 5%), which gives a doubling time of 6.1 hours and the estimated carrying capacity was 278 cells/μL (RSE 4.84%).

Low CEA-expressing tumor cell line CX1 showed only small increases in $CD25^+CD8^+$ T cells, reaching maximal levels in the range of 7 to 10 $CD25^+CD8^+$ cells/μL at concentration of 4,000 to 100,000 pmol/L of cibisatamab. This was approximately 20-fold lower as compared with MKN45. The baseline levels (control group) as well as the levels from the low dose groups (6–160 pmol/L) fluctuated between 1.5 and 7 cells/μL. Tumor cell growth over time (**Fig. 4B**) was

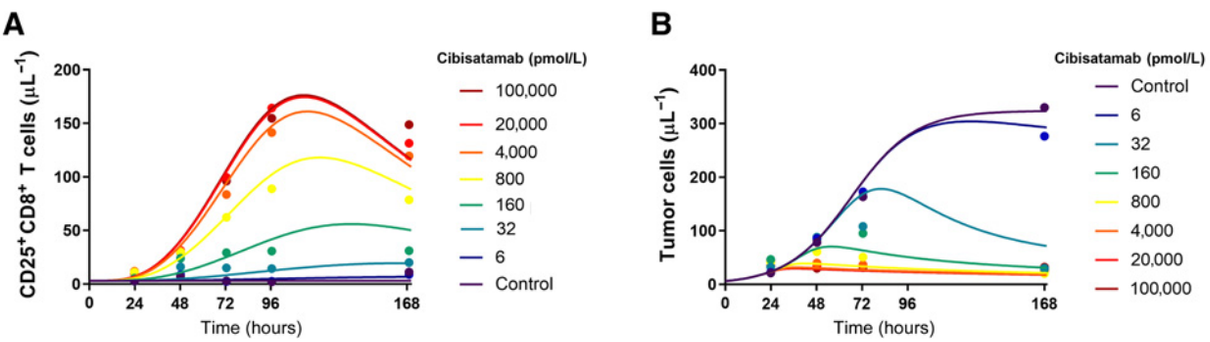


**Figure 3.**

Model fit of $CD25^+CD8^+$ T-cell (**A**) and MKN45 tumor cell (**B**) time-profiles at various cibisatamab concentrations. Dots represent the actual data as the mean of triplicate values, and lines represent the model fit. Individual triplicate values can be found in Supplementary Figs. S2A and S2B.

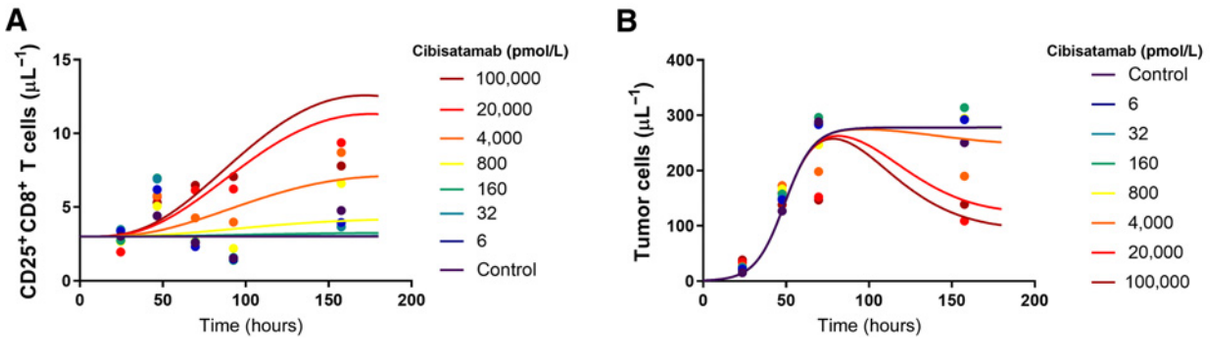


**Figure 4.**

Model prediction of $CD25^{+}CD8^{+}$ T-cell (**A**) and CX1 tumor cell (**B**) time-profiles at various cibisatamab concentrations. Dots represent the actual data as mean triplicate values, and lines represent the simulated profiles. Individual triplicate values can be found in Supplementary Figs. S2C and S2D.

half maximally reduced at 20,000 and 100,000 pmol/L cibisatamab. Furthermore, for the tested concentration range, no increase in cytokine was detected (Supplementary Figs. S3N–S3R).

Due to the large difference in target expression, there was a considerable change in predicted synapses per cell formed. The lower CEA expression in CX1 decreased scaling factor $\delta$, thereby restricting synapse-mediated T-cell activation.

In summary, the model correctly predicted a dose-dependent effect on $CD25^{+}CD8^{+}$ cells with a very low increase of approximately 9 cells/μL. In addition, the predicting model captured the effects on tumor cell growth, which was described as a concentration dependent partial tumor inhibition with a clear concentration-dependency (**Fig. 4B**).

### Prediction of tumor cytotoxicity over a broad range of target expression densities

We used the presented model to project the cibisatamab-induced cytotoxicity to a data set of 110 different tumor cell lines, with CEA surface densities ranging from 1 to 200,000 per cell (3). These cells were treated with 20 nmol/L cibisatamab and cytotoxicity was recorded 48 hours after treatment.

A simulation of cytotoxicity shows that the model can reliably predict the observed cytotoxicity over the whole CEA expression range. The model could distinguish between responding cells (>10% cytotoxicity, green squares) and nonresponding cells (<10% cytotoxicity, orange circles) under these experimental conditions. A clear switch between no/low killing and high killing is present, with a cut-off value around 10,000 CEA/cell (**Fig. 5**). The shaded area is delineated by the 5% and 95% percentiles of the individual predictions. A part of the cell lines falls outside the prediction interval, which may be due to cell line specific factors, assay differences or a process not yet captured by our model.

### Quantitative relationship between drug concentration, immune synapses, T-cell activation, and cytotoxicity

After demonstrating that the model was able to predict the drug effect across a broad range of tumor cells, we wanted to investigate the relationship between formation of synapses as a function of drug

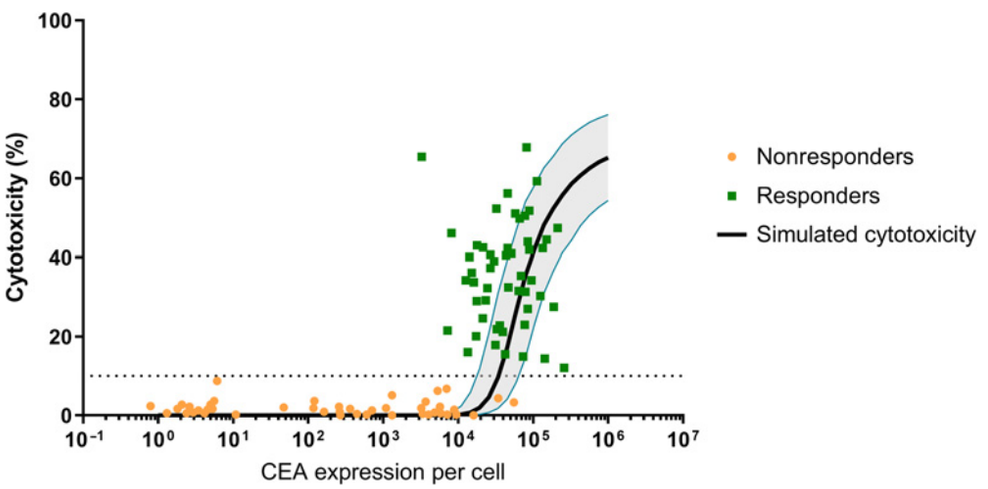


**Figure 5.**

Impact of CEA expression on tumor cytotoxicity after 48 hours at a cibisatamab concentration of 20 nmol/L. Orange dots and green squares represent nonresponding and responding tumor cell lines, respectively. Black line represents model-predicted cytotoxicity. The blue lines represent the 5% and 95% percentiles of the Monte Carlo simulations. The dotted line represents 10% cytotoxicity.

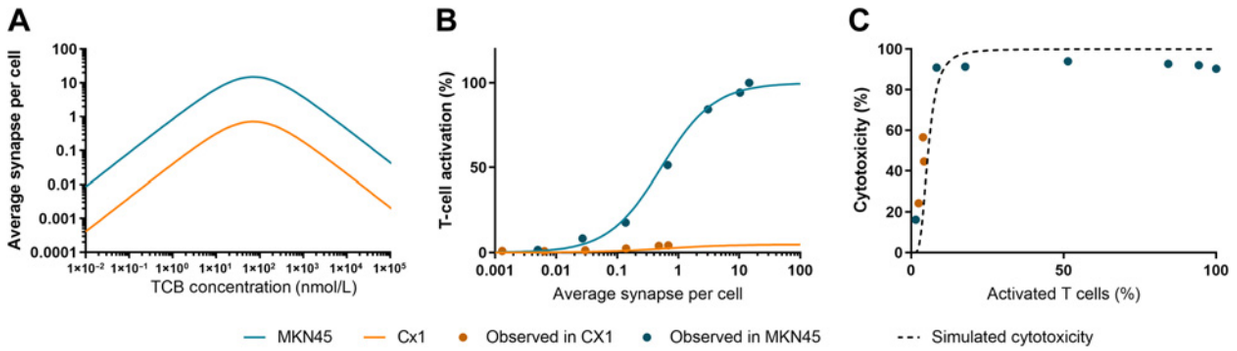


**Figure 6.**

Simulated differences in cibisatamab-induced effects between MKN45 and CX1 cell lines. **A,** Average immunologic synapse count formed per tumor cell in function of TCB concentration. **B,** Percentage of T-cell activation in function of synapse count per tumor cell. Simulations overlaid with observed T-cell activations in both cell lines. **C,** Maximal percentage of theoretical cytotoxicity in function of T-cell activation. Simulation (dashed line) overlaid with observed cytotoxicity for MKN45 (blue circles) and CX1 (orange circles) in function of the highest T-cell activation (in %) observed for each dose treatment group in both cell lines.

concentration (**Fig. 6A**), the relative T-cell activation as a function of synapses per cell (**Fig. 6B**) and the relative cytotoxicity as a function of activated T cells (**Fig. 6C**).

**Figure 6A** shows the predicted synapse per cell over a range of cibisatamab concentrations in MKN45 ($CEA^{high}$; **Fig. 6A**, blue curve) or CX1 ($CEA^{low}$; **Fig. 6A**, orange curve) cell line. For both cell lines, the profiles are parallel to each other with CX1 being 20-fold lower. In both cases, a bell-shaped profile is observed and the amount of immune synapse formed will increase with increasing TCB concentrations up to a maximal threshold, after which increasing TCB concentrations negatively affect synapse formation. In both cases, peak synapse formation occurs at a cibisatamab concentration of approximately 68 nmol/L.

The model suggests that stimulation of T cells depends on the number of immune synapses formed per tumor cell and on the target expression level, relative to a reference system. **Figure 6B** shows percent of T-cell activation as a function average synapses. Observed (symbols) and predicted (lines) data are shown for MKN45 (in blue) and CX1 (in orange). T-cell activation was expressed relative to the highest observed value of $CD25^+CD8^+$ cells, which was set to 100% and the respective maximal observed values from each treatment group was normalized accordingly. We observed the highest T-cell activation in the MKN45 cell line at 96 hours with 20 nmol/L cibisatamab and we took this value as 100% T-cell activation. We observed the highest T-cell activation in the CX1 cell line at 168 hours with 20 nmol/L cibisatamab. This level of activation corresponded to 4.3% of the maximal T-cell activation observed in MKN45. These fractions of T-cell activation were well in line with the simulated profiles (**Fig. 6B**). Although both cell lines differ strongly in maximal response with regards to T-cell activation, the model correctly predicted the relationship of T-cell activation and synapses per cell. Interestingly, for the same range of synapse per cell, the predicted and observed response of T-cell activation was much lower with CX1 as compared with MKN45. In line with proposed model, we concluded from these findings that the drug effect of cibisatamab on T-cell activation not only depends on number of synapses per cell but also on the relative CEA expression level.

The proposed model suggests that tumor cell killing depends on the increase in activated T cells over baseline levels, which is described as the increase in $CD25^+CD8^+$ T cells. We therefore explored the relationship between the cytotoxicity and maximal $CD25^+CD8^+$ T-cell counts. The highest observed concentration of $CD25^+CD8^+$ T cells was observed for 20 nmol/L cibisatamab in MKN45 and was set to 100% and normalized the maximal $CD25^+CD8^+$ for each treatment group and cell lines accordingly. **Figure 6C** shows good agreement between the predicted and observed cytotoxicity in function of maximal T-cell activation for each dose level.

## Discussion

In the presented work, we provided a mathematical model that extends the current knowledge on *in vitro* TCB activity by including a biomarker of T-cell activation. By linking ternary complex formation to T-cell activation, the proposed model predicts correctly a dose-dependent and transient increase in $CD25^+CD8^+$ T cells, which results into tumor cell killing observed in *in vitro* experiments with a high (MKN45) and a low (CX1) target expressing cell line tested over a broad range of cibisatamab concentrations. Furthermore, the model was capable of capturing the tumor lysis profile across a very broad range of CEA expression densities.

Bispecific antibodies redirecting T cells to kill tumor cells are a promising therapeutic modality in cancer immunotherapy. The mechanisms behind TCB mediated T-cell redirection and tumor cell killing have been investigated and it has been described that the initiation or extent of TCB activity is multifactorial as the bispecific antibody needs to bind both its binding partners before exerting its effect. Various mathematical models have been proposed to investigate these processes *in vivo* or *in vitro* and have been applied to address relevant questions related to the development of these modalities. We have expanded on existing models describing TCB activity by linking tumor cell killing to T-cell activation.

A common denominator between these models is the assumption that the formation of immunologic synapses is driving directly or indirectly the cytotoxic effects. T cells have been used as a link between synapse formation and tumor cell killing. These were either total T-cell counts (13) or a virtual pool of activated T cells without actual data (8, 11). In our study with cibisatamab, we used *in vitro* experiments to build a mechanistic model that integrates formation of synapses resulting into T-cell activation and tumor cell killing. The model captures the dynamics of tumor cell and $CD25^+$ cytotoxic T cells over time. It was successfully applied to predict cytotoxicity as a function of target expression and to predict the time course profiles of

activated T cells and tumor cell killing of a low expression cell line based on the modeling results using high expression cell line.

CD25 is the alpha-chain of the trimeric IL2 receptor and a known marker for T-cell activation [18]. CD25 expression is inducible on effector T cells and functions within auto- and paracrine feedback loops with IL2. Binding of IL2 to CD25 will result in receptor-mediated internalization of IL2, while also inducing higher expression of CD25 on the cell surface [19]. Therefore, we mechanistically linked T-cell activation—indicated by CD25 expression induction on the cell surface—to tumor cell killing in our model. We were capable to well describe killing of the high expressing tumor cell line as well as the associated T-cell activation.

The extent of synapse formation is dictated by the expression level of CD3 and tumor antigen, tumor cell concentration, the affinity of the TCB to both antigens, and the TCB concentration in the system. A change in antigen expression impacts the amplitude at which immune synapse can be formed as there will be more or less target available for the TCB to bind to. The TCB concentration has a more ambiguous impact on synapse formation. Higher TCB concentrations will increase synapse concentrations until the optimum is reached. TCB concentrations above that optimum promote the dimerization between TCB and a single antigen, rather than formation of ternary complexes (the actual immune synapses), as was discussed elsewhere (9, 14). The relationship between the binding affinities to both targets will determine at what TCB concentration the tipping point in synapse formation will occur. In the binding model that we used, the TCB concentration at which the bell-shaped curve peaks corresponds to the geometric mean of the bindings affinities from both binding arms (15). Therefore, information on binding affinities can inform on the TCB concentration range resulting in maximal synapses per cell, which may be relevant for experimentation. Our model suggests that ternary complex formation as well as T-cell activation and tumor lysis is decreased at high TCB concentration. However, it has not been shown experimentally and further *in vitro* tests could be conducted to confirm this hypothesis.

In this work, we used an *in vitro* system as this allows is to have a well-controlled environment to investigate the relationship between all elements of this complex pharmacological response. Our work is in line with previous findings showing that *in vitro* efficacy is closely related to target expression (3). Moreover, a clear threshold was observed *in vitro* at which the system switches from minimal to complete tumor killing, and which was well captured by the model. However, it should be noted that this quantitative insight may not reflect the clinically relevant threshold, which may be dependent on other factors and is beyond the scope of the work. CEA expression is the main differentiator in our model. Besides influencing how many immune synapses will be formed, CEA expression also directly affects the extent of T-cell activation in our model. Natural immune synapse formation is a very complex mechanism that involves many TCR–pMHC complexes clustering together in a small patch on the cell surface to induce T-cell activation (16). Size and stability of the cluster depends on the number of TCR–pMHC complexes that can be formed in that area (17, 18). Therefore, we hypothesized that the density of the TCB-targeted tumor antigen will affect the probability that sufficient immune synapses are formed in close proximity to elicit T-cell activation. As a result, cells with higher antigen densities have a higher chance to activate T cells when engaged. Consequently, a certain immune synapse density may exhibit more or less T-cell activation based on the target expression level. This peculiar dependency between target expression, immune synapse density, and T-cell activation predicted by the model is backed by the experimental data as depicted in **Fig. 6**. Conversely, tumor cell lysis is unambiguously linked to the extent of T-cell activation.

We predicted cytotoxicity in function of a broad range of CEA densities (**Fig. 5**). We included a Monte Carlo simulation to also account for the random effects captured by the model. As the simulation was run with system-related parameters taken from MKN45 such as $k_g$ and $K$ values, we allowed a higher level of individual variability on these parameters by fixing the random effects at 0.3.

Our simulation was capable of distinguishing responder from nonresponder cell lines based on CEA expressing level. Moreover, the simulation nicely captured the general profile of increasing cytotoxicity with expression level. Our model underpredicted a part of the responding cell lines, which accounts for 27.4% of the cell lines. Potential causes for this discrepancy are discussed below.

An immune response is a multifactorial process, whereas T-cell activation by formation of ternary complexes is the first step in TCB activity, and there are many processes that will impact T-cell activation and the interaction with tumor cells. The presence of costimulatory or inhibitory receptors may change the responsiveness of the system to TCB treatment. Interestingly, we observed an increase in PD1-positivity in the $CD8^+$ T cells from 10% to 70% over the course of the assay (Supplementary Fig. S3L), with a clear dose dependency. Differences in baseline levels of PD1 on T cells and PD-L1 on tumor cells could be one of the factors attributing to the variability in cytotoxicity between cell lines observed in **Fig. 5**. Higher levels of PD1 also suggest potential susceptibility to anti-PD1 therapy. The presence of regulatory T-cells (Tregs) may also dampen T-cell response. Baseline levels of Tregs could be one of the factors contributing to donor-to-donor variability. This warrants further investigation. The impact of anti-PD1 or other combination therapies to boost the immune response could be investigated with experiments, requiring further expansion of the model to capture these therapeutic conditions.

Bacac and colleagues showed that in tumor-bearing mice, tumors became PD-L1 positive upon cibisatamab treatment (3). Cibisatamab is also being studied in patients both as a monotherapy and in combination with anti-PD-L1 antibodies. Radiologic tumor shrinkage was observed in 50% of patients treated in combination with anti-PD-L1 therapy, as opposed to 11% of patients that only received monotherapy (7).

TCBs target antigens that are overexpressed in tumors. However, the prevalence of the antigen is often not tumor exclusive and it can be found at lower levels in healthy cells. This could result in the occurrence of on-target/off-tumor toxicities. In early drug discovery, the model presented here could help with selecting the best compound properties with respect to the expected antigen expression level in tumor and healthy cells.

Besides target expression described here, there are many more variables that influence TCB activity. Bluemel and colleagues showed that antigen size and epitope location affected TCB potency (19). More specifically, MCSP and EpCAM binding BiTE constructs showcased higher potency when targeting membrane-proximal epitopes and truncated variants of antigens.

TCB valency appears to play an important role. Cibisatamab is bivalent for CEA and monovalent for CD3e to increase tumor selectivity. Multivalency is commonly used to increase the functional affinity of a molecule and often also the potency. Besides that, target affinity has been shown to affect the biodistribution in mice (20).

Many different formats are currently under development (for overview see ref. 21). The effect of compound size and format on TCB activity is not well understood. However, they do play a big role in the PK and disposition of the TCB in the body. Depending on the

format, TCBs may have similar PK profiles as classical mAbs, or could differ massively (22). Ellerman performed an extensive review of the most well studied variables (23). The limitation of the current model is that it has been build and verified with one TCB molecule and further TCBs should be tested to evaluate if the model is generalizable and if it can be applied to predict the outcome of T-cell activation and killing for scenarios when the binding affinity is modified. In addition, the model assumes a simplistic binding model, which does not fully capture the bivalency of cibisatamab to the tumor target. Furthermore, the current binding model in place assumes independent binding of CD3 and tumor target to form trimolecular complexes, which is a simplified process assuming that the system is well stirred and no spatial organization between the different binding partners is taken into account.

The presented model can be used to investigate the impact of target expression on TCB activity, or which target affinity would be optimal for a given expression level. The model can be further expanded to be more broadly applicable. Betts and colleagues showed the translational value of implementing a systems model into a larger PKPD framework, by linking both PK and PD models together (10). As a result, they were able to calculate the concentration to reach tumor stasis in mice and predict TCB disposition in patients. Because our model takes TCB concentration as an input, it could be incorporated into a holistic PKPD framework, linking intratumoral TCB concentrations to T-cell activation and tumor cell killing. A model to capture tumor uptake of TCBs is being developed (Eigenmann, M. J.; unpublished data).

In general, such methodology can be used to derive relevant therapeutic indices for TCBs. To achieve this, the model needs to be supported by longitudinal data of tumor killing, T-cell activation and cytokine release.

Due to the inherently human-specific nature of TCBs, animal models are often not appropriate or limited to recapitulate the pharmacologic processes. The use of *in vitro*-based assays is therefore of increasing importance (24–26). Moreover, appropriate experimental design is seminal to maximize the gain from these *in vitro* studies. This work presents a synergy between modeling and experimentation, which helps to dissect complexity and decrease the amount of *in vitro* data required to quantify drug action.

Essentially, model development with *in vitro* data from a single tumor cell line and model verification with data from another tumor cell line with lower antigen density gave confidence in the ability to predict cytotoxicity over a broad range of antigen densities. The paradigm of learn-and-confirm proved to be sufficient to generate a model that is predictive for the *in vitro* activity of cibisatamab. A similar set-up can be performed for other T-cell bispecifics, allowing for simulation of efficacy under different target expression levels and characterization of a cytotoxic threshold.

## Authors' Disclosures

T. Lehr reports grants from Aspen Pharmaceuticals, grants from Boehringer Ingelheim, grants from Neovii, grants from Bayer, and grants from Apogenix outside the submitted work. No disclosures were reported by the other authors.

## Authors' Contributions

**A.J. Van De Vyver:** Conceptualization, software, formal analysis, visualization, methodology, writing–original draft. **T. Weinzierl:** Conceptualization, supervision, writing–review and editing. **M.J. Eigenmann:** Formal analysis, visualization, methodology, writing–review and editing. **N. Frances:** Software, methodology, writing–review and editing. **S. Herter:** Conceptualization, data curation, formal analysis, investigation, writing–review and editing. **R.B. Buser:** Data curation, formal analysis, investigation. **J. Somandin:** Data curation, formal analysis, investigation. **S. Diggelmann:** Data curation, formal analysis, investigation. **F. Limani:** Data curation, formal analysis, investigation. **T. Lehr:** Supervision, methodology, writing–review and editing. **M. Bacac:** Conceptualization, resources, supervision, writing–review and editing. **A.-C. Walz:** Conceptualization, supervision, visualization, methodology, writing–review and editing.

## Acknowledgments

This work was sponsored by F. Hoffmann-La Roche Ltd. The authors would like to thank colleagues from Roche Innovation Center Zürich; Anne Freimoser for kindly helping with the interpretation of the affinity data of cibisatamab; and Tanja Fauti for the fruitful discussions on the *in vitro* data sets and providing valuable feed-back.

The costs of publication of this article were defrayed in part by the payment of page charges. This article must therefore be hereby marked *advertisement* in accordance with 18 U.S.C. Section 1734 solely to indicate this fact.

Received April 24, 2020; revised August 3, 2020; accepted November 17, 2020; published first December 9, 2020.

## References

1. Yu L, Wang J. T cell-redirecting bispecific antibodies in cancer immunotherapy: recent advances. J Cancer Res Clin Oncol 2019;145:941–56.
2. Kaplan JB, Grischenko M, Giles FJ. Blinatumomab for the treatment of acute lymphoblastic leukemia. Invest New Drugs 2015;33:1271–9.
3. Bacac M, Fauti T, Sam J, Colombetti S, Weinzierl T, Ouaret D. A novel carcinoembryonic antigen T-cell bispecific antibody (CEA TCB) for the treatment of solid tumors. Clin Cancer Res 2016;22:3286–97.
4. Li J, Piskol R, Ybarra R, Chen Y-JJ, Li J, Slaga D, et al. CD3 bispecific antibody–induced cytokine release is dispensable for cytotoxic T cell activity. Sci Transl Med 2019;11:eaax8861.
5. Boudousquie C, Bossi G, Hurst JM, Rygiel KA, Jakobsen BK, Hassan NJ. Polyfunctional response by ImmTAC (IMCgp100) redirected CD8(+) and CD4(+) T cells. Immunology 2017;152:425–38.
6. Hammarstrom S. The carcinoembryonic antigen (CEA) family: structures, suggested functions and expression in normal and malignant tissues. Semin Cancer Biol 1999;9:67–81.
7. Gonzalez-Exposito R, Semiannikova M, Griffiths B, Khan K, Barber LJ, Woolston A, et al. CEA expression heterogeneity and plasticity confer resistance to the CEA-targeting bispecific immunotherapy antibody cibisatamab (CEA-TCB) in patient-derived colorectal cancer organoids. J Immunother Cancer 2019;7:101.
8. Campagne O, Delmas A, Fouliard S, Chenel M, Chichili GR, Li H, et al. Integrated pharmacokinetic/pharmacodynamic model of a bispecific CD3xCD123 DART molecule in nonhuman primates: evaluation of activity and impact of immunogenicity. Clin Cancer Res 2018;24:2631–41.
9. Jiang X, Chen X, Carpenter TJ, Wang J, Zhou R, Davis HM, et al. Development of a Target cell-Biologics-Effector cell (TBE) complex-based cell killing model to characterize target cell depletion by T cell redirecting bispecific agents. mAbs 2018;10:876–89.
10. Betts A, Haddish-Berhane N, Shah DK, van der Graaf PH, Barletta F, King L, et al. A translational quantitative systems pharmacology model for CD3 bispecific molecules: application to quantify T cell-mediated tumor cell killing by P-cadherin LP DART((R)). AAPS J 2019;21:66.
11. Chen X, Haddish-Berhane N, Moore P, Clark T, Yang Y, Li H, et al. Mechanistic projection of first-in-human dose for bispecific immunomodulatory P-cadherin LP-DART: an integrated PK/PD modeling approach. Clin Pharmacol Ther 2016;100:232–41.
12. Friberg LE, Henningsson A, Maas H, Nguyen L, Karlsson MO. Model of chemotherapy-induced myelosuppression with parameter consistency across drugs. J Clin Oncol 2002;20:4713–21.

13. Ferl GZ, Reyes A, Sun LL, Cheu M, Oldendorp A, Ramanujan S, et al. A preclinical population pharmacokinetic model for anti-CD20/CD3 T-cell-dependent bispecific antibodies. Clin Transl Sci 2018;11:296–304.
14. Schropp J, Khot A, Shah DK, Koch G. Target-mediated drug disposition model for bispecific antibodies: properties, approximation, and optimal dosing strategy. CPT Pharmacometrics Syst Pharmacol 2019;8:177–87.
15. Douglass EF Jr, Miller CJ, Sparer G, Shapiro H, Spiegel DA. A comprehensive mathematical model for three-body binding equilibria. J Am Chem Soc 2013; 135:6092–9.
16. Kupfer A. Signaling in the immunological synapse: defining the optimal size. Immunity 2006;25:11–3.
17. Manz BN, Jackson BL, Petit RS, Dustin ML, Groves J. T-cell triggering thresholds are modulated by the number of antigen within individual T-cell receptor clusters. Proc Natl Acad Sci U S A 2011;108:9089–94.
18. González PA, Carreño LJ, Coombs D, Mora JE, Palmieri E, Goldstein B, et al. T cell receptor binding kinetics required for T cell activation depend on the density of cognate ligand on the antigen-presenting cell. Proc Natl Acad Sci U S A 2005;102:4824.
19. Bluemel C, Hausmann S, Fluhr P, Sriskandarajah M, Stallcup WB, Baeuerle PA, et al. Epitope distance to the target cell membrane and antigen size determine the potency of T cell-mediated lysis by BiTE antibodies specific for a large melanoma surface antigen. Cancer Immunol Immunother 2010;59:1197–209.
20. Mandikian D, Takahashi N, Lo AA, Li J, Eastham-Anderson J, Slaga D, et al. Relative target affinities of T-cell-dependent bispecific antibodies determine biodistribution in a solid tumor mouse model. Mol Cancer Ther 2018;17: 776–85.
21. Spiess C, Zhai Q, Carter PJ. Alternative molecular formats and therapeutic applications for bispecific antibodies. Mol Immunol 2015;67:95–106.
22. Chen Y, Xu Y. Pharmacokinetics of bispecific antibody. Curr Pharmacol Rep 2017;3:126–37.
23. Ellerman D. Bispecific T-cell engagers: towards understanding variables influencing the in vitro potency and tumor selectivity and their modulation to enhance their efficacy and safety. Methods 2019;154:102–17.
24. Harper J, Adams KJ, Bossi G, Wright DE, Stacey AR, Bedke N, et al. An approved in vitro approach to preclinical safety and efficacy evaluation of engineered T cell receptor anti-CD3 bispecific (ImmTAC) molecules. PLoS One 2018;13: e0205491.
25. Dudal S, Hinton H, Giusti AM, Bacac M, Muller M, Fauti T, et al. Application of a MABEL approach for a T-cell-bispecific monoclonal antibody: CEA TCB. J Immunother 2016;39:279–89.
26. Mattson B, Menard K, Hamon D, Pizutti D, Chen E, Romero M, et al. Abstract A11: preclinical assessment of CD3 bispecific antibody efficacy: a comparison of humanized mouse models bearing xenografts and syngeneic mouse models using surrogate antibodies. Cancer Res 2018;78:A11.

***Manuscript 2***

# *A novel approach for quantifying the pharmacological activity of T-cell engagers utilizing in vitro time-course experiments and streamlined data analysis*

*Arthur Van De Vyver, Miro Eigenmann, Meric Ovacik, Christian Pohl, Sylvia Herter, Tina Weinzierl, Tanja Fauti, Christian Klein, Thorsten Lehr, Marina Bacac, Antje-Christine Walz*

Journal: AAPS journal

Publishing date: December 3rd 2021

DOI: 10.1208/s12248-021-00637-2

URL: https://link.springer.com/article/10.1208/s12248-021-00637-2

*The AAPS Journal* (2022) 247
https://doi.org/10.1208/s12248-021-00637-2

*Research Article*

# A Novel Approach for Quantifying the Pharmacological Activity of T-Cell Engagers Utilizing *In Vitro* Time Course Experiments and Streamlined Data Analysis

**Arthur Van De Vyver[1,2] · Miro Eigenmann[1] · Meric Ovacik[3] · Christian Pohl[4] · Sylvia Herter[4] · Tina Weinzierl[4] · Tanja Fauti[4] · Christian Klein[4] · Thorsten Lehr[2] · Marina Bacac[4] · Antje-Christine Walz[1,5]**

*Received 5 May 2021; accepted 11 August 2021*

***Abstract.*** CD3-bispecific antibodies are a new class of immunotherapeutic drugs against cancer. The pharmacological activity of CD3-bispecifics is typically assessed through *in vitro* assays of cancer cell lines co-cultured with human peripheral blood mononuclear cells (PBMCs). Assay results depend on experimental conditions such as incubation time and the effector-to-target cell ratio, which can hinder robust quantification of pharmacological activity. In order to overcome these limitations, we developed a new, holistic approach for quantification of the *in vitro* dose–response relationship. Our experimental design integrates a time-independent analysis of the dose–response across different time points as an alternative to the static, "snap-shot" analysis based on a single time point commonly used in dose–response assays. We show that the potency values derived from static*in vitro* experiments depend on the incubation time, which leads to inconsistent results across multiple assays and compounds. We compared the potency values from the time-independent analysis with a model-based approach. We find comparably accurate potency estimates from the model-based and time-independent analyses and that the time-independent analysis provides a robust quantification of pharmacological activity. This approach may allow for an improved head-to-head comparison of different compounds and test systems and may prove useful for supporting first-in-human dose selection.

**KEY WORDS:** CD3-bispecifics; *in vitro* dose–response; MABEL; PKPD; quantitative pharmacology

## INTRODUCTION

CD3-bispecific antibodies are a growing class of promising therapies in the field of immuno-oncology (1). Since the clinical success with blinatumomab—a CD19 × CD3-bispecific antibody that was approved by the FDA in 2014 for acute lymphoblastic leukemia (2, 3)—a variety of different CD3-bispecific antibodies or antibody fragments have been designed. More than 200 CD3-bispecifics are currently in development as novel cancer immunotherapies (1, 4). CD3-bispecifics activate an anti-cancer immune response by redirecting T-cells to the tumor (5), with promising anti-cancer activity (6–8) in both hematological (9) and solid (10) tumors.

The pharmacological response is based on tumor antigen recognition combined with CD3-mediated T-cell recruitment. This involves a cascade of events including T-cell

**Supplementary Information** The online version contains supplementary material available at https://doi.org/10.1208/s12248-021-00637-2.

Arthur Van De Vyver and Miro Eigenmann authors contributed equally.

[1] Roche Pharma Research & Early Development, Pharmaceutical Sciences, Roche Innovation Center Basel, Grenzacherstrasse 124, CH-4070 Basel, Switzerland
[2] Department of Clinical Pharmacy, Saarland University, Saarbrücken, Germany
[3] Preclinical Translational Pharmacokinetics, South San Francisco, CA, Genentech, USA
[4] Roche Pharma Research and Early Development, Roche Innovation Center Zürich, Wagistrasse 10, 8952 Schlieren, Switzerland
[5] To whom correspondence should be addressed. (e–mail: antje-christine.walz@roche.com)

Published online: 03 December 2021

activation and proliferation, cytokine release with involvement of innate immune cells, and T-cell-mediated tumor lysis (11–13)—distinct biological processes that occur on different time scales (14–16). CD3-bispecifics' efficacy (tumor cell toxicity) and safety (*e.g.*, cytokine release) are both related to the mechanism of action. These effects can be investigated*in vitro* as a basis for determining the minimum anticipated biological effect level (MABEL) dose for first-in-human (FIH) clinical trials (17). Due to the lack of cross-reactive animal species for some of the CD3-bispecifics (18–20),*in vitro* test systems are often utilized for pharmacological profiling of this class of molecules (20). In addition,*in vitro* analysis is suited to differentiate and to select compounds and is—in conjunction with in vivo PK/PD analysis—an important pillar for human PK/PD prediction (21).

The appropriate pharmacological quantification*in vitro* may help to improve the therapeutic index of these immune agonists, allowing for the selection of the most favorable compounds during early drug discovery. Appropriate quantification is also critical for predicting a clinically relevant, safe, and pharmacologically active starting dose that will reduce the number of patients exposed to subtherapeutic dose levels in FIH studies. This is a key challenge for CD3-bispecific therapy development (17). Based on a retrospective assessment of 17 CD3-bispecifics, Saber and colleagues conclude that there is no generalizable approach for MABEL-based dose selection applicable to all CD3-bispecifics (17). They highlight that FIH dose selection based on 30%*in vitro* pharmacological activity of the most sensitive readout results in doses that are substantially lower than the optimal biological dose, the recommended human dose, or the maximum tolerated dose in patients. In addition, a 2018 FDA workshop on the preclinical and translational safety assessment of CD3-bispecifics concluded that it is still unclear which*in vitro* experimental conditions (*e.g.*, effector-to-target ratio, target cell choice, assay duration, assay endpoints) are most appropriate for quantitative clinical translation and FIH starting dose prediction (22).

In the presented study, we suggest a modified experimental design and data analysis to explore and leverage*in vitro* data and to derive a more robust pharmacological quantification and a more appropriate integration of the multiple drug-induced PD responses that occur on different time scales. Often, the*in vitro* quantification of CD3-bispecifics is done at a single time point. The derived potency value is highly dependent on the incubation time and susceptible to time point selection bias. Consequently, the apparent potency for a specific compound varies from time point to time point (23). We demonstrated that the dose–response analysis derived from static*in vitro* experiments, as traditionally applied, depends on the incubation time and that this "snap-shot" analysis leads to inconsistent results. To overcome this limitation, we developed a more holistic approach for quantification of the*in vitro* dose–response relationship that considers the time course of the pharmacodynamic (PD) responses and that enables*in vitro* comparison of different readouts (*e.g.*, cytokine release and cytotoxicity) or of different test systems (*e.g.*, cancer cell line, organoids from a tumor or healthy tissue). This approach includes an*in vitro* experimental design that allows us to monitor the time course of the pharmacological responses and a subsequent time-independent dose–response analysis integrating all measured time points (24). As a result, we obtain a more robust readout that provides more consistent insights into the pharmacological activity of CD3-bispecifics. We also developed an automated data analysis workflow that can be applied to these large datasets. Finally, we illustrate how the proposed approach can be implemented to compare the pharmacological activity across test systems and compounds and how these pharmacological insights can be utilized in early drug discovery and development.

## MATERIALS AND METHODS

### Materials

The CD3-bispecifics (also called T-cell bispecifics; TCBs) CEA-TCB (cibisatamab), CEACAM5-TCB, and the FolR1-TCB affinity variants were produced in-house (Roche, Basel, Switzerland). Compound characteristics are summarized in Table I. The full list of all materials, cell lines, and reagents can be found in supplemental section S1.1.

### Methods

#### *Generation of Stably Transduced Cell Lines Expressing Human FolR1*

HEK 293 T cells were transduced with lentiviral particles to express human folate receptor 1 (FolR1) on their cell membrane. A high ($FolR1^{high}$) and a low ($FolR1^{low}$) target-expressing variant was created, with a surface density of 505,000 and 20,000 molecules/cell, respectively. Details on the generation of the stably transduced cell lines are summarized in supplemental section S1.2. Cell surface density of FolR1 was determined by QIFIKIT (Agilent Dako).

#### *Experimental Design of T-Cell-Dependent Cellular Cytotoxicity Assay*

The*in vitro* pharmacology of cibisatamab and CEACAM5-TCB was tested with a T-cell-dependent cellular cytotoxicity (TDCC) assay and flow cytometric analysis for tumor lysis

**Table I** Summary of Tested CD3-Bispecifics

| Compound | Molecular weight (KDa) | Avidity to TA (nM) | Affinity to CD3 (nM) |
|---|---|---|---|
| CEA-TCB | 194 | 48.6[a] | 3.7[b] |
| CEACAM5-TCB | 194 | 13.12[a] | 3.7[b] |
| FolR1$^{high}$-TCB | 194 | 2.2[b] | 3.7[b] |
| FolR1$^{low}$-TCB | 194 | 60[b] | 3.7[b] |

[a]Determined with FRET as described in Van De Vyver et al. (25). [b]Determined with surface plasmon resonance; *TCB*, T-cell bispecific; *kDa*, kilodalton; *TA*, tumor antigen

and immune-phenotyping. Additionally,*in vitro* pharmacology of FolR1-TCB variants was tested with an alternative TDCC method that included real-time monitoring of fluorescent tumor cells by incuCyte.

*FACS Based Assay to Monitor Tumor Cell Count After Treatment with Cibisatamab and CEACAM5-TCB* The experimental protocol for*in vitro* activity testing of cibisatamab has been previously described (25). This protocol was also applied to the*in vitro* testing of CEACAM5-TCB. Briefly, two cell lines expressing the oncofetal antigen CEA (carcinoembryonic antigen), MKN45 (high copy number: 230,000–690,000 CEA per cell) and CX1 (low copy number: 2000–11,000 CEA per cell), were seeded at a density of 30,000 cells/well in an effector-to-target ratio of 10:1 with human PBMCs and incubated at varying concentrations of cibisatamab (0, 6, 32, 160, 800, 4000, 20,000, & 100,000 pM) or CEACAM5-TCB (0, 1, 6, 32, 160, 800, 4000, & 20,000 pM). At 24 h, 48 h, 72 h, 96 h, and 168 h, supernatants were collected for cytokine analysis, and cell pellets were used for flow cytometric analysis. FACS analysis was performed for tumor cell counting and immune-phenotyping of T-cells on the expression of CD3, CD4, CD8, CD25, PD-1, and TIM-3.

*IncuCyte Assay to Monitor Tumor Cell Cytotoxicity with FolR1-TCB* Staining of tumor cells and PBMCs compatible with incuCyte imaging was performed as per the manufacturer's instructions (Sartorius). IncuCyte NucLight Rapid Red was used to fluorescently label the nucleus of HEK cells.

A total of 10,000 FolR1-expressing FolR1$^{high}$ or FolR1$^{low}$ tumor cells were seeded in flat-bottom 96-well plates and co-cultured with 100,000 PBMCs in assay medium (RPMI1640 + 20% FCS + 1% GlutaMax). Dilutions of either a high-affinity or a low-affinity FolR1-TCB were added to reach the final drug concentrations (0.5, 5, 50, 500, 5000, and 50,000 pM). For the negative control, 50 µL of assay medium was added. All conditions were performed in triplicate. The co-cultures were incubated over 4 days in a Sartorius incuCyte Zoom (humidified, 37 °C, 5% $CO_2$) for automated imaging at 3-h intervals. All co-cultures were duplicated fivefold to allow for supernatant sampling at 18 h, 44 h, 68 h, and 94 h.

*Cytokine Measurements*

At the indicated time points (18 h, 44 h, 68 h, and 94 h), the plates were centrifuged and 25 µL of supernatant was collected from each well. Cytokines IL2, IL6, IL10, IFNγ, and TNFα were measured with a multiplexed cytometric bead array.

*Statistics and Data Analysis* Experiments were performed in triplicate and data were processed as median values. Where applicable, the experimental data are reported as mean values with corresponding standard error (SEM). Values that are below their lower limit of quantification (LLOQ) are reported as ½ LLOQ. Estimated dose–response parameters are reported with their respective relative standard error (%RSE).

*Dose–Response Analysis*

Dose–response curves were generated based either on a single time point or on the time-independent PD effect using WinNonlin (Phoenix 8.2, Certara). This time-independent response is computed as an area under the curve of effect (AUCE) in the readout for the PD response over time for each tested TCB concentration. For estimation of the potency parameter $EC_{50}$, a simple or inhibitory sigmoidal model was fitted to the data (Eq. (1)).

$$E = E_0 + \frac{E_{max} * TCB^{\gamma}}{EC_{50}^{\gamma} + TCB^{\gamma}} \quad (1)$$

$E$ is the value of the experimental readout. In static analysis, $E$ is the actual readout, and in time-independent analysis, $E$ is either the calculated $AUCE$ value of the readout or the maximum value ($R_{max}$) of the readout. $TCB$ is the independent variable, corresponding to the concentration of the CD3-bispecific. $E_0$ is the baseline level of the readout or $AUCE$, $E_{max}$ is the maximum change in $E$, $\gamma$ is the Hill coefficient, and $EC_{50}$ is the drug concentration resulting in a half-maximum effect. An additive residual error was used to fit Eq. (1) to the respective experimental data. Based on Eq. (1), the concentration leading to 30% pharmacological activity ($PA_{30\%}$) was derived as follows:

$$PA_{30\%} = EC_{50} * \left(\frac{30\%}{100\% - 30\%}\right)^{\frac{1}{\gamma}} \quad (2)$$

If a sigmoidal dose–response relationship could not be established, a threshold concentration was estimated by fitting the data to the hockey-stick model (26) (Eq. (3)).

$$E = E_0 + S * \left(TCB - TCB_{threshold}\right) * P^{+} \quad (3)$$

$TCB_{threshold}$ is the threshold drug concentration for eliciting the PD effect above baseline ($AUCE_0$) and $S$ is the change in effect when the drug concentration is greater than the threshold value. $P^{+}$ is a derived variable that is zero when drug concentration is below the threshold concentration and one when the drug concentration is above the threshold concentration.

*Automated Dose–Response Analysis with Python* An automated dose–response analysis was conducted using Python. The data file was curated using *pandas* library. The Python code is provided in a GitHub repository (https://github.com/PKPD-coder/time-independent_analysis_in_vitro.git) and can be updated for other datasets. The workflow of the automated analysis is illustrated in Figure S1. Further details are summarized in supplemental section S2.

*Predicting Tumor Growth Inhibition with PK/PD Modeling*

The observed cell counts from cibisatamab and CEACAM5-TCB were fitted to a delayed tumor kill model (27) in Monolix (version 2019R2, Lixoft, France) to estimate the respective $EC_{50}$ values of tumor cytotoxicity. The tumor growth model (Eq. (8)) assumes a logistic tumor growth with $k_g$ representing the tumor growth rate and K the carrying capacity, which can be interpreted as the maximum tumor cell number that can be reached. The drug effect ($k_{el}$) is based on a sigmoidal dose–response relationship (Eq. (4)) with $E_{max}$ representing maximum cytotoxicity and $TCB$ representing the actual drug concentration. A delayed drug effect is assumed and described by means of three transit compartments (Eqs. (5)–(6)) with $\boldsymbol{\tau}$ describing the transit kinetics (27). The model parameters (fixed effects) were estimated and the standard errors of the random effects were fixed to 10% during model fitting. A combined error model was used.

$$k_{el} = E_{max} * \frac{TCB}{EC_{50} + TCB} \quad (4)$$

$$dk_1/dt = \frac{1}{\boldsymbol{\tau}} * (k_{el} - k_1) \quad (5)$$

$$dk_2/dt = \frac{1}{\boldsymbol{\tau}} * (k_1 - k_2) \quad (6)$$

$$dk_3/dt = \frac{1}{\boldsymbol{\tau}} * (k_2 - k_3) \quad (7)$$

$$k_1\,(0) = k_2\,(0) = k_3\,(0) = 0$$

$$dTumor/dt = k_g * \left(1 - \frac{Tumor}{K}\right) - k_3 * Tumor \quad (8)$$

*Trimeric Complex Prediction*

The concentration of trimeric complexes formed between the tumor target, CD3 and CD3-bispecific antibody, was estimated under quasi-equilibrium assumptions and based on the equations derived by Schropp and colleagues (28). The corresponding equations are summarized in supplemental section S3 (Eq. S1-S7). A Python script is provided in order to perform the calculation (https://github.com/PKPD-coder/time-independent_analysis_in_vitro.git).

## RESULTS

### *In Vitro* Dose–Response Analysis

Using a TDCC assay, we assessed the PD effects of cibisatamab (CEA-TCB) on MKN45 tumor cell lines expressing CEA, co-cultured with human PBMCs *in vitro*. The *in vitro* kinetics of tumor cell cytotoxicity, cytokine release, and T-cell activation induced by cibisatamab are shown in Fig. 1 and Figure S2. Cytokine release is shown for IL2 (Fig. 1a) and IL6 (Fig. 1b), as well as IL10, IFNγ, and TNFα (Figure S2). T-cell activation was monitored by measuring $CD8^{+}CD25^{+}$ T-cells (Fig. 1c). Tumor cell killing was captured by monitoring the tumor cell count dynamics in the absence and presence of the drug (Fig. 1d).

For all tested PD readouts, we observed a clear dose–response. PD effects increased with increased drug concentration. Each readout displayed a maximum response at a different time point. Table II summarizes the observed maximum response time ($t_{max}$) for each readout. IL2 had the fastest response, with a maximum release at the first observed time point (24 h) at all drug concentrations followed by a rapid decline in the presence of constant drug exposure. However, T-cell activation increased over time, reaching a maximum level of activation in $CD8^{+}CD25^{+}$ T-cells at 96 h, when IL2 levels were no longer detectable. We observed measurable IL6 released at each time point, with peaks occurring between 48 and 96 h depending on the drug concentration, followed by a slow decrease in IL6 concentration. IL10 (Figure S2H) and IFNγ (Figure S2J) showed a similar release pattern to IL6, while TNFα (Figure S2I) showed a similar release pattern to IL2, with a peak after 24 h followed by a rapid decrease.

The results of the static dose–response analysis are displayed in the insets of Figs. 1a–d showing time-dependent $EC_{50}$ values observed for various PD readouts. Notably, the

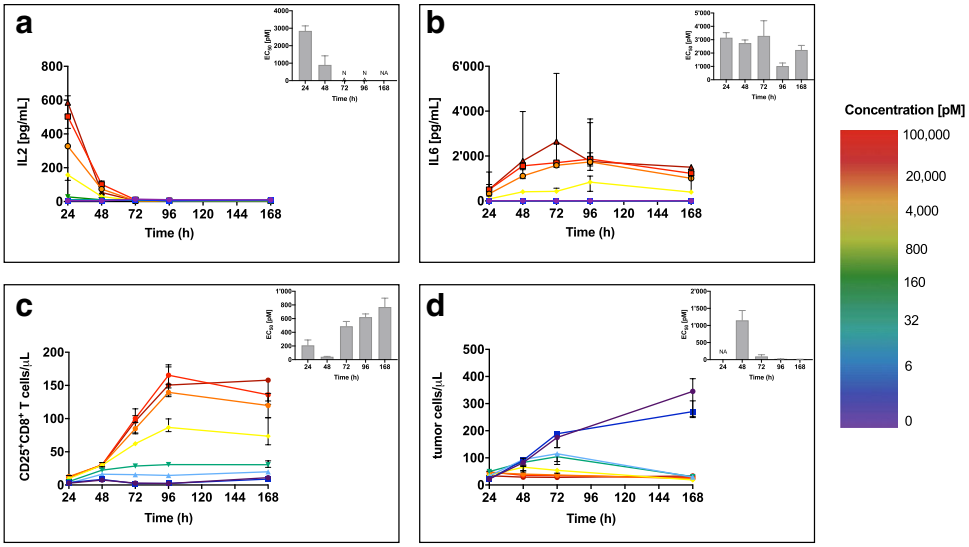


**Fig. 1** Time course of pharmacodynamic response of cibisatamab tested in a T-cell-dependent cytotoxicity assay on MKN45 tumor cells co-cultured with human PBMC (E:T 10:1). Dose–response over time is shown for **a** IL2 release; **b** IL6 release; **c** T-cell activation measured as CD25 + CD8 + T-cells; and **d** drug-related tumor cell cytotoxicity. The static $EC_{50}$ potency estimates for each time point are displayed in the inset plots. Results are shown as the median and range of the replicates

$EC_{50}$ estimates for each readout varied between 3- and 110-fold across the different time points.

## Time-Independent Quantification of Drug Response

Subsequently, we performed a time-independent, two-step *in vitro* analysis to quantify and compare the dose–response on the various PD readouts of the TDCC assays (Fig. 2). We illustrate this approach for IL6. First, we compute the time-independent PD effect as the area-under-the-effect-curve (AUCE) with the trapezoidal rule (Fig. 2a and inset equation). We then fit a sigmoidal drug effect model to the drug concentration-AUCE curve (Fig. 2b). We overlaid this curve with the dose–response of IL6 release ($R_{max}$), indicating that there is good agreement between estimated exposure–response relationships derived based on AUCE and $R_{max}$ for IL6. Table II summarizes the estimated $EC_{50}$ values and corresponding Hill coefficients. Figure 2c shows the overlay of the derived pharmacological profiles of tumor cytotoxicity, T-cell activation, and IL2 and IL6 release. Furthermore, for all tested readouts, the dose–response relationship was similar when the time-independent or the maximum effect was used (supplemental Figure S3).

In the tested time frame, tumor cytotoxicity (Fig. 2c, red curve) was the most sensitive readout for cibisatamab, with an $EC_{50}$ 38-fold lower than T-cell activation and approximately 145- and 96-fold lower than IL2 and IL6 release, respectively. In the tested *in vitro* system, maximum tumor cytotoxicity ($IC_{99}$) was reached at a concentration of 155 pM cibisatamab, which approximately corresponds to the $EC_5$ for IL2 and IL6 release.

**Table II** Dose–Response Analysis of Cibisatamab Tested on MKN45, Time of Maximal Response, and Dynamic Potency

| Parameter | $T_{max}$ (h) | EC50 (pM) (%RSE) | Hill coefficient (%RSE) |
|---|---|---|---|
| Activated cytotoxic T-cells ($CD25^+CD8^+$) | 96 | 596 (13) | 0.91 (11) |
| Tumor cell cytotoxicity | 96 | 15.7 (27) | 2.07 (31) |
| IL2 | 24 | 2280 (16) | 1.19 (17) |
| IL6 | 72 | 1501 (16) | 1.28 (17) |
| IL10 | 48 | 1890 (17) | 1.09 (16) |
| TNFα | 24 | 1437 (19) | 0.88 (15) |
| IFNγ | 48 | 409 (3.0) | 1.49 (3.0) |
| $CD4^+CD25^+$ | 96 | 686 (5.0) | 1.24 (5.0) |
| $CD4^+PD1^+$ | 168 | 545 (9.0) | 1.22 (10) |

$T_{max}$, time of maximal response; *%RSE*, relative standard error in percentage

## Accuracy of AUCE-Based Method to Estimate $EC_{50}$

We compared the results of the time-independent dose–response analysis to those obtained using a model-based approach (22). For this exercise, we considered the tumor cytotoxicity of two drugs with low (cibisatamab, $K_D = 48.6$ nM) and high (CEACAM5-TCB, $K_D = 13.1$ nM) binding affinities for the same tumor target (CEA). We tested the drugs on two different cell lines with low (CX1) and high (MKN45) target expression levels allowing for four separate comparisons.

We monitored the drugs' effect on perturbation of tumor cell growth dynamics by measuring tumor cell count with FACS and used this as a basis to quantify tumor cell cytotoxicity and drug activity. We derived the model-based potency parameters by fitting the model (Eqs. (4)–(5)) to the observed tumor cell count data for all four scenarios. Figure 3a shows the $EC_{50}$ estimates with the corresponding %RSE values represented as horizontal error bars. Since the mathematical model effectively captures the pharmacodynamic effects

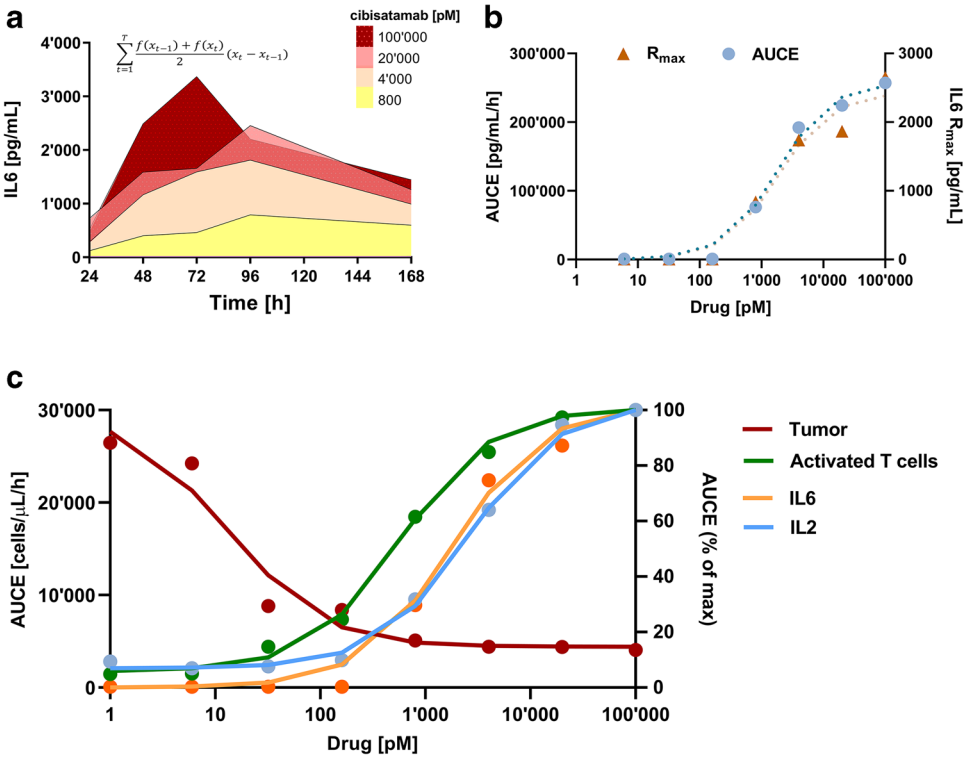


**Fig. 2** Time-independent analysis workflow example for cibisatamab. **a** Integration with trapezoidal interpolation (inset equation) of dose–response curves for IL6 release over time yields individual area-under-the-effect-curve (AUCE; shaded areas) for each TCB concentration. **b** Overlay of dose–response curves for IL6 release based on AUCE (blue circles) or maximum response ($R_{max}$, orange triangle). **c** Time-independent dose–response comparison between tumor cell cytotoxicity (red), T-cell activation (green), IL2 (blue), and IL6 (orange) release

over time of all four scenarios and model-misspecification was excluded, we regard the estimated $EC_{50}$ value as a good approximation of the "reference" potency, which can be used as a benchmark for the static and time-independent analysis. The estimated parameters and %RSE values are summarized in supplemental table S1. The model fit and observed data are shown in Figure S4.

Finally, we assessed the accuracy of the AUCE-based analysis and compared the corresponding $EC_{50}$ values from all four tested scenarios to those estimated by model fitting (Fig. 3a). All four $EC_{50}$ values are at the line of identity, suggesting good agreement between the AUCE-based potency values and the model-derived method. The same method was applied to assess the accuracy of the static approach considering all four time points (Fig. 3b). In three out of the four scenarios tested, the variability of the potency estimates between the time points spanned multiple orders of magnitude; 25% of values deviated more than fivefold from the model-based estimate.

## Time Course Analysis Using Transfected Cell Lines

As a next step, we tested an *in vitro* image-based TDCC kinetic assay that also incorporated cytokine kinetic profiling as a less labor-intensive alternative to flow cytometry-based methods. We measured tumor cell cytotoxicity via live-cell imaging (incuCyte), which enables real-time visualization of viable tumor cells transfected with a red

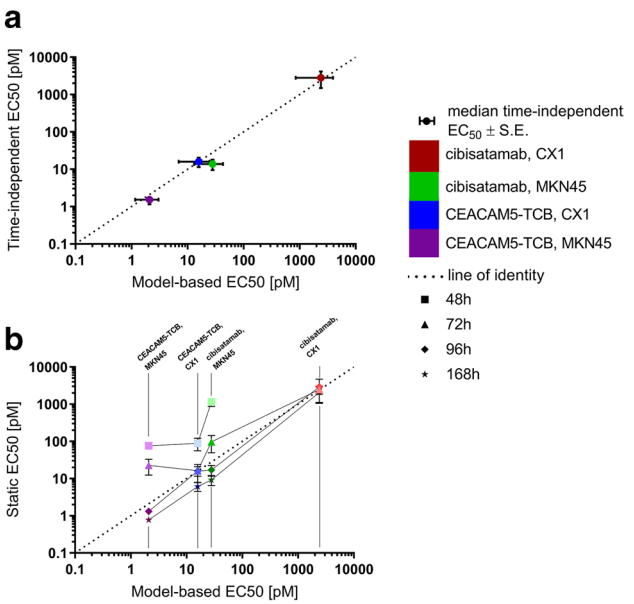


**Fig. 3** Comparison of tumor cell-killing potency ($EC_{50}$) of cibisatamab and CEACAM-TCB, tested on CX1 and MKN45 tumor cell lines derived by modeling (displayed on the x-axis; %RSE are shown as horizontal error bars): **a** time-independent $EC_{50}$ derived from AUCE (displayed on the y-axis; %RSE is shown as vertical error bars) or **b** static $EC_{50}$ per given time point (displayed on the y-axis; % RSE is shown as vertical error bars)

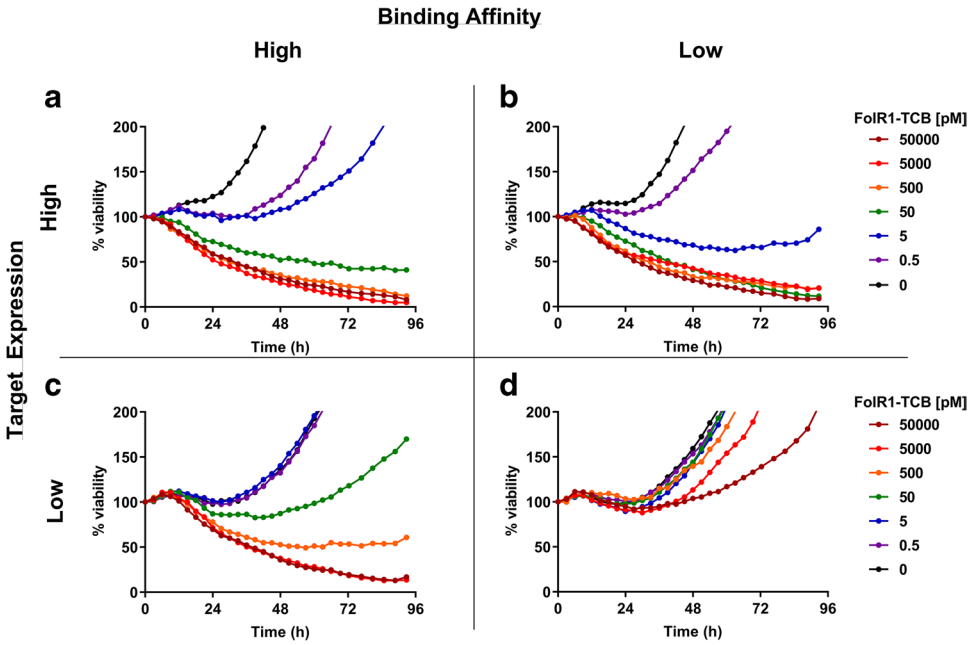


**Fig. 4** Time course profiles of tumor cells treated with high (**a**, **c**) and low (**b**, **d**) affinity FolR1-TCB on HEK transduced cell lines with high (**a**, **b**) and low (**c**, **d**) FolR1 expression. For better visualization of the higher doses, the y-axis is truncated at 200% viability. The complete plots can be found in Figure S6. The profiles of cytokine release are summarized in Figure S7

fluorescent protein (RFP) with fluorescence microscopy at standard cell culture conditions (humidified, 37 °C, 5% $CO_2$). We tested two different CD3-bispecific drugs with high ($K_D$ = 2.2 nM) and low ($K_D$ = 60 nM) binding avidity for FolR1 (FolR1-TCBs) and assessed their pharmacological activity on RFP-transfected HEK cells with low (20,000 FolR1/cell) and high (505,000 FolR1/cell) expression levels co-cultured with PBMCs from a healthy donor. Figure 4 shows the time course profiles of tumor cell cytotoxicity reported as percent viable cells. In all tested scenarios, there was a clear dose–response. We observed maximum tumor cell cytotoxicity in all cases except when the low-affinity FolR1-TCB was incubated with the low FolR1-expressing cell line, which did not result in either measurable tumor cell cytotoxicity or cytokine release. In all four cases, we observed an early decrease in viability occurring over the first 24 h followed by a recovery and regrowth of the tumor cells except for the higher concentrations. The time course of different readouts as well as the time that it takes to reach the maximal effect ($T_{max}$) varies across readouts and test systems (Fig. 1, Table II, Supplemental table S2). As a consequence, the estimated potencies may also vary across the different time points, as illustrated for TNFα (Supplemental figure S5).

The time span between the decrease in viability and the recovery was different for each scenario. The longest time to regrowth was observed for the high-affinity FolR1-TCB on a high expression cell line. In addition, we quantified the dose-responses of all four scenarios with the time-independent analysis of cytokine release. These results are summarized in Table III and displayed in Fig. 5.

As an illustrative example of how to assess a molecule's therapeutic index, we compared the dose-responses of efficacy and safety readouts of the high- and low-affinity variant of FolR1-TCB on high and low target-expressing cells. Here, we again used tumor cell cytotoxicity as a readout for efficacy. For safety, we used IL6 release, assuming that, in this case, IL6 release is a relevant safety marker of on-target toxicity. When comparing the dose–response on the high expression cell line (Fig. 5a), both affinity variants have a similar potency for tumor lysis whereas the high-affinity compound has an eightfold higher potency for IL6 release associated with an approximately twofold higher maximum release (higher $E_{max}$).

**Table III** AUCE Dose–Response Analysis of FolR1-TCB Affinity Variants Tested on Transfected HEK Cells with High and Low FolR1 Expression

| Test system | Tumor cell cytotoxicity $EC_{50}$ (pM) (%RSE) | Hill (%RSE) | IL6 release, $EC_{50}$ (pM) (%RSE) | Hill (%RSE) |
|---|---|---|---|---|
| Low-affinity FolR1-TCB, low target expression | N.I | N.I | N.I | N.I |
| High-affinity FolR1-TCB, low target expression | 30.1 (63) | 1 (57) | N.I | N.I |
| Low-affinity FolR1-TCB, high target expression | 0.42 (15) | 1.3 (35) | 1026 (36) | 0.63 (18) |
| High-affinity FolR1-TCB, high target expression | 0.28 (43) | 0.35 (22) | 116 (26) | 1.3 (23) |

*N.I.*, not identifiable; *na*, not applicable

As a second illustrative example of how to assess the selectivity of a compound between high and low target expression, we compared the changes in pharmacological activity of both FolR1-TCB variants based on target expression (Fig. 5b and c). The high-affinity variant (Fig. 5b) induced maximal tumor lysis in both cell lines, whereas the low-affinity variant (Fig. 5c) showed selective tumor cell cytotoxicity with no effects on the low-expression cell line and maximal cytotoxicity in the high expression cell line.

More specifically, the high-affinity FolR1-TCB was approximately 100-fold more potent towards the high expression tumor cell line compared with the low-expression line (Fig. 5b). Furthermore, a 40-fold higher maximum IL6 response was observed for the high expression cell line. For the low-expression cell line, a sigmoidal model could not be fitted. A threshold concentration for IL6 release was observed to be 500 pM. The dose–response analysis of low-affinity FolR1-TCB targeting high- and low-expression cells (Fig. 5c) showed that there was only minimal tumor lysis and no IL6 release in the low-expression cell line, suggesting that low-expression tissues would be minimally targeted by the low-affinity variant.

In addition, we calculated the theoretical trimeric complexes at the corresponding $EC_{50}$ (table S3) of both binders in the high expression cell line (Eq. S1-S7, supplemental section S3). As a result, a 20-fold higher trimeric complex concentration is estimated for the high-affinity binder.

### Retrospective MABEL Dose Prediction for Cibisatamab

In order to illustrate the value of the time-independent PK/PD analysis, we conducted a retrospective dose prediction based on the dataset and results for cibisatamab presented in this manuscript (Fig. 2, Table II). The retrospective MABEL dose was based on $PA_{30\%}$ of IL6 release in the high CEA-expression cell line (MKN45), which was the same cell line as previously used to derive the FIH starting dose (19). The $PA_{30\%}$ of IL6 release was calculated (Eq. (2)), with the estimated $EC_{50}$ and the corresponding Hill coefficient (Table II). The MABEL dose is predicted to result in a $C_{max}$ (maximal serum concentration) that corresponds to this pharmacological readout. Assuming that the dose of cibisatamab dissolves initially in the human serum with a typical volume of 3000 mL (29), a predicted MABEL dose of 450 µg is obtained (Table IV).

## DISCUSSION

In the present study, we propose a simple yet comprehensive method for accurately quantifying the pharmacological activity of CD3-bispecific antibodies. The cascade of events

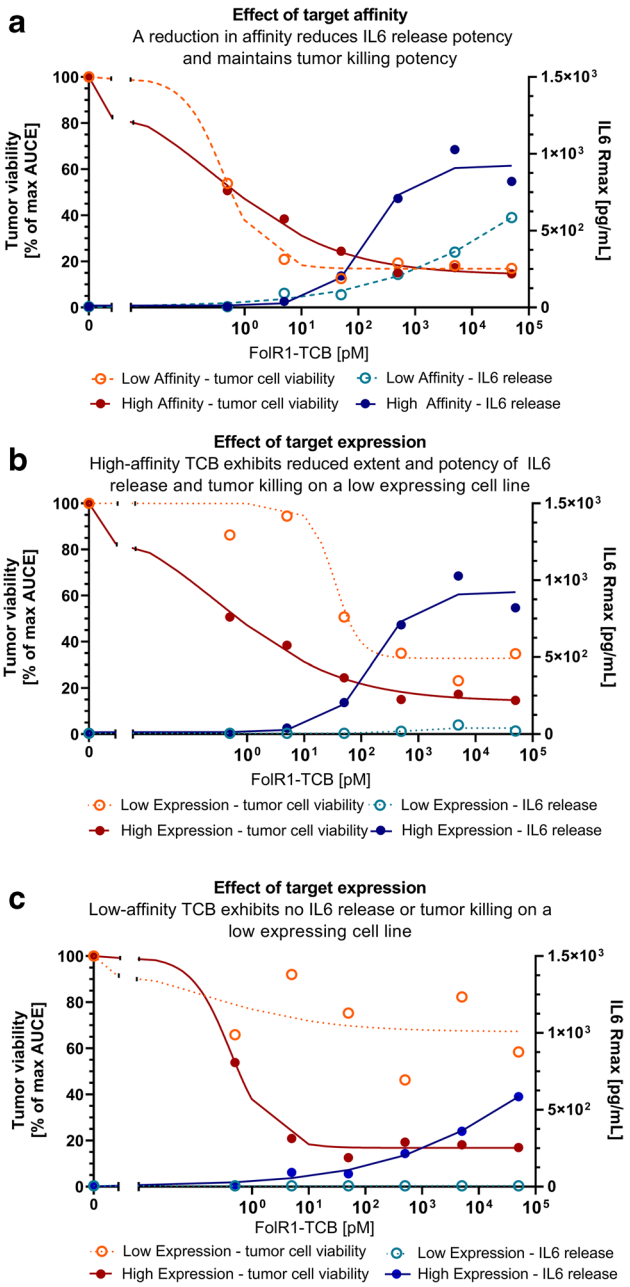


**Fig. 5** Time-independent dose-responses of high- and low-affinity FolR1-TCB variants tested in high- and low-expression cell lines. Dose–response of tumor cell cytotoxicity is expressed as the cumulative effect of tumor cell viability normalized to the control group (% of max AUCE, orange symbols, left y-axis) and dose–response of IL6 release is shown as the maximum response ($R_{max}$, blue symbols, right y-axis). Symbols have been overlaid with the sigmoidal model fit of the data (solid/dotted lines). **a** Head-to-head comparison of high-affinity FolR1-TCB (solid circles) and low-affinity FolR1-TCB (open circles) tested on a high-expressing tumor cell line. **b** Head-to-head comparison of dose–response with high-affinity FolR1-TCB tested on a high (solid circles) and low (open circles) expressing cell line. **c** Head-to-head comparison of dose–response with low-affinity FolR1-TCB tested on a high (solid circles) and low (open circles) expressing cell line

that lead to drug-induced cytotoxicity and cytokine release (11–13) can be investigated *in vitro* as a basis for determining the MABEL dose for FIH clinical trials (17). In a recent FDA guidance (30) on the development of bispecific antibodies with agonistic properties, reference is made to the FDA's retrospective dose prediction of CD3-bispecifics (17) using *in vitro* assays. These are often done at a single time point, which can lead to a variation in the apparent potency of a given compound because of differences in incubation time and time point selection bias (23). In the present work, we found that this variation could span several orders of magnitude (Fig. 3b). We also showed that this bias could be circumvented by estimating the drug's potency based on the dynamic effect over time, a time-independent metric, which is computed as the area-under-the-effect-curve. We demonstrated a reliable and accurate potency estimate using this method by cross-validating it with a model-based estimation.

In line with earlier observations (14–16), we found that the kinetics of the various pharmacodynamic processes triggered by CD3-bispecifics differ, such as tumor cell killing, T cell activation, and cytokine release. Based on these findings, we conclude that it is impossible to find a single optimal time point for all readouts. Instead, we suggest monitoring the various PD readouts over time and comparing these with their respective AUCE-based potency value in order to gain a more holistic understanding of the drug's pharmacological activity.

As observed in the presented datasets with cibisatamab, CEACAM5-TCB, and high- and low-affinity FolR1-TCBs, the time it takes for the PD readouts to reach their peak effect ($T_{max}$) varies across different readouts and test systems (supplemental table S2) and is often not known a priori. We therefore propose a tailored approach to enable an integrated PK/PD analysis of readouts that occur on different timescales (Fig. 6) and show it can be applied in drug discovery and development. For drug candidate selection, there are two options proposed. This is either done based on a single PD readout (*e.g.*, potency on tumor cytotoxicity) and with a static analysis or based on the anticipated therapeutic index, in which case, time course analysis of the corresponding safety and efficacy readouts is recommended (Fig. 6a).

The exposure–response relationship of readouts, including potency, steepness of response, and maximal effect is expected to differ between test systems. Prerequisites for a thorough pharmacological assessment are the selection of the appropriate test systems as well as the appropriate design of the assay. This will enable the investigators to derive integrated quantitative insights and to select a relevant PD readout for the MABEL-based dose prediction. Together with information on the target biology in a healthy and diseased context as well as other supporting data, a time-independent *in vitro* analysis could provide a more rational basis to select and justify relevant readouts for a starting dose selection with minimal pharmacological activity and lower risk for adverse effects. This justification needs to be done on a case-by-case basis and will be supported by the integrated quantitative analysis. An important point to consider for the dose–response analysis is that not every concentration-dependent increase of effect can be captured with a sigmoidal $E_{max}$ model. For those cases, we suggest estimating a threshold concentration at which minimal effects are expected (26). Especially in the context of adverse effects, this can be utilized to calculate the anticipated exposure margins (20) and to potentially give guidance on the dose-escalation scheme.

In order to demonstrate its utility in the context of FIH dose selection, we have conducted a retrospective MABEL prediction for cibisatamab and compared it to the clinical data (31). The actual MABEL starting dose was originally determined as the $EC_{20}$ of tumor cytotoxicity with a static analysis (19). Here, we evaluated the exposure–response of efficacy (cytotoxicity) *versus* safety (IL6 release) with the integrated analysis in the same high-expressing cell line (MKN45) as previously utilized (19) to ensure the safety of patients with high tumor target expression.

The proposed analysis confirms that for cibisatamab, tumor cell cytotoxicity was the most sensitive readout as defined on the estimated potency value ($EC_{50}$). Furthermore, it is suggested that cibisatamab has a favorable therapeutic index when comparing IL6 release to cytotoxicity in the MKN45 cell line (Fig. 2c). Based on this integrated *in vitro* PK/PD assessment, a $PA_{30\%}$ on IL6 release is selected as a basis for the MABEL dose of 450 µg. It was ninefold higher than the original starting dose of 50 µg and—when comparing it to clinical data—with an acceptable safety profile. This was 50-fold below the dose (2.5 mg) at which pharmacological activity was observed in clinics and ~ 80-fold below the reported MTD of 400 mg (31). In summary, the proposed MABEL approach is safe and may reduce the number of patients exposed at subtherapeutic dose levels during dose escalation.

In order to tailor and simplify this approach, we proposed a workflow where the first detailed time course analysis of various readouts is conducted with only one or a few PBMC donors in order to assess the potency and maximal response for each readout in a time-independent fashion (Fig. 6b). For quantification of the donor-to-donor variability and to reduce the overall work package, the PD endpoint of interest can subsequently be tested with multiple PBMC donors at a single time point. With such a stepwise approach, the process can be efficiently adapted and tailored based on the specific needs and questions for a given project.

This is applicable in early CD3-bispecific discovery and development in order to select favorable tumor-selective compounds tailored to the target of interest, to explore the

**Table IV** Comparison of a Retrospective Dose Calculation Based on Time-Independent Experiments and the Actual First-in-Human Dose Applied in Clinics

| Parameter | Retrospective dose prediction | Applied FIH dose |
|---|---|---|
| Definition of MABEL | $C_{max}$ corresponding to PA30, IL6 release in MKN45* | $C_{max}$ corresponding to EC20 of cytotox in MKN45 at 48 h*** |
| EC20 (ng/mL) | 100 | 46*** |
| PA30 (ng/ml) | 150 | 80**** |
| Assumed human plasma Volume (mL)** | 3000 | 3000 |
| MABEL dose (µg) | 450 | 50*** |

*Data presented in Fig. 1 and Table II; **Davies et al. (29), ***reported FIH starting dose (Dudal et al. [19]), ****back-calculated from EC20, using Eq. (2) and assuming a Hill coefficient of 1

therapeutic index of different molecules, or to define and assess the ideal compound properties for a given therapeutic target (4, 5, 32). Most tumor targets considered for therapeutic applications are overexpressed in tumor tissue and exhibit lower target expression levels in most healthy tissues, which allows for selective targeting of tumor cells with limited cytotoxicity in normal tissue (33). In these cases, the goal is to identify CD3-bispecifics with favorable compound properties that selectively kill tumor cells while exhibiting limited or no cytotoxicity to non-targeted tissue. To illustrate this, two compounds with different binding affinities for the same epitope on a both high- and low-expression target cell lines were compared with regards to their pharmacological profiles. Here, we highlight the utility of real-time imaging systems such as incuCyte or real-time cellular impedance like xCELLigence (34) that generate richer datasets and are less labor- and time-intensive than analogous workflows that use flow cytometry (35) in early drug discovery. The generation of time course data is especially important since cytotoxicity kinetics may differ between cell lines as we observe in the present study and has been reported for TCR-like CD3-bispecifics (36). In addition, the presented case example shows the value of a data-driven approach for compound selection. Here, a binder with higher affinity did not result in higher potency on tumor cytotoxicity as one may have anticipated based on in silico prediction that relate the formation of trimeric complexes to cytotoxicity (21, 37). The time-independent analysis of the high- and low-affinity FolR1-TCB revealed similar potency ($EC_{50}$) values, but a steeper dose–response curve and a more favorable therapeutic index for the low-affinity binder. Further investigations are needed to better understand the various factors that trigger cytotoxicity beyond the formation of trimeric complexes (25).

Time-independent analysis enables the meaningful quantitative characterization of *in vitro* experiments, provided that the experimental design is appropriate. An informative dose range includes doses that span from minimum to full effect and a tailored observation period that captures the time course of the PD readouts of interest. However, these TDCC assays are dependent on the experimental conditions, such as the source of human PBMCs (*e.g.*, isolated PBMCs, whole blood, frozen/fresh PBMCs, purified T cells), the use of adherent or soluble cancer cell lines, the absolute number as well as the concentration of individual cell types, the PBMC donor-to-donor variability, and which can hamper robust quantification of the pharmacological activity. Another important consideration to *in vitro* experiments is the effector-to-target (E:T) cell ratio. The physiological effector-to-tumor (E:T) ratio in patients' tumors is not always known, highly variable, and will depend on the site of action (*i.e.*, blood *versus* solid tumors). For illustration, the anticipated E:T ratio for solid tumors is reported with 1:150 (21, 38, 39). However, it has been discussed that—for *in vitro* assays—higher E:T ratios (*e.g.*, 2:1, 5:1, 10:1) are needed to compensate for the short assay duration of only a few days (34). While the time course PK/PD approach is certainly an improvement over the static assessment, it has limitations. It does not provide a potency estimate independent of all of these assay conditions and it does not allow project the outcome of other scenarios such as predicting tumor cell cytotoxicity as a function of target expression (25, 37). Instead, it is suggested to use a model-based approach (as proposed by Chen et al. (15), Betts et al. (21), Jiang et al. (37)) to get a potency estimate that can possibly predict the response with varying E:T ratios or to predict other untested scenarios. However, this would require time course data, and therefore, the proposed experimental design is suitable for complementary analysis.

The proposed method of time-independent analysis can be seen as complementary to PK/PD modeling in the early development of CD3-bispecifics. It provides a pragmatic means of comparing efficacy and safety data without the risk of time bias. Time-independent therapeutic indices may prove to be an important asset when comparing compounds. In order to facilitate this analysis, an automated workflow has been developed that generates graphic and textual

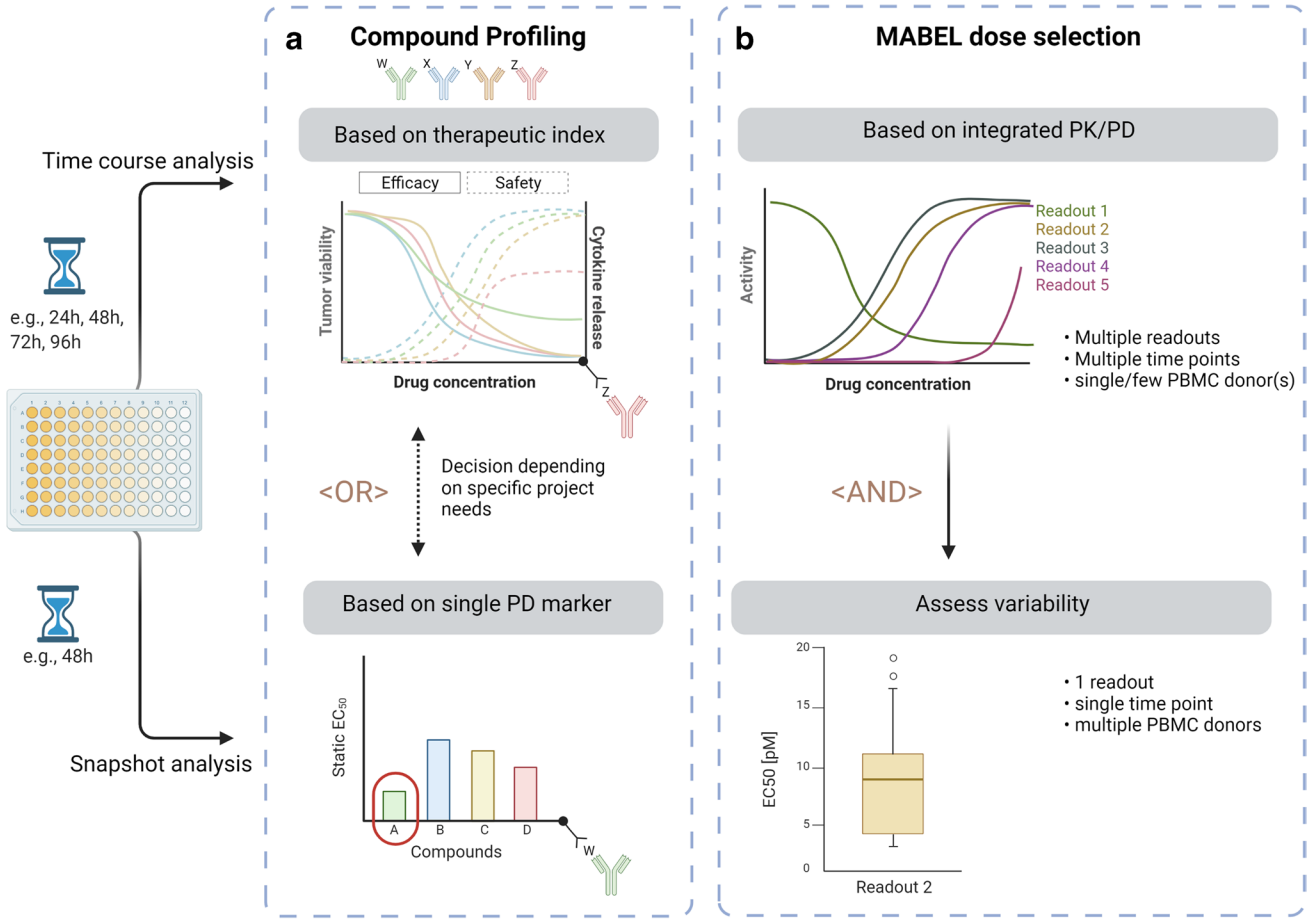


**Fig. 6** A schematic overview of strategic overview and decision tree for the complementary use of time-independent and static analyses in the early development of CD3-bispecifics is provided. **a** Two alternative options are depicted for compound profiling and candidate selection (*e.g.*, compounds W, X, Y, or Z). The upper panel illustrates compound selection based on the most favorable *in vitro* safety/efficacy balance applying a time-independent analysis on multiple readouts. The lower panel shows a static analysis based on a single readout. **b** For MABEL dose selection, a stepwise approach is proposed. First, a time-independent analysis is suggested to enable comparison across various readouts without the risk of time bias. This can be conducted with one or only a few PBMC donors (upper panel). For quantification of the donor-to-donor variability and to reduce the overall work package, the PD endpoint of interest can subsequently be tested with multiple PBMC donors at a single time point informed by the time-independent analysis (lower panel)

outputs. This allows scientists to analyze, plot, and evaluate the data. The framework is intended to help scientists conduct a holistic analysis of their data instead of focusing on a single readout or experimental condition. The results of this automated analysis should be examined, and, if needed, further analysis can be conducted to address any remaining questions.

## CONCLUSIONS

Our time-independent PK/PD analysis enables robust quantification of the pharmacological activity of CD3-bispecifics and provides more accurate potency estimates than traditionally applied *in vitro* methods. We developed a leaner and less labor-intensive experimental protocol for the classical T-cell-mediated cytotoxicity assay for monitoring the time course of tumor cell cytotoxicity and cytokine release with real-time imaging. We also created a semi-automated workflow to quantify the pharmacological response. Improved *in vitro* assays and analysis methods may increase their translational relevance and pave the way for less animal experimentation. The proposed method enables head-to-head comparison of drug candidates based on their anticipated therapeutic index and may improve the identification of relevant FIH dose estimations of CD3-bispecifics.

**Acknowledgements** This work was supported by F. Hoffmann-La Roche Ltd. The authors would like to thank Jitka Somandin, Florian Limani, Sarah Diggelmann, Melanie Knobloch, Mudita Pincha, Simon Patrick Keiser, and Simone Lang from Roche Innovation Center Zürich for their technical expertise and support in the lab. The authors would

like to thank Ken Wang from Roche Innovation Center Basel for support and constructive feedback on the automated workflow in Python. The authors would also like to thank Kelly Van der Borght for the insightful discussions. Editorial support was provided by Anshin BioSolutions Corp. Some of the figures have been generated with Biorender.com.

**Author Contribution** A.J. Van De Vyver: data collection, analysis and interpretation, visualization, methodology, writing, review, and editing; M.J. Eigenmann: data collection, analysis, visualization, methodology, writing, review, and editing; M. Ovacik: data analysis and data interpretation, automated workflow, methodology, writing, review, and editing; C. Pohl: data collection, data interpretation writing, and review; S. Herter: conceptualization, data collection, and review; T. Weinzierl: conceptualization, supervision, review; T. Fauti: conceptualization, supervision, and review; M. Bacac: conceptualization, supervision, and review; A.-C. Walz: conceptualization, supervision, data analysis and interpretation, methodology, writing, review, and editing; T. Lehr: interpretation, visualization, methodology, review; C. Klein: interpretation, review.

**Declarations**

**Conflict of Interest** A. Van De Vyver, M. Eigenmann, M. Ovacik, C. Pohl, S. Herter, T. Weinzierl, T. Fauti, C. Klein, M. Bacac, and A-C. Walz were employed by F. Hoffmann-La Roche Ltd. at time of submission of this manuscript. T. Weinzierl, T. Fauti, C. Klein, M. Bacac, and A-C. Walz declare patents and stock ownership with Roche. T. Lehr reports grants from Neovii, grants from Boehringer Ingelheim, and grants from Aspen outside the submitted work.



## References

1. Upadhaya S, Hubbard-Lucey VM, Yu JX. Immuno-oncology drug development forges on despite COVID-19. Nat Rev Drug Discov. 2020;19(11):751–2. https://doi.org/10.1038/d41573-020-00166-1.
2. Ali S, Moreau A, Melchiorri D, Camarero J, Josephson F, Olimpier O, *et al*. Blinatumomab for acute lymphoblastic leukemia: the first bispecific T-cell engager antibody to be approved by the EMA for minimal residual disease. Oncologist. 2020;25(4):e709–15. https://doi.org/10.1634/theoncologist.2019-0559.
3. Ribera J-M, Genescà E, Ribera J. Bispecific T-cell engaging antibodies in B-cell precursor acute lymphoblastic leukemias: focus on blinatumomab. Therapeutic Advances in Hematology. 2020;11:2040620720919632. https://doi.org/10.1177/2040620720919632.
4. Vafa O, Trinklein ND. Perspective: designing T-cell engagers with better therapeutic windows. Front Oncol. 2020;10:446. https://doi.org/10.3389/fonc.2020.00446.
5. Ellerman D. Bispecific T-cell engagers: towards understanding variables influencing the in vitro potency and tumor selectivity and their modulation to enhance their efficacy and safety. Methods (San Diego, Calif). 2019;154:102–17. https://doi.org/10.1016/j.ymeth.2018.10.026.
6. Krishnamurthy A, Jimeno A. Bispecific antibodies for cancer therapy: a review. Pharmacol Ther. 2018;185:122–34. https://doi.org/10.1016/j.pharmthera.2017.12.002.
7. Suurs FV, Lub-de Hooge MN, de Vries EGE, de Groot DJA. A review of bispecific antibodies and antibody constructs in oncology and clinical challenges. Pharmacol Ther. 2019;201:103–19. https://doi.org/10.1016/j.pharmthera.2019.04.006.
8. Yu S, Li A, Liu Q, Yuan X, Xu H, Jiao D, *et al*. Recent advances of bispecific antibodies in solid tumors. J Hematol Oncol. 2017;10(1):155. https://doi.org/10.1186/s13045-017-0522-z.
9. Velasquez MP, Bonifant CL, Gottschalk S. Redirecting T cells to hematological malignancies with bispecific antibodies. Blood. 2018;131(1):30–8. https://doi.org/10.1182/blood-2017-06-741058.
10. de Miguel M, Umana P, Gomes de Morais AL, Moreno V, Calvo E. T cell-engaging therapy for solid tumors. Clin Cancer Res. 2020. https://doi.org/10.1158/1078-0432.ccr-20-2448.
11. Bacac M, Fauti T, Sam J, Colombetti S, Weinzierl T, Ouaret D. A novel carcinoembryonic antigen T-cell bispecific antibody (CEA TCB) for the treatment of solid tumors. Clin Cancer Res. 2016;22. https://doi.org/10.1158/1078-0432.ccr-15-1696.
12. Bossi G, Buisson S, Oates J, Jakobsen BK, Hassan NJ. ImmTAC-redirected tumour cell killing induces and potentiates antigen cross-presentation by dendritic cells. Cancer Immunol Immunother. 2014;63(5):437–48. https://doi.org/10.1007/s00262-014-1525-z.
13. Li J, Piskol R, Ybarra R, Chen Y-JJ, Li J, Slaga D, *et al*. CD3 bispecific antibody–induced cytokine release is dispensable for cytotoxic T cell activity. Sci Transl Med. 2019;11(508):eaax8861. https://doi.org/10.1126/scitranslmed.aax8861.
14. Aigner M, Feulner J, Schaffer S, Kischel R, Kufer P, Schneider K, *et al*. T lymphocytes can be effectively recruited for ex vivo and in vivo lysis of AML blasts by a novel CD33/CD3-bispecific BiTE antibody construct. Leukemia. 2013;27(5):1107–15. https://doi.org/10.1038/leu.2012.341.
15. Chen X, Haddish-Berhane N, Moore P, Clark T, Yang Y, Li H, *et al*. Mechanistic projection of first-in-human dose for bispecific immunomodulatory P-cadherin LP-DART: an integrated PK/PD modeling approach. Clin Pharmacol Ther. 2016;100(3):232–41. https://doi.org/10.1002/cpt.393.
16. Nazarian AA, Archibeque IL, Nguyen YH, Wang P, Sinclair AM, Powers DA. Characterization of bispecific T-cell Engager (BiTE) antibodies with a high-capacity T-cell dependent cellular cytotoxicity (TDCC) assay. J Biomol Screen. 2015;20(4):519–27. https://doi.org/10.1177/1087057114561405.
17. Saber H, Del Valle P, Ricks TK, Leighton JK. An FDA oncology analysis of CD3 bispecific constructs and first-in-human dose selection. Regul Toxicol Pharmacol. 2017;90:144–52. https://doi.org/10.1016/j.yrtph.2017.09.001.
18. Schaller TH, Snyder DJ, Spasojevic I, Gedeon PC, Sanchez-Perez L, Sampson JH. First in human dose calculation of a single-chain bispecific antibody targeting glioma using the MABEL approach. J Immunother Cancer. 2020;8(1). https://doi.org/10.1136/jitc-2019-000213.
19. Dudal S, Hinton H, Giusti AM, Bacac M, Muller M, Fauti T, Colombetti S, Heckel T, Giroud N, Klein C, Umaña P, Benincosa L, Bachl J, Singer T, Bray-French K. Application of a MABEL Approach for a T-Cell-Bispecific Monoclonal Antibody: CEA TCB. J Immunother. 2016;39(7):279–89. https://doi.org/10.1097/CJI.0000000000000132.

20. Harper J, Adams KJ, Bossi G, Wright DE, Stacey AR, Bedke N, *et al*. An approved in vitro approach to preclinical safety and efficacy evaluation of engineered T cell receptor anti-CD3 bispecific (ImmTAC) molecules. PLoS ONE. 2018;13(10):e0205491. https://doi.org/10.1371/journal.pone.0205491.
21. Betts A, Haddish-Berhane N, Shah DK, van der Graaf PH, Barletta F, King L, *et al*. A translational quantitative systems pharmacology model for CD3 bispecific molecules: application to quantify T cell-mediated tumor cell killing by P-cadherin LP DART((R)). AAPS J. 2019;21(4):66. https://doi.org/10.1208/s12248-019-0332-z.
22. Kamperschroer C, Shenton J, Lebrec H, Leighton JK, Moore PA, Thomas O. Summary of a workshop on preclinical and translational safety assessment of CD3 bispecifics. J Immunotoxicol. 2020;17(1):67–85. https://doi.org/10.1080/1547691X.2020.1729902.
23. Hoffmann P, Hofmeister R, Brischwein K, Brandl C, Crommer S, Bargou R, *et al*. Serial killing of tumor cells by cytotoxic T cells redirected with a CD19-/CD3-bispecific single-chain antibody construct. Int J Cancer. 2005;115(1):98–104. https://doi.org/10.1002/ijc.20908.
24. Eigenmann M, Herter S, Diggelmann S, Limani F, Somandin J, Frances N, *et al*. PAGE 27 (2018) Abstr 8621 [www.page-meeting.org/?abstract=8621]. 2018.
25. Van De Vyver AJ, Weinzierl T, Eigenmann MJ, Frances N, Herter S, Buser RB, *et al*. Predicting tumor killing and T-cell activation by T-cell bispecific antibodies as a function of target expression: combining in vitro experiments with systems modeling. Molecular Cancer Therapeutics. 2020:molcanther.0269.2020. https://doi.org/10.1158/1535-7163.MCT-20-0269.
26. Lutz WK, Lutz RW. Statistical model to estimate a threshold dose and its confidence limits for the analysis of sublinear dose-response relationships, exemplified for mutagenicity data. Mutat Res. 2009;678(2):118–22. https://doi.org/10.1016/j.mrgentox.2009.05.010.
27. Lobo ED, Balthasar JP. Pharmacodynamic modeling of chemotherapeutic effects: application of a transit compartment model to characterize methotrexate effects in vitro. AAPS PharmSci. 2002;4(4):E42-E. https://doi.org/10.1208/ps040442.
28. Schropp J, Khot A, Shah DK, Koch G. Target-mediated drug disposition model for bispecific antibodies: properties, approximation, and optimal dosing strategy. CPT Pharmacometrics Syst Pharmacol. 2019;8(3):177–87. https://doi.org/10.1002/psp4.12369.
29. Davies B, Morris T. Physiological parameters in laboratory animals and humans. Pharm Res. 1993;10(7):1093–5. https://doi.org/10.1023/A:1018943613122.
30. FDA Center for Drug Evaluation and Research and Center for Biologics Evaluation and Research. Guidance for Industry: Bispecific Antibody Development Programs. FDA Maryland; 2021. p. 10.
31. Tabernero J, Melero I, Ros W, Argiles G, Marabelle A, Rodriguez-Ruiz ME. Phase Ia and Ib studies of the novel carcinoembryonic antigen (CEA) T-cell bispecific (CEA CD3 TCB) antibody as a single agent and in combination with atezolizumab: preliminary efficacy and safety in patients with metastatic colorectal cancer (mCRC). J Clin Oncol. 2017;35. https://doi.org/10.1200/JCO.2017.35.15_suppl.3002.
32. Chen W, Yang F, Wang C, Narula J, Pascua E, Ni I, *et al*. One size does not fit all: navigating the multi-dimensional space to optimize T-cell engaging protein therapeutics. MAbs. 2021;13(1):1871171. https://doi.org/10.1080/19420862.2020.1871171.
33. Staflin K, Zuch de Zafra CL, Schutt LK, Clark V, Zhong F, Hristopoulos M, *et al*. Target arm affinities determine preclinical efficacy and safety of anti-HER2/CD3 bispecific antibody. JCI Insight. 2020;5(7). https://doi.org/10.1172/jci.insight.133757.
34. Cerignoli F, Abassi YA, Lamarche BJ, Guenther G, Santa Ana D, Guimet D, *et al*. In vitro immunotherapy potency assays using real-time cell analysis. PLoS ONE. 2018;13(3):e0193498. https://doi.org/10.1371/journal.pone.0193498.
35. Gelles JD, Mohammed JN, Santos LC, Legarda D, Ting AT, Chipuk JE. Real-time integration of cell death mechanisms and proliferation kinetics at the single-cell and population-level using high-throughput live-cell imaging. bioRxiv. 2019:596239. https://doi.org/10.1101/596239.
36. McCormack E, Adams KJ, Hassan NJ, Kotian A, Lissin NM, Sami M, *et al*. Bi-specific TCR-anti CD3 redirected T-cell targeting of NY-ESO-1- and LAGE-1-positive tumors. Cancer Immunol Immunother. 2013;62(4):773–85. https://doi.org/10.1007/s00262-012-1384-4.
37. Jiang X, Chen X, Carpenter TJ, Wang J, Zhou R, Davis HM, *et al*. Development of a Target cell-Biologics-Effector cell (TBE) complex-based cell killing model to characterize target cell depletion by T cell redirecting bispecific agents. MAbs. 2018;10(6):876–89. https://doi.org/10.1080/19420862.2018.1480299.
38. Del Monte U. Does the cell number 10(9) still really fit one gram of tumor tissue? Cell cycle (Georgetown, Tex). 2009;8(3):505–6. https://doi.org/10.4161/cc.8.3.7608.
39. Kovacsovics-Bankowski M, Chisholm L, Vercellini J, Tucker CG, Montler R, Haley D, *et al*. Detailed characterization of tumor infiltrating lymphocytes in two distinct human solid malignancies show phenotypic similarities. J Immunother Cancer. 2014;2(1):38. https://doi.org/10.1186/s40425-014-0038-9.

***Manuscript 3***

*Cytokine release syndrome by T-cell-redirecting therapies: can we predict and modulate patient risk?*

Journal: AACR Clinical Cancer Research

Publishing date: July 26th 2021

DOI: 10.1158/1078-0432.ccr-21-0470.

URL: https://clincancerres.aacrjournals.org/content/27/22/6083.full-text.pdf

# Cytokine Release Syndrome By T-cell–Redirecting Therapies: Can We Predict and Modulate Patient Risk?

Arthur J. Van De Vyver[1,2], Estelle Marrer-Berger[1], Ken Wang[1], Thorsten Lehr[2], and Antje-Christine Walz[1]

## ABSTRACT

T-cell–redirecting therapies are promising new therapeutic options in the field of cancer immunotherapy, but the development of these modalities is challenging. A commonly observed adverse event in patients treated with T-cell–redirecting therapies is cytokine release syndrome (CRS). Its clinical manifestation is a burden on patients, and continues to be a big hurdle in the clinical development of this class of therapeutics. We review different T-cell–redirecting therapies, discuss key factors related to cytokine release and potentially leading to CRS, and present clinical mitigation strategies applied for those modalities. We propose to dissect those risk factors into drug-target-disease–related factors and individual patient risk factors. Aiming to optimize the therapeutic intervention of these modalities, we illustrate how the knowledge on drug-target-disease–related factors, such as target expression, binding affinity, and target accessibility, can be leveraged in a model-based framework and highlight with case examples how modeling and simulation is applied to guide drug discovery and development. We draw attention to the current gaps in predicting the individual patient's risk towards a high-grade CRS, which requires further considerations of risk factors related, but not limited to, the patient's demographics, genetics, underlying pathologies, treatment history, and environmental exposures. The drug-target-disease–related factors together with the individual patient's risk factors can be regarded as the patient's propensity for developing CRS in response to therapy. As an outlook, we suggest implementing a risk scoring system combined with mechanistic modeling to enable the prediction of an individual patient's risk of CRS for a given therapeutic intervention.

## Introduction

The advent of immunotherapies has sparked a revolution in cancer patients' treatment and care over the last couple of decades. By harnessing the patient's immune system to fight cancer, we have witnessed some promising outcomes where patients experienced a long-term or even permanent remission from cancers that until then were thought to be incurable, and sometimes even untreatable (1). At an ever-increasing pace, pharmaceutical companies and academic institutions are developing new and more powerful immunotherapies that aim to resolve problems encountered with previous generation therapies (2). T-cell bispecific antibodies and antibody fragments (CD3-bispecifics), chimeric antigen receptor (CAR)-T cells, and engineered TCR-T cells belong to the T-cell–redirecting therapies. Only a few of them already reached the market, and almost all are indicated for hematologic malignancies (3–9).

Some of these T-cell–redirecting therapies have lived up to the promise by providing unpreceded high response rates in patients. However, the other side of the coin for this class of therapies is the risk for cytokine release syndrome (CRS), which is the most frequent serious adverse event associated with these therapies. CRS generally occurs within hours to days after treatment starts; it is largely reversible but also represents a major cause of morbidity (10–14).

CRS develops when extensive on-target related T-cell engagement and subsequent activation of bystander immune cells and nonimmune cells, such as endothelial cells, lead to a massive release of cytokines, which in turn induce tissue damage, capillary leakage, neurologic events, and multiorgan failure (10, 15). The American Society for Transplantation and Cellular Therapy (ASTCT) defines CRS as "a supraphysiologic response following any immune therapy that results in the activation or engagement of endogenous or infused T cells and/or other immune effector cells. Symptoms can be progressive, must include fever at the onset, and may include hypotension, capillary leak (hypoxia) and end organ dysfunction (16)." Building on this, a recently published white paper on CRS provides core principles for defining CRS. It considers the therapeutic modality, symptom manifestation, timing, and response to intervention (17).

The goal of our review is to examine the key factors influencing cytokine release, potentially leading to CRS, triggered by T-cell–redirecting therapies. We discuss the utility of computational models to guide target selection, explore desirable compound properties, and influence clinical development. Therefore, our findings should generate new insights into how to improve the therapeutic benefit–risk profile of T-cell–redirecting therapies by minimizing inflammatory cytokine release and mitigating CRS. **Figure 1** summarizes the key questions in the discovery and development of novel T-cell–redirecting therapies and illustrates the major factors affecting cytokine release and the risk for CRS formation. **Table 1** summarizes our results of the literature research on factors that may influence the risk for CRS toxicity as reported *in vitro, in vivo*, and in the clinics. **Table 2** provides an overview of all T-cell engagers that were considered in this review. A more extensive overview of T-cell–redirecting therapies that are under development can be found in refs. 8, 18, and 19. Modeling approaches can be used to quantitatively characterize experimental or clinical data in order to better understand the pharmacokinetics (PK) and pharmacodynamics (PD) of a drug. Model-informed drug development (MID3) is becoming increasingly widespread among pharmaceutical companies and regulatory agencies (20, 21). We illustrate how the knowledge on drug-target-disease–related factors can be leveraged in a model-based framework to improve these modalities and to optimize therapeutic treatment (**Fig. 2**). We summarize various

[1]Roche Pharma Research & Early Development, Pharmaceutical Sciences, Roche Innovation Center Basel, Switzerland. [2]Saarland University, Department of Clinical Pharmacy, Saarbrücken, Germany.

**Corresponding Author:** Arthur J. Van De Vyver, Grenzacherstrasse 124, 4070 Basel, Switzerland, Phone: 0041/787158333; E-mail: arthur.van_de_vyver@roche.com

Clin Cancer Res 2021;27:6083–94

**doi:** 10.1158/1078-0432.CCR-21-0470

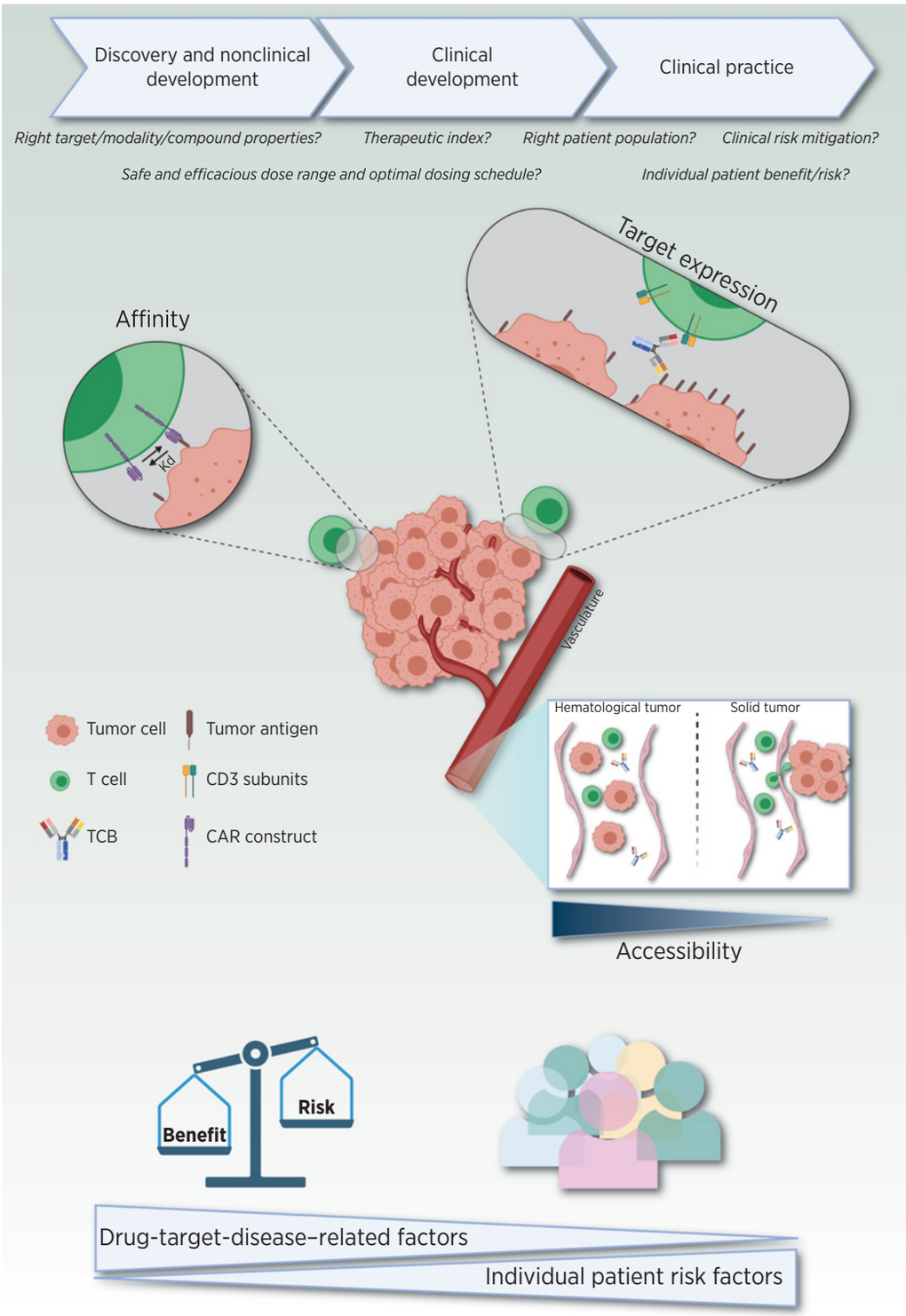


**Figure 1.**

The successful development of safe and efficacious cancer immunotherapies requires many considerations. There are pivotal questions during the development of T-cell–redirecting therapies and good understanding of these questions is key from the discovery phase up until clinical practice. Drug-target-disease–related factors, such as binding affinity, target expression, and target accessibility that may affect cytokine release need to be identified. In addition, individual risk factors that may put the patients at risk for developing cytokine release syndrome are key considerations. Both are important to establish a benefit–risk profile for the patient and allow optimizing the treatment strategy. Kd, dissociation constant; TCB, T-cell bispecific antibody. Adapted from an image created with BioRender.com.

**Table 1.** Factors that may trigger cytokine release and may increase the risk for CRS as reported *in vitro, in vivo*, and in the clinics.

| Factors | Dependency | Observed for | *In vitro* | *In vivo* | In patients | References |
|---|---|---|---|---|---|---|
| Tumor antigen affinity | Strong | CD3-bispecific, CAR-T | X | X | X | 30, 43, 47 |
| CD3 affinity | Strong | CD3-bispecific | X | X | | 15, 42, 44, 45 |
| Tumor burden | Strong | CD3-bispecific, CAR-T | X | X | X | 31–33, 35, 36 |
| Expression level | Strong | CD3-bispecific, CAR-T | X | X | X | 24–26, 30, 34 |
| Target accessibility | Medium[a] | CD3-bispecific, CAR-T | | X | X | 39, 53, 59, 94 |
| Indication | Medium[a] | CD3-bispecific, CAR-T | | | X | 60 |
| Cell types | Medium | ACT | | X | X | 65, 68, 84, 99 |
| Lymphodepletion | Strong | ACT | | | X | 31, 36, 65, 99 |

Abbreviation: ACT, adoptive cell therapy, which includes both CAR and autologous T cells.
[a]Due to limited information. Corresponding references are provided for T-cell–redirecting therapies.

**Table 2.** Overview of T-cell–redirecting therapies discussed in this review, including applicable brand names, generic and other relevant names, tumor target specificity, developmental status, and other relevant information.

| Therapeutic modality | Brand name | Generic/other names[a] | Tumor target specificity | Developmental status and additional remarks | References |
|---|---|---|---|---|---|
| **Adoptive cell therapies** | | | | | |
| CD19-CAR-T | Kymriah | tisagenlecleucel (CTL019) | CD19 | Marketed<br>$Kd_{CD19}$ = 0.32 nmol/L | 47, 74 |
| | Yescarta | axicabtagene ciloleucel (KTA-C19) | | Marketed | 9 |
| | N/A | CAT19 | | Clinical development<br>~50-fold higher dissociation rate of CD19-binder than Kymriah. | 47 |
| HER2-CAR-T | N/A | N/A | HER2 | Nonclinical development | 46 |
| EGFR-CAR-T | N/A | N/A | EGFR | Nonclinical development | 46 |
| CAIX-CAR-T | N/A | N/A | CAIX | Clinical development<br>Clinical trial identifier: DDHK97–29/P00.0040C | 108 |
| CD22-CAR-T | N/A | M971BBz | CD22 | Clinical development | 35 |
| BCMA-CAR-T | N/A | 1. idecabtagene vicleucel<br>2. ciltacabtagene autoleucel | BCMA | Clinical development<br>Idecabtagene vicleucel received FDA approval for the treatment of MM in 03/2021 | 36 |
| GD2-CAR-T | N/A | 14.2GA-CAR | GD2 | Nonclinical development | 28 |
| **CD3-bispecific antibodies** | | | | | |
| EpCAMxCD3-bispecific | Removab | catumaxomab | EpCAM | Withdrawn<br>First approved CD3-bispecific antibody (2009)<br>Market withdrawal in 2017 | 3 |
| CD19-BiTE | Blincyto | blinatumomab | CD19 | Marketed<br>BiTE | 92 |
| P-cadherin-X-CD3-bispecific | N/A | LP-DART (PF-06671008) | P-cadherin | Clinical development<br>DART | 48 |
| CD20xCD3-bispecific | N/A | mosunetuzumab (BTCT4465A, RG7828) | CD20 | Clinical development | 95 |
| HER2xCD3-bispecific | N/A | HER2 –TDB (BTRC4017A, RG61942) | HER2 | Clinical development<br>Affinity variants from trastuzumab (clone 4D5) were used as the HER2 binding arm | 30 |
| CEA-TCB | N/A | cibisatamab (RG-7802, RO-6958688) | CEA | Clinical development<br>Format contains 2 CEA-binders, 1 CD3-binder | 26 |

Abbreviations: BCMA, B-cell maturation antigen; BiTE: Bispecific T-cell Engager; CAIX, carbonic anhydrase IX; CD, cluster of differentiation; CEA, carcinoembryonic antigen; DART, Dual-Affinity Re-Targeting; EGFR, epidermal growth factor receptor; EpCAM, epithelial cell adhesion molecule; GD2, disialioganglioside; HER2, epidermal growth factor receptor 2; Kd, equilibrium dissociation constant; MM, multiple myeloma.
[a]All nonbrand names that are affiliated with the therapy, to facilitate literature and database search.

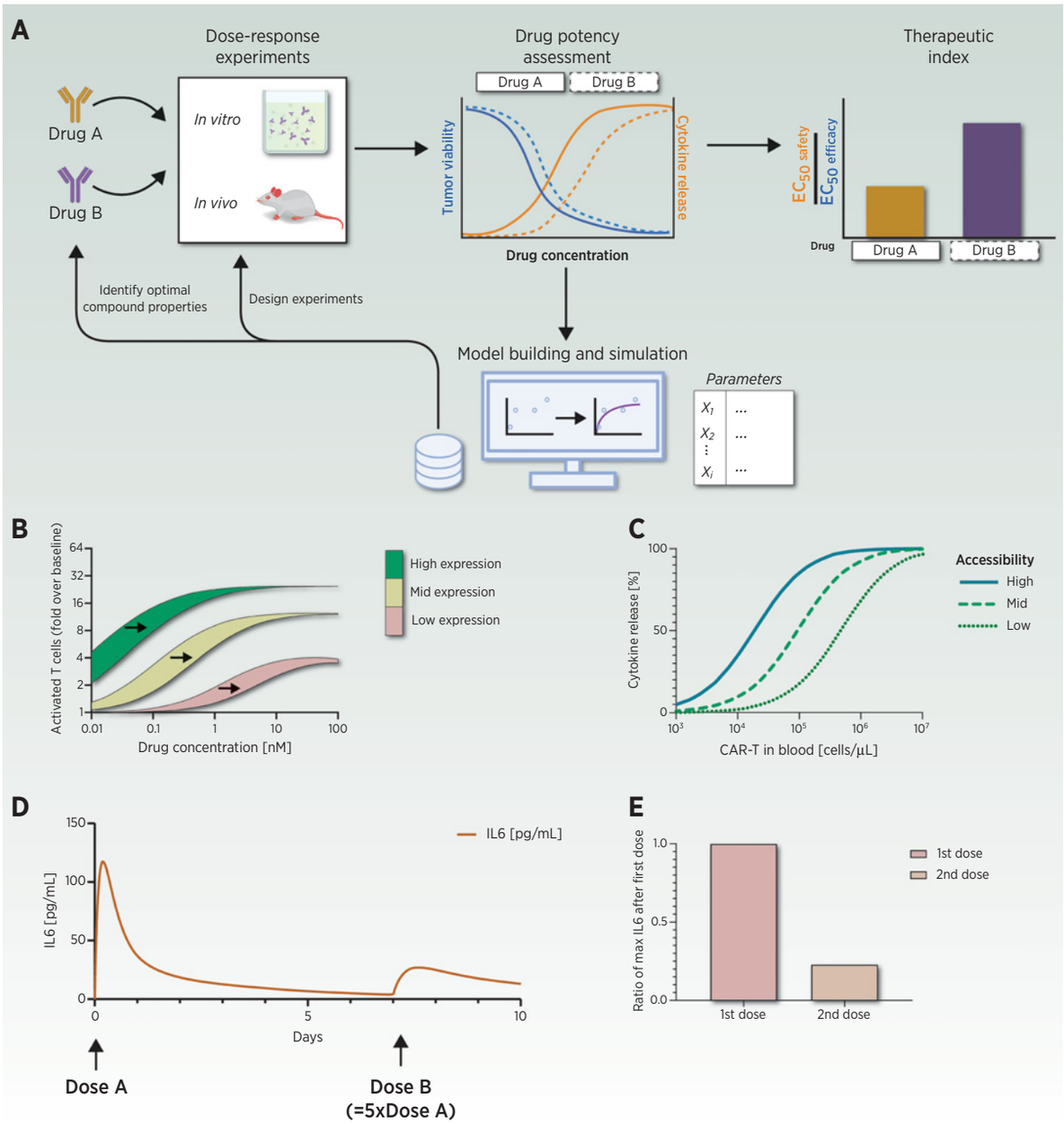


**Figure 2.**

Illustration on how modeling and simulation combined with experimentation can be utilized to guide discovery and development of T-cell–redirecting therapies. Model codes are provided in an online repository (https://github.com/PKPD-coder/Modeling_Cytokine_Release.git) **A,** The goal in early drug discovery is to select drug candidates with favorable risk–benefit profiles using a model-based framework. Here, nonclinical experiments are designed and conducted to enable assessment of dose responses for markers of efficacy (e.g., tumor killing) and safety (e.g., cytokine release) and a therapeutic index is derived on the basis of the ratio of $EC_{50safety}/EC_{50efficacy}$. Furthermore, longitudinal dose-response data are suited for the development of mechanistic models suited to explore the optimal compound properties *in silico*, which then can be tested and confirmed experimentally. Quantitative approaches can be used to maximize the information yield from experiments and to design new experiments. They are useful to explore drug effects under certain conditions and anticipate their therapeutic index. **B–E,** Simulation studies from published computational models that are discussed in the main text (27, 39, 97) are presented. **B,** The extent of T-cell activation *in vitro* depends on the target density (green, high; yellow, intermediate; red, low) and binding affinity as predicted by Van De Vyver and colleagues (27). The arrows show the potency shift caused by a 4-fold decrease in binding affinity to the tumor target. **C,** Prediction of local PD effects as a function of systemic CAR-T concentration based on a physiologically based PK/PD model as proposed by Singh and colleagues (39). Predicted cytokine release in tumor (xenograft mice) upon CAR-T-cell treatment assuming varying degrees of tumor accessibility. **D** and **E,** *in silico* exploration of cytokine release with step-up dosing using the model from Chen and colleagues (97). **D,** Simulated IL6 release upon step-up dosing [dose A at time 0, dose B (5xA) at day 7] of a CD3-bispecific T-cell engager in a patient with a hematologic tumor. **E,** Relative drop in maximal IL6 release after stepped dosing with the compound computed on the basis of simulation shown in **D**. Adapted from an image created with BioRender.com.

strategies to mitigate CRS and improve patient safety. Whereas the cytokine release coming from the drug-target-disease interplay can be computationally modeled, each patient will have a different propensity for developing CRS in response to this cytokine excursion. This highlights the need to distinguish between cytokine release and CRS. For instance, an IL6 level of 200 pg/mL postadministration of a CD3-bispecific can be associated with a CRS grade 3 in one patient, while being asymptomatic in another patient (22, 23), clearly pointing to further individual patient risk to be included in the equation in order to predict who will be at risk of developing a high-grade CRS. Therefore, we discuss patient characteristics that may put them at higher risk for developing severe CRS. As an outlook, we propose to fill this gap by providing a quantitative framework that combines mechanistic modeling for the given therapeutic treatment with a risk scoring method that integrates all relevant patient/individual specific risk factors to predict the probability of CRS for each patient (**Fig. 3**).

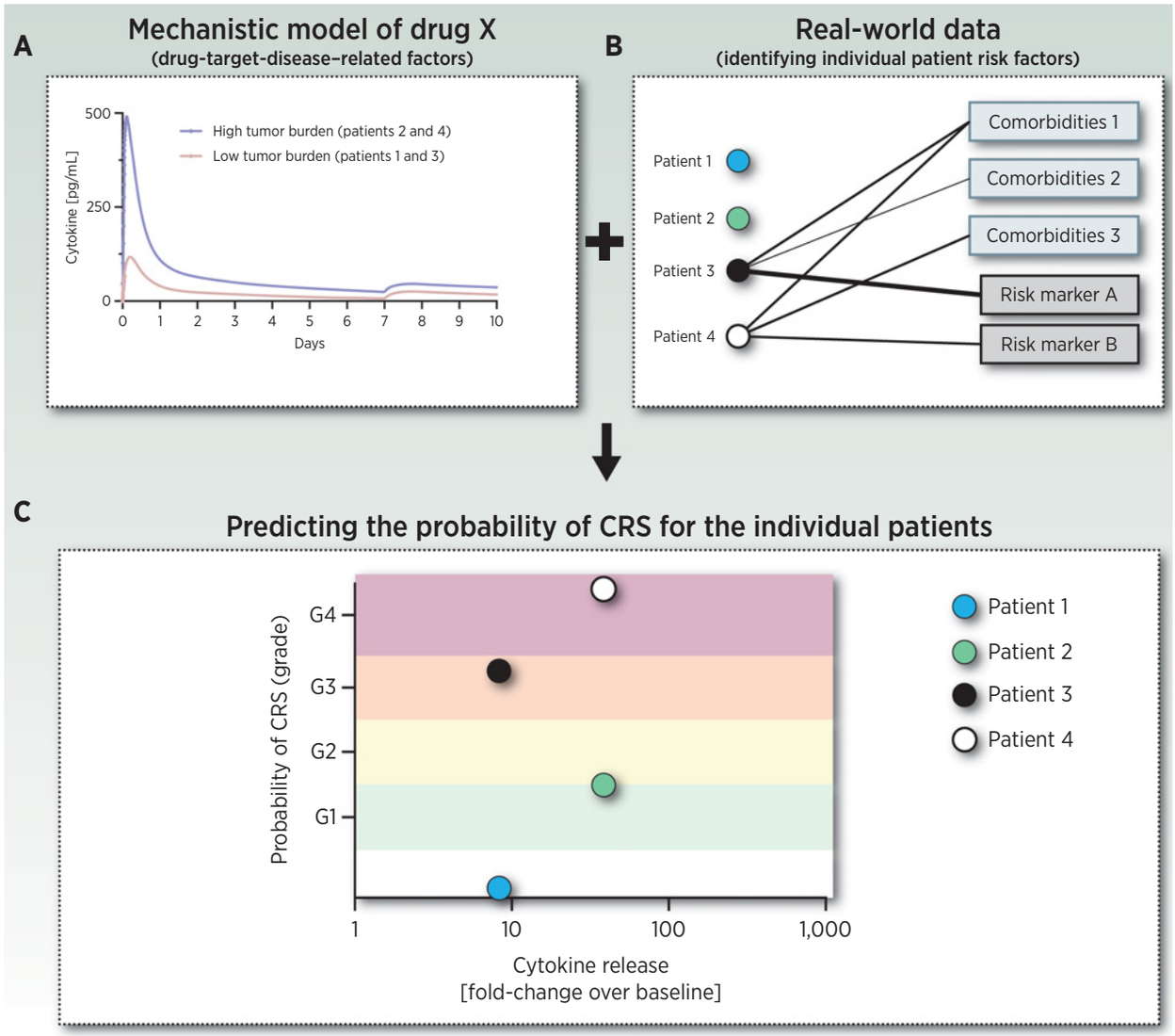


**Figure 3.**

Conceptual framework to predict the probability of severe CRS for the individual patient based on mechanistic modeling of a given therapeutic intervention and on individual patient risk scores derived from real-world data considering a large number of therapeutic interventions. **A,** For a given therapeutic intervention, cytokine release profiles can be predicted using mechanistic models built for the drug of interest. For illustration, the cytokine release of two patients with high and low tumor burden after step-up dosing is simulated. **B,** Individual patient risk factors for severe CRS formation, e.g., demographics, age, comorbidities, and lifestyle, are captured in risk scoring tables derived from real-world data considering a broad range of therapeutic interventions for which CRS has been clinically observed. **C,** Prediction of the probability of CRS for the individual patients. Here, we illustrated the use-cases of 4 hypothetical patients with ALL that are treated with a hypothetical CD3-bispecific and simulated the respective probability of CRS for these individual patients. It was assumed that patients 1 and 3 have a low tumor burden whereas patients 2 and 4 have a high tumor burden. Regarding the individual risk profile, patients 1 and 2 have a low, and patients 3 and 4 have a high risk profile. Adapted from an image created with BioRender.com.

## Drug–target Interaction, Pharmacologic Response, and Disease Context

### Target expression and cytokine release

T-cell–redirecting therapies rely on the interaction with tumor cells to convey their mechanism of action. The extent of which depends on the density of target antigen on the tumor cell surface (**Fig. 1**). Various nonclinical *in vitro* and *in vivo* studies showed a strong correlation between target expression and the pharmacologic response of CD3-bispecifics (24–27) as well as of CAR-T-cell therapy (28, 29).

In addition, most targets are not restricted to tumor tissue and can be found on healthy tissues. The selectivity of the therapy will, therefore, depend on differences concerning location and target expression level between tumor and healthy tissues (30).

The available target pool is defined by the target density and number of tumor cells. A dependency between tumor load and CRS has been described. Blinatumomab, a CD3-bispecific targeting CD19 on B cells, propagated a higher CRS risk in patients with acute lymphoblastic leukemia (ALL) with high leukemic burden (31). A correlation between disease burden and the level of cytokine excursion and CRS severity was reported in patients treated with CD19-CAR-T (32–34) as well as with CD22-CAR-T (35) and BCMA-CAR-T (36) therapies.

The complex relationship between target expression and cytokine release can be investigated with systems pharmacology models. For instance, models that incorporate immune synapse formation by CD3-bispecifics are well suited to capture changes in target expression (37, 38). Van De Vyver and colleagues expanded on these models by making activated T cells rather than immune synapses the driver for tumor cell killing. They concluded that T-cell activation depends on both synapse formation and on the target expression level on the tumor cell surface. Such a model is useful to predict tumor killing in function of target expression (**Fig. 2B**) or define the threshold to elicit tumor killing (27). Singh and colleagues developed a systems model to capture the effect of target expression on the activity of HER2- and EGFR-CAR-T cells *in vitro* (39). The release of IFNγ, CAR-T expansion, and tumor lysis increased with increased target density.

Tumor selectivity could be improved with "pro-drug" like engineering approaches for CD3-bispecifics. The goal is to administer the CD3-bispecific compound in its pharmacologically inactive form and that will be converted proteolytically or biochemically into its pharmacologically active form in the tumor microenvironment (40, 41).

### Binding affinity and cytokine release

For T-cell–redirecting therapies, the binding affinity to the tumor target, and in addition for CD3-bispecifics, the binding affinity to the T cell, are important properties (**Fig. 1**). Binding affinity has implications on their activity (42–45). Understanding this relationship is paramount to select optimal compound properties.

In a retrospective FDA analysis, Saber and colleagues looked into the binding affinities of multiple CD3-bispecifics that undergo clinical testing. Among those, the most common toxicity was CRS. They reported a trend of better tolerability among the compounds when affinity to CD3 was lower than to the tumor target, even though they did not mention whether there was any link with CRS (15).

Several studies explored the relationship of binding affinity to the tumor target and CD3. Preclinical *in vivo* studies with HER2-CD3-bispecific antibodies (30) showed that a high CD3-affinity variant as well as higher HER2-binding affinity variants had a lower benefit/risk profile. While higher inflammatory cytokine release was observed with the higher binding affinity molecules, there was no additional gain in antitumor effects. Similar results have been observed with HER2-CAR-T cells (46). A high-affinity variant induced tumor regression for a longer time by preventing regrowth compared to the low-affinity variant, but the high-affinity variant also induced maximal cytokine release *in vitro* even at low HER2 copy numbers, suggesting it may have a worse benefit/risk profile.

On the basis of these data, Singh and colleagues built a systems pharmacology model to investigate the impact of target binding affinity of CAR-T cells (39). They could make predictions about other CAR-T therapies, explore the impact of varying binding affinity on tumor lysis and cytokine release, and enable translation from *in vitro* data to *in vivo* predictions. Ghorashian and colleagues developed a new CD19-CAR-T therapy, called CAT19. The CAR-construct developed for CAT19 binds with a low affinity to an epitope on CD19, largely similar to the epitope bound by the approved CD19-CAR-T therapy Kymriah (tisagenlecleucel; ref. 47). As a result, CAT19 exhibited superior proliferative and cytotoxic potential *in vitro* and *in vivo*, with lower cytokine release compared with Kymriah. In addition, good antitumor responses and a favorable safety profile without any severe CRS was observed in pediatric patients with ALL. This finding suggests that cytokine release is not required to induce clinical efficacy.

*In silico* simulations facilitate the exploration of suitable compound properties. Systems pharmacology models have been developed to identify the most promising drug candidate based on their compound properties, and even for dose selection. **Figure 2A** gives an illustrative example of how dose-response analyses and *in silico* models can aid in selecting optimal compound properties for a given target (**Fig. 2A**; refs. 37, 38, 48). Jiang and colleagues developed a mechanistic model to describe synapse formation and subsequent tumor killing *in vitro* with the aim to select the desired compound properties for optimal tumor lysis by CD3-bispecifics (37). A similar model framework was used to derive the first-in-human dose for LP-DART, a proprietary format CD3-bispecific using the Dual-Activity Re-Targeting (DART) platform that targets P-cadherin (48). **Figure 2B** illustrates the impact of varying binding affinity of CD3-bispecifics.

### Target accessibility and CRS

To predict the safety and efficacy profile of a T-cell–redirecting therapy, accessibility of the target in healthy and tumor tissues (**Fig. 1**) needs to be investigated. The accessibility to the tumor for therapeutic interventions will depend on the tissue involved, the anatomic location, the vasculature, the specific tumor type, and the presence of metastases (49). Indeed, the biggest clinical successes for this kind of therapy have been observed for hematologic tumors, while effective treatment of solid tumors remains to be demonstrated (50, 51). The accessibility of a hematologic or fluid tumor is usually high while CD3-bispecifics and T cells need to surmount physical barriers in order to reach and effectively target a solid tumor (52, 53). Accessibility will affect the exposure to the treatment and may therefore affect the extent of local cytokine release. Moreover, cytokines are short-lived and therefore systemic cytokine levels may not necessarily reflect intratumoral cytokine release.

The disposition of CD3-bispecific antibodies and antibody fragments depends on the extravasation and lymphatic flow, resulting in different tissue partitioning. These physiologic processes of antibody disposition are captured in physiologically based PK models that can be utilized to predict the local drug concentration of CD3-bispecifics (54–56). It has also been observed that compound size and binding affinity play an important role in tumor uptake (57, 58). The notion of target accessibility becomes even

more important for CD3 bispecifics and adoptive cell therapies targeting a solid tumor (7, 58).

Modeling and simulation are helpful to deconvolute the factors that affect tumor accessibility and to make suggestions on optimal compound properties. For instance, Singh and colleagues aimed to predict local drug effects of CAR-T cells *in vivo*. For this, they developed a multiscale mathematical model to describe both the pharmacokinetics (based on mouse data) and pharmacodynamics (based on *in vitro* data) of CAR-T cells (39). In **Fig. 2C**, we illustrate how this model is useful to investigate the impact of altered accessibility on intratumoral cytokine release.

Local drug administration may improve the therapeutic window. For example, catumaxomab—a CD3-bispecific against EpCAM—showed good tolerability in ovarian cancer patients when administered via intraperitoneal injection (3). In contrast, intravenous dosing of catumaxomab was less tolerated (59).

The impact of target accessibility on the therapeutic window in different indications has been reported for both CAR-T cells and CD3-bispecifics. In the case of B-cell–related ALL versus non-Hodgkin lymphoma (B-NHL), it was found that CRS occurs together with CD19-CAR-T expansion and that both are correlated with disease burden in ALL but not NHL (60). Generally, ALL is a solely blood-borne neoplasia whereas NHL has a solid tumor involvement in the lymphatic tissue (61) and may therefore be less accessible as a whole, reducing the effect of disease burden on T-cell activity.

### Adoptive cell therapies: lymphodepletion, cell subtypes, and CRS

Lymphodepletion with cyclophosphamide and/or fludarabine prior to adoptive cell therapy (ACT) is common practice (62, 63). Lymphodepletion removes the circulating T cells, providing more space for CAR-T or TCR-T cells to expand (64); the concurrent removal of regulatory T cells also eliminates potential immunosuppressive cues (63). The enhanced proliferation of the engineered T cells leads to improved antitumor effects but also increased incidence of CRS (36, 65, 66). Due to lack of direct evidence, it is unclear whether lymphodepletion increases the incidence for all-grade CRS; however, increased risk for high-grade CRS (> grade 3) has been shown in two independent analyses (63, 67).

There is limited evidence that the cell contents of the ACT infusion product may affect the propensity for CRS. For instance, in a pediatric neuroblastoma population, infusion of purified $CD4^+$ and $CD8^+$ GD2-CAR-T cells (by removal of other mononuclear cells) boasted a higher potency for cytokine release compared with the nonpurified product and necessitated dose deescalation (68). However, at lower doses the purified product had a markedly improved risk–benefit profile.

Multiple lines of evidence point out the differences between $CD4^+$ and $CD8^+$ T-cell subsets in ACT with respect to expansion and persistence (65, 69–71). The difference in treatment efficacy and safety is however not well understood.

In terms of noncanonical cell types, engineered CAR-NK cells are being investigated as a suitable alternative to CAR-T cells as they show similar tumor lytic potential with less cytokine release (72).

On the molecular scale, the structure of the CAR construct also influences its cytokine-inducing potential. Multiple generations of CAR constructs have been developed that are structurally different (36, 60, 73). The effect of these differently structured CAR constructs on CRS formation is not well understood. Schuster and colleagues reported that patients treated with Kymriah or Yescarta, each containing different costimulatory domains, had a 58% and 93% incidence of any-grade CRS, respectively (74).

Alternatives to the viral production of CAR-T cells are being investigated to improve both the manufacturing efficiency and safety profile. For instance, the use of transposons to manufacture CAR-T cells eliminates the risk for insertional mutagenesis (75). A phase I clinical trial of patients with advanced NHL and ALL that received hematopoietic stem cell transplantation with adjuvant transposon-based CAR-T-cell therapy produced favorable safety and efficacy profiles (76). Similarly, mRNA-based CAR-T cells have been developed that induce transient expression of the CAR construct to prevent long-term toxicity. As a consequence, this modality would require repeated administration and offers the possibility to stop dosing in case of serious adverse events, which is not feasible with virally transduced (i.e., stably expressing) CAR-T cells that are administered only once and persist over a long period (73, 77, 78).

## Considering Individual Patient Risk

It has been challenging to establish robust correlations between cytokine levels and CRS severity grades. Moreover, individual patients may respond differently to cytokine excursion, thus demonstrating that patients' specific characteristics influence the body's pathophysiologic reaction to cytokine release. The predisposing factors for high-grade CRS in individual patients have not yet been investigated comprehensively; however, some negative synergies leading to the exacerbation of pathophysiology can be anticipated. A hallmark of acute inflammation, whether naturally triggered (infection) or drug-induced, is the increased vascular permeability leading to the escape (capillary leakage) of an exudate into the tissues (edema). Numerous criteria, which are taken into account for the grading of CRS, are directly related to the increased vascular permeability and its consequences on the cardiovascular and cardio-pulmonary systems, i.e., hypotension, hypoxia, and dyspnea (16). Thus, genetic polymorphisms associated to—or preexisting pathologies/comorbidities involving—chronic inflammation, endothelial dysfunctions, and barrier impairments should be factored in when considering the consequences of cytokine release. Endothelial dysfunction and/or inflammation is present in several cardiovascular and metabolic conditions such as hypertension, chronic heart failure, peripheral arterial disease, atherosclerosis, diabetes, obesity, septic shock, and chronic renal failure (79–81). Lifestyle-related conditions have also been identified as independent risk factors for endothelial dysfunction. These include obesity, hyperlipidemia, hypertension, age, and smoking (82). A recent study by Hong and colleagues on a small cohort of COVID-19 patients identified hypertension history as a significant risk factor for severe CRS (83), and baseline endothelial activation (thrombocytopenia) has been described to be predictive for higher-grade CRS (84). The aforementioned pathologies have underlying endothelial oxidative stress and chronic inflammation in common. The association of obesity and severe dengue gives a relevant example, where chronic inflammation and pro-inflammatory adipokines found in obese individuals cause endothelial and platelet dysfunction, predisposing them to severe dengue defined by stronger proinflammatory cytokine responses and more severe immunopathology after viral infection (85).

Certain associations between demographics/comorbidities and increased cytokine levels were recently strengthened in the context of the comprehensive immunopathology investigation of COVID-19 (22). Namely, of demographic variables, age and sex were significantly associated with cytokine levels, especially IL6. Considering

comorbidities, TNFα and IL8 were significantly increased in patients with chronic kidney disease, diabetes, and hypertension. TNFα was also increased in patients with congestive heart failure, and IL6 and IL8 were elevated in patients with a history of atrial fibrillation.

The commonality between viral infections and T-cell–redirecting therapies is the polyclonal T-cell activation. In both contexts, activated T cells release IFNγ, which activates monocytes/macrophages to produce additional cytokines such as IL6, TNFα, and IL10. These cytokines can elicit flu-like symptoms, vascular leakage, diarrhea, cardiomyopathy, lung injury, and acute phase response. IL6 triggers effects such as vascular leakage, activation of the complement, and coagulation cascade inducing disseminated intravascular coagulation, which are characteristics of severe CRS.

Many cytokines and inflammatory mediators increase vascular permeability by activating and structurally changing the endothelium; in turn, activated endothelium has an enhanced capability for (i) T-cell migration (86) and (ii) release of proinflammatory cytokines. Endothelial cells activated by IL6 will upregulate Ang2 signaling and produce oxygen radicals, leading to endothelial dysfunction (87), which critically contributes to the pathogenesis of CRS, both by amplifying the inflammation and as a target organ for capillary leak syndrome, hypotension, and coagulopathy. In a CD19-CAR-T-cell therapy phase I/II study in patients with various B-cell malignancies, Hay and colleagues (67) observed that a pretreatment activated endothelium status as defined by elevated vWF and Ang2/Ang1 ratio was predictive of severe CRS.

A solid base of literature supports the role of underlying diseases in exacerbating CRS related to viral infections and the implication of endothelial cells in producing IL6 and hypotension seen in severe CRS with T-cell–redirecting therapies (88, 89). However, there is not yet any literature that exposes direct associations of underlying pathologies (i.e., endothelial dysfunction) with higher CRS grades for T-cell–redirecting therapies.

Furthermore, clinical fitness appears not to be a reliable predictor for CRS formation. Hay and colleagues found that there was no significant difference in CRS formation induced by CD19-CAR-T therapy between patients with Karnofsky scores (a measure of clinical fitness) of 60%–70%, 80%–90%, and 100% (67). Because patients that are in poor health conditions are usually excluded from clinical trials, we have no information on the link between low clinical performance scores and the propensity for CRS formation. Moreover, patients that have an objectively good clinical performance score may still be suffering from underlying ailments that remain undetected and that pose an increased risk for CRS formation.

For instance, for immune checkpoint inhibitors, it has been reported that underlying comorbidities may affect its safety: a history of kidney dysfunction of at least grade 3 was identified as an independent risk factor for immune-related adverse events (90). Although these findings do not specifically reflect CRS and T-cell–redirecting therapies, they still suggest caution to be taken when dealing with patients suffering from these ailments and who will receive immunostimulatory treatment.

Taken together, more research and leveraging real-world data and details on individual patient characteristics will need to be collected to improve the prognosis of the individual patient's risks concerning CRS.

Identification of the main additional contributors is paramount to be able to predict reliably which patients are at risk for developing high-grade CRS triggered by a T-cell–redirecting therapy. This should guide the decision-making regarding individual dosing schemes and choice of mitigation or salvage strategies.

## Clinical Mitigating Strategies

Investigators have been studying various approaches to downplay undesirable immune effects while still maintaining a therapeutically active treatment (**Table 3**). Li and colleagues demonstrated that cytokine release is dispensable for antitumor activity. They showed *in vitro* as well as in a mouse study that tumor killing is maintained even when cytokine release is lowered by mitigating strategies (91). Dosing strategies can be applied to reduce the risk for cytokine release. One option is to give patients with a high tumor burden a low initial dose to dampen the cytokine response (66, 69). Alternatively, step-up dosing is frequently applied in clinics for CD3-bispecifics (59, 92–94). By fractionating the dose into two or more steps, cytokine release is dampened with each subsequent step, which was demonstrated for HER2xCD3-bispecific antibody *in vitro* and *in vivo* (30, 91) and was also observed clinically for mosunetuzumab (a CD20xCD3-bispecific; ref. 95).

Li and colleagues demonstrated with nonclinical experiments that repeat dosing with CD3 bispecifics strongly reduces cytokine release with subsequent doses. They also showed that a reduction in cytokine release did not affect the tumor-killing potential of the therapy. The optimal (step-up) dosing strategies can be explored *in silico* (for illustration, see **Fig. 2D** and **E**). PK/PD models have been developed by Jiang and colleagues for blinatumomab (96) and by Chen and colleagues for blinatumomab and P-cadherin LP-DART (97) that incorporate mechanistic insights to simulate the cytokine-mitigating effects of dose fractionation. The model from Jiang and colleagues assumes that the reduction in tumor burden after the first dose is responsible for the reduced cytokine release upon repeat dosing, whereas the model from Chen and colleagues assumes that the main driver behind reduced cytokine release is a build-up of tolerance in the

**Table 3.** Toxicity-mitigating strategies for T-cell–redirecting therapies that are either in development or already applied in clinics.

| Strategy | Modality[a] | Example | Clinical application[b] | References |
|---|---|---|---|---|
| Inverse dose-adjustment | All | BCMA-CAR-T | Yes | 31 |
| Cytoreduction | All | Blinatumomab | Yes | 69 |
| Cytokine blockade | All | Tocilizumab, Ienlizumab | Yes | 84, 91, 101, 103, 104, 106 |
| Corticosteroids | All | Dexamethasone | Yes | 99, 100 |
| Target masking | All | Anti-CAIX mAb | Yes | 108 |
| Dose fractionation | CD3-bispecific | Mosunetuzumab, blinatumomab | Yes | 59, 91–94 |
| Kinase inhibitors | All | Dasatinib | No | 84, 107 |

[a]Modalities to which the strategy is applicable.
[b]Whether the strategies are currently being tested in clinics.

immune system. The exact mechanism still needs to be elucidated, but current data would support a combination of both hypotheses (91, 96). Similarly, Hosseini and colleagues developed a mechanistic model based on nonclinical data of mosunetuzumab and clinical data of blinatumomab to construct a virtual patient population and used it to simulate the effects of dose fractionation on cytokine release and efficacy of these compounds. These simulations supported the implementation of dose fractionation in an ongoing phase I trial of mosunetuzumab (98).

Other mitigation strategies aim to reduce the propensity of T cells and accessory cells to induce CRS after target engagement. The most common example is the use of corticosteroids, which has shown to prevent fatal CRS events and pushed up the MTD in patients (84, 99, 100). Cytokine sequestration and receptor blocking are used to prevent downstream cytokine signaling that may be harmful, which is further supported by the preclinical findings that cytokines are dispensable for therapeutic efficacy of T-cell–engaging therapies (84, 100, 101).

Tocilizumab is an anti-IL6R antibody that is FDA approved as a salvage therapy in case of CRS induced by CAR therapy. It has been used to great success to reverse CRS in all approved anti-CD19 T-cell–redirecting therapies against B-ALL (tisagenlecleucel, axicabtagene ciloleucel, blinatumomab; refs. 102, 103). A recent line of evidence suggests the superiority of tocilizumab over corticosteroids pretreatment to combat CRS because blocking IL6 receptor does not affect the tumor-killing potential of T cells, in contrast to corticosteroids (104). Despite the promising results, it is unknown what the best timing for tocilizumab intervention is during the course of CRS to balance efficacy and safety (105). Recently, a prospective clinical trial of pediatric patients with B-ALL treated with CD19-CAR-T cells was carried out where cohorts were formed based on disease burden (106). Risk-adapted preemptive treatment of tocilizumab was performed to reduce the incidence of grade 4 CRS. The high tumor burden (i.e., high-risk) cohort received tocilizumab early, when persistent fever was reported but before development of CRS. Compared with a historical cohort that received standard CRS management, preemptive tocilizumab treatment markedly reduced the incidence of grade 4 CRS.

Kinase inhibitors such as dasatinib have shown to rapidly reduce T-cell activity and could be used as a salvage therapy in case of severe toxicities. However, it will also hamper the treatment efficacy (84, 107).

For CAR-T cells, the administration of mAbs targeting the same antigen has been explored as a mitigation strategy to reduce on-target toxicity. In a phase I trial, patients with metastatic renal cell carcinoma were treated with CAR-T cells targeting CAIX. There were signs of liver toxicity at low doses, which were attributed to reactivity against CAIX-expressing healthy liver tissue. By administering anti-CAIX antibodies prior to CAR-T-cell treatment, thereby saturating the liver target pool, the investigators managed to prevent liver toxicities and allow higher CAR-T-cell doses to be given (108).

## Conclusion: Limitations and Outlook

Using a data-driven modeling framework, we are well equipped to investigate the complex relationship between drug-target-disease–related factors and cytokine release.

Given the complexities and the interdependencies of the drug-target-disease–related factors of the T-cell–redirecting therapies, we argue that it is not meaningful to look at the factors in isolation when trying to optimize their effectiveness by balancing the beneficial versus the adverse effects. Instead, we suggest the use of mathematical modeling, integrating all those processes in mechanistic terms supported by the generated data. We can utilize this to select the most favorable compound properties for a given target in a given indication and to optimize the dosing regimen with minimized inflammatory cytokine release while maximizing antitumor effects for patients.

We have presented various case studies highlighting the value of model-based approaches to guide drug discovery and development of T-cell engagers. The success of these modeling approaches is highly dependent on the collaboration between *in vitro* and *in silico* scientists, and the appropriate study design of the *in vitro* experiments as well as the nonclinical and clinical studies. This includes the collection of relevant PK and PD data measured repeatedly over time. In addition, it is recommended to explore a broad dose range capturing minimal to maximal drug effects.

However, while these models are well suited to predict cytokine release, they are not suited to predict the individual risk of severe CRS in patients because the risk of CRS is multifactorial and not only dependent on the magnitude of cytokine release (22, 23, 83, 84). While it was shown that on a population level there is a higher cytokine release observed in CRS, there is significant overlap in the range of cytokine levels in patients that are associated with no or with high CRS risk (22, 23). Therefore, the risk for a patient to experience high-grade CRS depends on the patient's propensity for developing CRS in response to therapy, which can be regarded as a combination and interplay of both the drug-target-disease–related factors and the individual patient's risk factors.

As an outlook, we propose to fill this gap by providing a quantitative framework that combines mechanistic modeling for the given therapeutic treatment with a risk scoring method that integrates all relevant patient/individual specific risk factors. The relevant risk factors can be derived from real-world data of a broad range of therapeutic interventions associated with CRS and the scoring method can be established using these data. **Figure 3** illustrates the conceptual framework of such an approach, which could enable personalized risk assessment. It aims to predict the probability of severe CRS for the individual patient (**Fig. 3C**), which is achieved by combining mechanistic modeling that considers the drug-target-disease–related factors to predict cytokine release for a given therapeutic intervention (**Fig. 3A**), and the consideration of the individual patient risk factors (**Fig. 3B**). To predict the risk of high or low grade of CRS, additional patient-specific risk factors such as hypertension history or endothelial activation can be integrated empirically with the mechanistically predicted cytokine response. To give a relevant example, the study from Han and colleagues (109) showed a machine learning–based approach to predict adverse events after spine surgery, taking into account patient-, diagnostic-, and procedure-related factors. In the case of T-cell–redirecting therapies, to establish such an empirical model, one would need a (large) data set where individual patient cytokine profiles and comorbidities (prior and during treatment) are recorded.

For prediction of the individual cytokine release profiles, we propose a data-driven approach utilizing mechanistic-based nonlinear mixed-effect PK/PD models tailored for the therapeutic intervention of interest. These approaches are suited to analyze sparse data, to quantify the dose–response relationships, and may explain the interpatient variability in mechanistic terms. For example, the individual cytokine response can be predicted as the result of a given drug–target relationship in the context of the individual disease factors such as tumor load and/or target expression. On the basis of the predicted cytokine profiles and the individual patient's risk factors, the patient's individual

risk for high-grade CRS could be predicted. We proposed to capture individual risk factors in risk-scoring tables derived from real-world data considering a broad range of therapeutic interventions for which CRS has been clinically observed (**Fig. 3B**). Because of the high dimension and the high complexity of all the elements, to dissect comprehensively the patient-specific risk factors, one would need to collect and analyze information-rich (ideally with high granularity) datasets from a large number of patients that reflect a cross-section of the entire population. Real-world data, ideally combining demography, well-curated electronic healthcare records (EHR), omics, and baseline screening data from a large number of patients, provide a promising opportunity. Besides the sample size, an agnostic and unbiased approach to mine and analyze the data, in particular, for the risk markers and comorbidities can be important to uncover the true picture.

We expect that the proposed optimized prediction models result in a better prognosis of the individual patient's risk and can be the basis of a classification of the risks. The individual or classified risk factors can subsequently be integrated in more standard classical approaches for further analyses or comparisons (i.e., ROC curves, logistic regression, and time-to-event).

As an initial step, our future efforts will first focus on the comprehensive and agnostic evaluation of demographic, comorbidity, clinical lab value, and genetic (where available) information from patients who experienced a drug-induced CRS. Real-world data sources ranging from the less granular claims data (e.g., Truven Marketscan) to more information-rich data/biobank (e.g., UK Biobank, Genomics England) will be used to identify the relevant individual risk factors to be considered in our next-generation quantitative framework, which will aim at differentiating between low- and high-risk patients for severe CRS induced by T-cell–redirecting therapies. Developing these risk scores will require further cross-disciplinary research among data scientists, physicians, and drug developers and will be an important step towards improved individual risk prediction of severe CRS with T-cell–redirecting therapy.

## Authors' Disclosures

A.J. Van De Vyver reports employment at F. Hoffmann-La Roche. E. Marrer-Berger reports employment at F. Hoffmann-La Roche. K. Wang reports employment at F. Hoffmann-La Roche. T. Lehr reports grants from Neovii, Boehringer Ingelheim, and Aspen outside the submitted work. A.-C. Walz reports employment at F. Hoffmann-La Roche.

## Acknowledgments

This work was supported by F. Hoffmann-La Roche Ltd. The authors would like to thank Christoph T. Berger from the Interdisciplinary Centre of Immunology at University Hospital Basel and Martin Stern from Clinical Development Oncology at Roche Innovation Center Zürich for critical review of the manuscript, and Alexander Skates from Roche Welwyn for his valuable comments on the methodology. Figures have been created with Biorender.com.

The costs of publication of this article were defrayed in part by the payment of page charges. This article must therefore be hereby marked *advertisement* in accordance with 18 U.S.C. Section 1734 solely to indicate this fact.

Received February 28, 2021; revised April 30, 2021; accepted June 11, 2021; published first June 23, 2021.

## References

1. Kruger S, Ilmer M, Kobold S, Cadilha BL, Endres S, Ormanns S, et al. Advances in cancer immunotherapy 2019 – latest trends. J Exp Clin Cancer Res 2019; 38:268.
2. Upadhaya S, Hubbard-Lucey VM, Yu JX. Immuno-oncology drug development forges on despite COVID-19. Nat Rev Drug Discov 2020;19:751–2.
3. Seimetz D, Lindhofer H, Bokemeyer C. Development and approval of the trifunctional antibody catumaxomab (anti-EpCAM x anti-CD3) as a targeted cancer immunotherapy. Cancer Treat Rev 2010;36:458–67.
4. Zheng P-P, Kros JM, Li J. Approved CAR T cell therapies: ice bucket challenges on glaring safety risks and long-term impacts. Drug Discov Today 2018;23: 1175–82.
5. O'Leary MC, Lu X, Huang Y, Lin X, Mahmood I, Przepiorka D, et al. FDA approval summary: tisagenlecleucel for treatment of patients with relapsed or refractory B-cell precursor acute lymphoblastic leukemia. Clin Cancer Res 2019;25:1142–6.
6. Labrijn AF, Janmaat ML, Reichert JM, Parren PWHI. Bispecific antibodies: a mechanistic review of the pipeline. Nat Rev Drug Discovery 2019;18:585–608.
7. Zhang J, Wang L. The emerging world of TCR-T cell trials against cancer: a systematic review. Technol Cancer Res Treat 2019;18:1533033819831068.
8. Ma S, Li X, Wang X, Cheng L, Li Z, Zhang C, et al. Current progress in CAR-T cell therapy for solid tumors. Int J Biol Sci 2019;15:2548–60.
9. Sharma P, King GT, Shinde SS, Purev E, Jimeno A. Axicabtagene ciloleucel for the treatment of relapsed/refractory B-cell non-Hodgkin's lymphomas. Drugs of today (Barcelona, Spain: 1998) 2018;54:187–98.
10. Shimabukuro-Vornhagen A, Gödel P, Subklewe M, Stemmler HJ, Schlößer HA, Schlaak M, et al. Cytokine release syndrome. J Immunother Cancer 2018;6:56.
11. Maker AV, Phan GQ, Attia P, Yang JC, Sherry RM, Topalian SL, et al. Tumor regression and autoimmunity in patients treated with cytotoxic T lymphocyte-associated antigen 4 blockade and interleukin 2: a phase I/II study. Ann Surg Oncol 2005;12:1005–16.
12. Caspi RR. Immunotherapy of autoimmunity and cancer: the penalty for success. Nat Rev Immunol 2008;8:970–6.
13. Young A, Quandt Z, Bluestone JA. The balancing act between cancer immunity and autoimmunity in response to immunotherapy. Cancer Immunol Res 2018; 6:1445–52.
14. Yiu HH, Graham AL, Stengel RF. Dynamics of a cytokine storm. PLoS One 2012;7:e45027.
15. Saber H, Del Valle P, Ricks TK, Leighton JK. An FDA oncology analysis of CD3 bispecific constructs and first-in-human dose selection. Regul Toxicol Pharmacol 2017;90:144–52.
16. Lee DW, Santomasso BD, Locke FL, Ghobadi A, Turtle CJ, Brudno JN, et al. ASTCT consensus grading for cytokine release syndrome and neurologic toxicity associated with immune effector cells. Biol Blood Marrow Transplant 38–25:625;2019.
17. Friends of Cancer Research. Harmonizing the definition and reporting of cytokine release syndrome (CRS) in immuno-oncology clinical trials [White paper]. Washington, D.C.: Friends of Cancer Research; 2021.
18. Suurs FV, Lub-de Hooge MN, de Vries EGE, de Groot DJA. A review of bispecific antibodies and antibody constructs in oncology and clinical challenges. Pharmacol Ther 2019;201:103–19.
19. Zhao L, Cao YJ. Engineered T cell therapy for cancer in the clinic. Front Immunol 2019;10:2250.
20. Wang Y, Zhu H, Madabushi R, Liu Q, Huang SM, Zineh I. Model-informed drug development: current US regulatory practice and future considerations. Clin Pharmacol Ther 2019;105:899–911.
21. Marshall S, Madabushi R, Manolis E, Krudys K, Staab A, Dykstra K, et al. Model-informed drug discovery and development: current industry good practice and regulatory expectations and future perspectives. CPT Pharmacometrics Syst Pharmacol 2019;8:87–96.
22. Del Valle DM, Kim-Schulze S, Huang H-H, Beckmann ND, Nirenberg S, Wang B, et al. An inflammatory cytokine signature predicts COVID-19 severity and survival. Nat Med 2020;26:1636–43.
23. Teachey DT, Lacey SF, Shaw PA, Melenhorst JJ, Maude SL, Frey N, et al. Identification of predictive biomarkers for cytokine release syndrome after chimeric antigen receptor T-cell therapy for acute lymphoblastic leukemia. Cancer Discov 2016;6:664–79.
24. Sapski S, Beha N, Kontermann RE, Müller D. Influence of antigen density and immunosuppressive factors on tumor-targeted costimulation with antibody-fusion proteins and bispecific antibody-mediated T cell response. Cancer Immunol Immunother 2020;69:2291–303.

25. Slaga D, Ellerman D, Lombana TN, Vij R, Li J, Hristopoulos M, et al. Avidity-based binding to HER2 results in selective killing of HER2-overexpressing cells by anti-HER2/CD3. Sci Transl Med 2018;10:eaat5775.
26. Bacac M, Fauti T, Sam J, Colombetti S, Weinzierl T, Ouaret D. A novel carcinoembryonic antigen T-cell bispecific antibody (CEA TCB) for the treatment of solid tumors. Clin Cancer Res 2016;22:3286–97.
27. Van De Vyver AJ, Weinzierl T, Eigenmann MJ, Frances N, Herter S, Buser RB, et al. Predicting tumor killing and T-cell activation by T-cell bispecific antibodies as a function of target expression: combining in vitro experiments with systems modeling. Mol Cancer Ther 2021;20:357–66.
28. Andersch L, Radke J, Klaus A, Schwiebert S, Winkler A, Schumann E, et al. CD171- and GD2-specific CAR-T cells potently target retinoblastoma cells in preclinical in vitro testing. BMC Cancer 2019;19:895.
29. Watanabe K, Terakura S, Martens AC, van Meerten T, Uchiyama S, Imai M, et al. Target antigen density governs the efficacy of anti–CD20-CD28-CD3 ζ chimeric antigen receptor–modified effector $CD8^{+}$T cells. J Immunol 2015;194:911–20.
30. Staflin K, Zuch de Zafra CL, Schutt LK, Clark V, Zhong F, Hristopoulos M, et al. Target arm affinities determine preclinical efficacy and safety of anti-HER2/CD3 bispecific antibody. JCI Insight 2020;5:e133757.
31. Frey N. Cytokine release syndrome: Who is at risk and how to treat. Best Pract Res Clin Haematol 2017;30:336–40.
32. Davila ML, Riviere I, Wang X, Bartido S, Park J, Curran K, et al. Efficacy and toxicity management of 19–28z CAR T cell therapy in B cell acute lymphoblastic leukemia. Sci Transl Med 2014;6:224ra25–ra25.
33. Brentjens RJ, Davila ML, Riviere I, Park J, Wang X, Cowell LG, et al. CD19-targeted T cells rapidly induce molecular remissions in adults with chemotherapy-refractory acute lymphoblastic leukemia. Sci Transl Med 2013;5:177ra38.
34. June CH, Sadelain M. Chimeric antigen receptor therapy. N Engl J Med 2018;379:64–73.
35. Fry TJ, Shah NN, Orentas RJ, Stetler-Stevenson M, Yuan CM, Ramakrishna S, et al. CD22-targeted CAR T cells induce remission in B-ALL that is naive or resistant to CD19-targeted CAR immunotherapy. Nat Med 2018;24:20–8.
36. Brudno JN, Kochenderfer JN. Recent advances in CAR T-cell toxicity: Mechanisms, manifestations and management. Blood Rev 2019;34:45–55.
37. Jiang X, Chen X, Carpenter TJ, Wang J, Zhou R, Davis HM, et al. Development of a target cell-biologics-effector cell (TBE) complex-based cell killing model to characterize target cell depletion by T cell redirecting bispecific agents. mAbs 2018;10:876–89.
38. Campagne O, Delmas A, Fouliard S, Chenel M, Chichili GR, Li H, et al. Integrated pharmacokinetic/pharmacodynamic model of a bispecific CD3xCD123 DART molecule in nonhuman primates: evaluation of activity and impact of immunogenicity. Clin Cancer Res 2018;24:2631–41.
39. Singh AP, Zheng X, Lin-Schmidt X, Chen W, Carpenter TJ, Zong A, et al. Development of a quantitative relationship between CAR-affinity, antigen abundance, tumor cell depletion and CAR-T cell expansion using a multiscale systems PK-PD model. mAbs 2020;12:1688616.
40. Geiger M, Stubenrauch K-G, Sam J, Richter WF, Jordan G, Eckmann J, et al. Protease-activation using anti-idiotypic masks enables tumor specificity of a folate receptor 1-T cell bispecific antibody. Nat Commun 2020;11:3196.
41. Boustany LM, Wong L, White CW, Diep L, Huang Y, Liu S, et al. Abstract A164: EGFR-CD3 bispecific Probody™ therapeutic induces tumor regressions and increases maximum tolerated dose >60 fold in preclinical studies. Mol Cancer Ther 2018;17:A164–A.
42. Ellerman D. Bispecific T-cell engagers: Towards understanding variables influencing the in vitro potency and tumor selectivity and their modulation to enhance their efficacy and safety. Methods 2019;154:102–17.
43. Harper J, Adams KJ, Bossi G, Wright DE, Stacey AR, Bedke N, et al. An approved in vitro approach to preclinical safety and efficacy evaluation of engineered T cell receptor anti-CD3 bispecific (ImmTAC) molecules. PLoS One 2018;13:e0205491.
44. Bortoletto N, Scotet E, Myamoto Y, D'Oro U, Lanzavecchia A. Optimizing anti-CD3 affinity for effective T cell targeting against tumor cells. Eur J Immunol 2002;32:3102–7.
45. Leong SR, Sukumaran S, Hristopoulos M, Totpal K, Stainton S, Lu E, et al. An anti-CD3/anti–CLL-1 bispecific antibody for the treatment of acute myeloid leukemia. Blood 2017;129:609–18.
46. Liu X, Jiang S, Fang C, Yang S, Olalere D, Pequignot EC, et al. Affinity-tuned ErbB2 or EGFR chimeric antigen receptor T cells exhibit an increased therapeutic index against tumors in mice. Cancer Res 2015;75:3596.
47. Ghorashian S, Kramer AM, Onuoha S, Wright G, Bartram J, Richardson R, et al. Enhanced CAR T cell expansion and prolonged persistence in pediatric patients with ALL treated with a low-affinity CD19 CAR. Nat Med 2019;25:1408–14.
48. Chen X, Haddish-Berhane N, Moore P, Clark T, Yang Y, Li H, et al. Mechanistic projection of first-in-human dose for bispecific immunomodulatory P-Cadherin LP-DART: an integrated PK/PD modeling approach. Clin Pharmacol Ther 2016;100:232–41.
49. Sambi M, Bagheri L, Szewczuk MR. Current challenges in cancer immunotherapy: multimodal approaches to improve efficacy and patient response rates. J Oncol 2019;2019:4508794.
50. Yu S, Li A, Liu Q, Yuan X, Xu H, Jiao D, et al. Recent advances of bispecific antibodies in solid tumors. J Hematol Oncol 2017;10:155.
51. Dahlén E, Veitonmäki N, Norlén P. Bispecific antibodies in cancer immunotherapy. Curr Opin Biotechnol 2018;6:3–17.
52. Lanitis E, Dangaj D, Irving M, Coukos G. Mechanisms regulating T-cell infiltration and activity in solid tumors. Ann Oncol 2017;28:xii18–32.
53. Morgan RA, Yang JC, Kitano M, Dudley ME, Laurencot CM, Rosenberg SA. Case report of a serious adverse event following the administration of T cells transduced with a chimeric antigen receptor recognizing ERBB2. Mol Ther 2010;18:843–51.
54. Eigenmann MJ, Karlsen TV, Krippendorff B-F, Tenstad O, Fronton L, Otteneder MB, et al. Interstitial IgG antibody pharmacokinetics assessed by combined in vivo- and physiologically-based pharmacokinetic modelling approaches. J Physiol 2017;595:7311–30.
55. Fronton L, Pilari S, Huisinga W. Monoclonal antibody disposition: a simplified PBPK model and its implications for the derivation and interpretation of classical compartment models. J Pharmacokinet Pharmacodyn 2014;41:87–107.
56. Jones HM, Zhang Z, Jasper P, Luo H, Avery LB, King LE, et al. A physiologically-based pharmacokinetic model for the prediction of monoclonal antibody pharmacokinetics from *in vitro* data. CPT: Pharmacometrics & Systems Pharmacology 2019;8:738–47.
57. Wittrup KD, Thurber GM, Schmidt MM, Rhoden JJ. Practical theoretic guidance for the design of tumor-targeting agents. Methods Enzymol 2012;503:255–68.
58. Lehmann S, Perera R, Grimm HP, Sam J, Colombetti S, Fauti T, et al. In vivo fluorescence imaging of the activity of CEA TCB, a novel T-cell bispecific antibody, reveals highly specific tumor targeting and fast induction of T-cell-mediated tumor killing. Clin Cancer Res 2016;22:4417–27.
59. Mau-Sørensen M, Dittrich C, Dienstmann R, Lassen U, Büchler W, Martinius H, et al. A phase I trial of intravenous catumaxomab: a bispecific monoclonal antibody targeting EpCAM and the T cell coreceptor CD3. Cancer Chemother Pharmacol 2015;75:1065–73.
60. Ormhøj M, Bedoya F, Frigault MJ, Maus MV. CARs in the lead against multiple myeloma. Curr Hematol Malig Rep 2017;12:119–25.
61. Szymańska K, Park S. Non-hodgkin lymphoma: diagnosis and treatment. In: Boffetta P, Hainaut P, editors. Encyclopedia of Cancer (Third Edition). Oxford, United Kingdom: Academic Press; 2019. p. 44–7.
62. Gattinoni L, Powell DJ Jr., Rosenberg SA, Restifo NP. Adoptive immunotherapy for cancer: building on success. Nat Rev Immunol 2006;6:383–93.
63. Thakar MS, Kearl TJ, Malarkannan S. Controlling cytokine release syndrome to harness the full potential of CAR-based cellular therapy. Front Oncol 2020;9:1529.
64. Yang JC. Toxicities associated with adoptive T-cell transfer for cancer. The Cancer Journal 2015;21:506–9.
65. Hunder NN, Wallen H, Cao J, Hendricks DW, Reilly JZ, Rodmyre R, et al. Treatment of metastatic melanoma with autologous CD4+ T cells against NY-ESO-1. N Engl J Med 2008;358:2698–703.
66. Frey NV, Shaw PA, Hexner EO, Gill S, Marcucci K, Luger SM, et al. Optimizing chimeric antigen receptor (CAR) T cell therapy for adult patients with relapsed or refractory (r/r) acute lymphoblastic leukemia (ALL). J Clin Oncol 2016;34:7002.
67. Hay KA, Hanafi LA, Li D, Gust J, Liles WC, Wurfel MM, et al. Kinetics and biomarkers of severe cytokine release syndrome after CD19 chimeric antigen receptor-modified T-cell therapy. Blood 2017;130:2295–306.
68. Louis CU, Savoldo B, Dotti G, Pule M, Yvon E, Myers GD, et al. Antitumor activity and long-term fate of chimeric antigen receptor–positive T cells in patients with neuroblastoma. Blood 2011;118:6050–6.
69. Ali SA, Shi V, Maric I, Wang M, Stroncek DF, Rose JJ, et al. T cells expressing an anti-B-cell maturation antigen chimeric antigen receptor cause remissions of multiple myeloma. Blood 2016;128:1688–700.

70. Yee C, Thompson JA, Byrd D, Riddell SR, Roche P, Celis E, et al. Adoptive T cell therapy using antigen-specific CD8+ T cell clones for the treatment of patients with metastatic melanoma: in vivo persistence, migration, and antitumor effect of transferred T cells. PNAS 2002;99:16168–73.
71. Mackensen A, Meidenbauer N, Vogl S, Laumer M, Berger J, Andreesen R. Phase I study of adoptive T-cell therapy using antigen-specific CD8+ T cells for the treatment of patients with metastatic melanoma. J Clin Oncol 2006; 24:5060–9.
72. Li Y, Hermanson DL, Moriarity BS, Kaufman DS. Human iPSC-derived natural killer cells engineered with chimeric antigen receptors enhance anti-tumor activity. Cell Stem Cell 2018;23:181–92.e5.
73. Maus MV, June CH. Making better chimeric antigen receptors for adoptive T-cell therapy. Clin Cancer Res 2016;22:1875–84.
74. Schuster SJ, Maziarz RT, Rusch ES, Li J, Signorovitch JE, Romanov VV, et al. Grading and management of cytokine release syndrome in patients treated with tisagenlecleucel in the JULIET trial. Blood Adv 2020;4:1432–9.
75. Magnani CF, Tettamanti S, Alberti G, Pisani I, Biondi A, Serafini M, et al. Transposon-based CAR T cells in acute leukemias: where are we going? Cells 2020;9:1337.
76. Kebriaei P, Singh H, Huls MH, Figliola MJ, Bassett R, Olivares S, et al. Phase I trials using sleeping beauty to generate CD19-specific CAR T cells. J Clin Invest 2016;126:3363–76.
77. Beatty GL, Gladney WL. Immune escape mechanisms as a guide for cancer immunotherapy. Clin Cancer Res 2015;21:687–92.
78. Singh N, Barrett DM, Grupp SA. Roadblocks to success for RNA CARs in solid tumors. Oncoimmunology 2015;3:e962974–e.
79. Esper RJ, Nordaby RA, Vilariño JO, Paragano A, Cacharrón JL, Machado RA. Endothelial dysfunction: a comprehensive appraisal. Cardiovascular Diabetology 2006;5:4.
80. Roumeliotis S, Mallamaci F, Zoccali C. Endothelial dysfunction in chronic kidney disease, from biology to clinical outcomes: a 2020 update. J Clin Med 2020;9:2359.
81. Bleakley C, Hamilton PK, Pumb R, Harbinson M, McVeigh GE. Endothelial function in hypertension: victim or culprit? The Journal of Clinical Hypertension 2015;17:651–4.
82. Widmer RJ, Lerman A. Endothelial dysfunction and cardiovascular disease. Glob Cardiol Sci Pract 2014;2014:291–308.
83. Hong R, Zhao H, Wang Y, Chen Y, Cai H, Hu Y, et al. Clinical characterization and risk factors associated with cytokine release syndrome induced by COVID-19 and chimeric antigen receptor T-cell therapy. Bone Marrow Transplant 2021;56:570–80.
84. Murthy H, Iqbal M, Chavez JC, Kharfan-Dabaja MA. Cytokine release syndrome: current perspectives. ImmunoTargets Ther 2019;8:43–52.
85. Gallagher P, Chan KR, Rivino L, Yacoub S. The association of obesity and severe dengue: possible pathophysiological mechanisms. J Infect 2020;81:10–6.
86. Molema G, Tervaert JW, Kroesen BJ, Helfrich W, Meijer DK, de Leij LF. CD3 directed bispecific antibodies induce increased lymphocyte-endothelial cell interactions in vitro. Br J Cancer 2000;82:472–9.
87. Su H, Lei C-T, Zhang C. Interleukin-6 signaling pathway and its role in kidney disease: an update. Front Immunol 2017;8:405.
88. Obstfeld AE, Frey NV, Mansfield K, Lacey SF, June CH, Porter DL, et al. Cytokine release syndrome associated with chimeric-antigen receptor T-cell therapy: clinicopathological insights. Blood 2017;130:2569–72.
89. Callender LA, Curran M, Bates SM, Mairesse M, Weigandt J, Betts CJ. The impact of pre-existing comorbidities and therapeutic interventions on COVID-19. Front Immunol 2020;11:1991.
90. Kartolo A, Sattar J, Sahai V, Baetz T, Lakoff JM. Predictors of immunotherapy-induced immune-related adverse events. Curr Oncol 2018;25:e403–e10.
91. Li J, Piskol R, Ybarra R, Chen Y-JJ, Li J, Slaga D, et al. CD3 bispecific antibody–induced cytokine release is dispensable for cytotoxic T cell activity. Sci Transl Med 2019;11:eaax8861.
92. Zhu M, Wu B, Brandl C, Johnson J, Wolf A, Chow A, et al. . Blinatumomab, a Bispecific T-cell Engager (BiTE®) for CD-19 targeted cancer immunotherapy: clinical pharmacology and its implications. Clin Pharmacokinet 2016;55: 1271–88.
93. Fiedler WM, Wolf M, Kebenko M, Goebeler M-E, Ritter B, Quaas A, et al. A phase I study of EpCAM/CD3-bispecific antibody (MT110) in patients with advanced solid tumors. J Clin Oncol 2012;30:2504.
94. Kebenko M, Goebeler M-E, Wolf M, Hasenburg A, Seggewiss-Bernhardt R, Ritter B, et al. A multicenter phase 1 study of solitomab (MT110, AMG 110), a bispecific EpCAM/CD3 T-cell engager (BiTE®) antibody construct, in patients with refractory solid tumors. OncoImmunology 2018;7:e1450710.
95. Bartlett NL, Sehn LH, Assouline SE, Bosch F, Diefenbach CS, Flinn I, et al. Managing cytokine release syndrome (CRS) and neurotoxicity with step-fractionated dosing of mosunetuzumab in relapsed/refractory (R/R) B-cell non-Hodgkin lymphoma (NHL). J Clin Oncol 2019;37:7518.
96. Jiang X, Chen X, Jaiprasart P, Carpenter TJ, Zhou R, Wang W. Development of a minimal physiologically-based pharmacokinetic/pharmacodynamic model to characterize target cell depletion and cytokine release for T cell-redirecting bispecific agents in humans. Eur J Pharm Sci 2020;146:105260.
97. Chen X, Kamperschroer C, Wong G, Xuan D. A modeling framework to characterize cytokine release upon T-cell-engaging bispecific antibody treatment: methodology and opportunities. Clin Transl Sci 2019;12:600–8.
98. Hosseini I, Gadkar K, Stefanich E, Li C-C, Sun LL, Chu Y-W, et al. Mitigating the risk of cytokine release syndrome in a Phase I trial of CD20/CD3 bispecific antibody mosunetuzumab in NHL: impact of translational system modeling. Systems Biology and Applications 2020;6:28.
99. Shah NN, Highfill SL, Shalabi H, Yates B, Jin J, Wolters PL, et al. CD4/CD8 T-cell selection affects chimeric antigen receptor (CAR) T-cell potency and toxicity: updated results from a phase I anti-CD22 CAR T-cell trial. J Clin Oncol 2020;38:1938–50.
100. Pishvaian M, Morse MA, McDevitt J, Norton JD, Ren S, Robbie GJ, et al. Phase 1 dose escalation study of MEDI-565, a bispecific T-cell engager that targets human carcinoembryonic antigen, in patients with advanced gastrointestinal adenocarcinomas. Clin Colorectal Cancer 2016;15:345–51.
101. Sterner RM, Sakemura R, Yang N, Cox MJ, Khadka R, Forsman CL, et al. GM-CSF blockade during chimeric antigen receptor T-cell (CART) therapy reduces cytokine release syndrome and neurotoxicity and may enhance CART effector functions. Biol Blood Marrow Transplant 2019;25:S4.
102. Si S, Teachey DT. Spotlight on tocilizumab in the treatment of CAR-T-cell-induced cytokine release syndrome: clinical evidence to date. Ther Clin Risk Manag 2020;16:705–14.
103. Porter D, Frey N, Wood PA, Weng Y, Grupp SA. Grading of cytokine release syndrome associated with the CAR T cell therapy tisagenlecleucel. J Hematol Oncol 2018;11:35.
104. Kauer J, Hörner S, Osburg L, Müller S, Märklin M, Heitmann JS, et al. Tocilizumab, but not dexamethasone, prevents CRS without affecting antitumor activity of bispecific antibodies. J Immunother Cancer 2020;8: e000621.
105. Frey N, Porter D. Cytokine release syndrome with chimeric antigen receptor T cell therapy. Biol Blood Marrow Transplant 2019;25:e123–e7.
106. Kadauke S, Myers RM, Li Y, Aplenc R, Baniewicz D, Barrett DM, et al. Risk-adapted preemptive tocilizumab to prevent severe cytokine release syndrome after CTL019 for pediatric B-cell acute lymphoblastic leukemia: a prospective clinical trial. J Clin Oncol 2021;39:920–30.
107. Kenderian SS, Ruella M, Shestova O, Kim MY, Klichinsky M, Chen F, et al. Ruxolitinib prevents cytokine release syndrome after CART cell therapy without impairing the anti-tumor effect in a xenograft model. Blood 2016; 128:652.
108. Lamers CH, Sleijfer S, van Steenbergen S, van Elzakker P, van Krimpen B, Groot C, et al. Treatment of metastatic renal cell carcinoma with CAIX CAR-engineered T cells: clinical evaluation and management of on-target toxicity. Mol Ther 2013;21:904–12.
109. Han SS, Azad TD, Suarez PA, Ratliff JK. A machine learning approach for predictive models of adverse events following spine surgery. The Spine Journal 2019;19:1772–81.